Socioenvironmental and demographic modifiers of aging in nonhuman animals

Marina Miriam Watowich

A dissertation

submitted in partial fulfillment of the

requirements for the degree of

Doctor of Philosophy

University of Washington

2022

Reading Committee:

Noah Snyder-Mackler, Chair

Daniel E.L. Promislow

Z. Yan Wang

Lauren J.N. Brent

Program Authorized to Offer Degree:

Biology

University of Washington

Abstract

Socioenvironmental and demographic modifiers of aging in nonhuman animals

Marina Miriam Watowich

Chair of the Supervisory Committee:
Noah Snyder-Mackler
Department of Biology

Across many species, chronological age is the greatest predictor of mortality and the leading risk factor for many non-communicable diseases. However, not all individuals within a species exhibit the same age-related declines in health. For example, some individuals develop early-onset of age-associated diseases while others never develop certain age-associated phenotypes. Understanding what predicts inter-individual pace of aging remains a key question in evolutionary biology and human health. It remains unknown how many intrinsic (e.g., body size) and extrinsic (e.g., environment) factors affect aging and, ultimately, health and survival. Further, aging is a complex phenotype that can vary across organ systems within an individual. Here, I investigated how several pertinent intrinsic and extrinsic variables impact age-related cognitive and immunological phenotypes in two species. First, I tested whether cognitive aging was associated with an intrinsic factor (i.e., body size) in domestic dogs, a species in which individuals have dramatically different rates of size-associated physical aging. I found that dogs from all breeds, regardless of size, showed approximately similar rates of cognitive aging, despite smaller breeds having lifespans approximately twice as long as larger breed dogs. Secondly, I tested how aging of the peripheral immune system, which can directly affect health and morbidity, was affected by an extrinsic modifier: extreme environmental adversity. Specifically, I investigated the extent to which a major hurricane affected immunological aging at the transcriptomic and epigenomic (i.e., DNA methylation) levels, in a key biomedical model organism (rhesus macaques). I found that 4% of genes and 13% of CpG

sites were significantly associated with exposure to a major hurricane and that post-hurricane differential expression and methylation were associated with inflammatory processes. Further, transcriptomic age of individuals sampled after the hurricane were predicted to be an average of 2 years older than individuals sampled before the storm, hinting that the hurricane may have accelerated transcriptomic aging in this population. Together, this work uncovers novel intrinsic and extrinsic modifiers of aging at cognitive and immune levels that are highly pertinent to an organism's health.

TABLE OF CONTENTS

ACKNOWLEDGEMENTS

This dissertation could not have been completed without the help and support of my collaborators and colleagues. I sincerely thank my coauthors for their invaluable mentorship and insight which has strengthened the projects in this dissertation, including Evan L. MacLean, Brian Hare, Josep Call, Juliane Kaminski, Ádám Miklósi, Amanda J. Lea, Kenneth L. Chiou, Michael J. Montague, Julie E. Horvath, James P. Higham, Lauren J. N. Brent, Michael L. Platt, Angelina V. Ruiz-Lambides, Melween I. Martínez, Josué Negrón, Daniel Phillips, Noah D. Simons, Elisabeth A. Goldman, Rachel Petersen, Sam Patterson, and Christina Costa. The scientific questions investigated herein would not be possible to ask without data collected by the Dognition team and citizen scientists who contributed by collecting data as part of the Dognition project, the Caribbean Primate Research Center staff who maintain the invaluable Cayo Santiago Field Station, especially Nahirí Rivera Barreto and Giselle Caraballo Cruz, as well as volunteers who contributed to Monkey Health Explorer in Zooniverse. I also sincerely thank my committee members, the Snyder-Mackler lab, and the broader research communities of which I am a part; each has contributed greatly to my growth as a scientist. Specifically, I would like to thank Daniel Promislow for his support throughout my graduate career; the Snyder-Mackler Lab including India Schneider-Crease, Kenny L. Chiou, Corbin S.C. Johnson, Alice Baniel, Sierra Sams, Brianah McCoy, Layla Brassington, Laura Newman, Mitchell R. Sanchez-Rosado, Trish Zintel, and Alex DeCasien; Jenny Tung, Luis Barreiro, Vasiliki Michopoulos, and Ryan Campbell for sharing data vital to this dissertation; Erin Siracusa, Eve Cooper, Clare Kimock, Arthur Fernandes, and Melissa Pavez Fox for the insightful conversations about rhesus behavior and being excellent fieldwork partners.

I also sincerely thank my family and friends for their support while I completed this dissertation. I have been grateful to have wonderfully supportive family and friends who have made this experience much more fun, enjoyable, and rewarding. I would like to thank my wife, Carly Busch, for her endless kindness, encouragement, and optimism, her ability to always have fun and bring joy to those around her, and for our many captivating scientific conversations. I thank my parents, Stephanie and Stanley Watowich, and my brother Matthew for being examples of excellence and generosity in all facets of life. I thank my extended family for their generosity, good humor, enthusiasm, and kindness. I thank all past and present members of the Snyder-Mackler lab for their friendship and for making the lab an intellectually stimulating, collaborative, and fun working environment. In particular, I thank India Schneider-Crease, Kenny Chiou, Corbin Johnson, and Alice Baniel for their guidance during the early stages

of my graduate career, their friendship throughout graduate school, and for making the lab a wonderfully collaborative and inspiring environment. Lastly, I sincerely thank Noah Snyder-Mackler for his guidance and mentorship which has helped me to become a better scientist, for cultivating a highly intellectually stimulating, collaborative, and fun working environment, for his relentless optimism, and for maintaining high standards and always helping raise others up to meet them.

Funding Sources

I am grateful to the many funders without whom this work would not be possible. This work was supported by the University of Washington, Department of Biology, and the National Institutes of Health (1F31AG072787-01A1). Work contributed from coauthors and collaborators was supported by: a Royal Society Research Grant (RGS/R1/191182), the National Brain Research Program (2017-1.2.1-NKP-2017-00002), the ELTE 576 Institutional Excellence Program (National Research, Development and Innovation Office; NKFIH-1157-8/2019-DT), the National Institutes of Health (R00AG051764, U19AG057377, R01AG060931, R01HD097732, R00-AG051764, P40-OD012217, R01-AG060931, R01-MH096875, R01-MH089484, R01-MH118203, F32-AG062120), and the National Science Foundation (1800558). Cayo Santiago Field Station is supported by the Office of Research Infrastructure Programs (ORIP) of the National Institutes of Health (2P40OD012217).

Chapter 1

Age influences domestic dog cognitive performance independent of average breed lifespan

Marina M. Watowich[1], Evan L. MacLean[2,3,4], Brian Hare[5,6], Josep Call[7], Juliane Kaminski[8], Ádám Miklósi[9,10], Noah Snyder-Mackler[1,11,12,13,14,15]

[1] Department of Biology, University of Washington, Seattle, WA 98195, USA
[2] School of Anthropology, University of Arizona, Tucson, AZ 85719, USA
[3] Department of Psychology, University of Arizona, Tucson, AZ 85721, USA
[4] Cognitive Science, University of Arizona, Tucson, AZ 85721, USA
[5] Department of Evolutionary Anthropology, Duke University, Durham, NC 27708, USA
[6] Center for Cognitive Neuroscience, Duke University, Durham, NC 27708, USA
[7] School of Psychology and Neuroscience, University of St Andrews, St Andrews, UK
[8] Centre for Comparative and Evolutionary Psychology, Department of Psychology, University of Portsmouth, Portsmouth, UK
[9] Department of Ethology, Eötvös Loránd University, Budapest, Hungary
[10] MTA-ELTE Comparative Ethology Research Group, Budapest, Hungary
[11] Center for Evolution & Medicine, Arizona State University, Tempe, AZ 85287, USA
[12] School of Life Sciences, Arizona State University, Tempe, AZ 85287, USA
[13] Department of Psychology, University of Washington, Seattle, WA 98195, USA
[14] Nathan Shock Center of Excellence in the Basic Biology of Aging, Department of Pathology, University of Washington, Seattle, WA 98195, USA
[15] Center for Studies in Demography and Ecology, University of Washington, Seattle, WA 98195, USA

Abstract

Across mammals, increased body size is positively associated with lifespan. However, within species, this relationship is inverted. This is well illustrated in dogs (*Canis familiaris*), where larger dogs exhibit accelerated life trajectories: growing faster and dying younger than smaller dogs. Similarly, some age-associated traits (e.g., growth rate and physiological pace of aging) exhibit accelerated trajectories in larger breeds. Yet, it is unknown whether cognitive performance also demonstrates an accelerated life course trajectory in larger dogs. Here, we measured cognitive development and aging in a cross-sectional study of over 4000 dogs from 66 breeds using nine memory and decision-making tasks performed by citizen scientists as part of the Dognition project. Specifically, we tested whether cognitive traits follow a compressed (accelerated) trajectory in larger dogs, or the same trajectory for all breeds, which would result in limited cognitive decline in larger breeds. We found that all breeds, regardless of size or lifespan, tended to follow the same quadratic trajectory of cognitive aging—with a period of cognitive development in early life and decline in later life. Taken together, our results suggest that cognitive

performance follows similar age-related trajectories across dog breeds, despite remarkable variation in developmental rates and lifespan.

Introduction

Across mammals, larger species tend to live longer than smaller species (Healy et al. 2014). Yet, within species this pattern is reversed (Metcalfe and Monaghan 2003; Austad 2010; Bartke 2017). This pattern is well-documented in domestic dogs (Galis et al. 2007; Kraus et al. 2013; Fan et al. 2016) where larger dog breeds (e.g., Bernese Mountain Dog, mean lifespan = 7 years) have an expected lifespan that is approximately half that of smaller breeds (e.g., Chihuahua, mean lifespan = 13 years; Jones et al. 2008). While large breeds take longer to mature than small breeds, they weigh disproportionately more, and therefore have faster growth rates and an accelerated pace of physiological aging (e.g., cellular damage; Fick et al. 2012; Kraus et al. 2013; Fan et al. 2016). Domestic dogs have been under strong artificial selection for at least 15,000 years (vonHoldt et al. 2010), which has driven extensive diversity in physical and life history traits (i.e., size, growth rate, lifespan). The large variation in these life history traits, in particular, have made dogs an invaluable model species for studying the underpinnings of age-related changes in health (Hoffman et al. 2018).

Domestic dogs also provide a powerful model in which to explore intraspecific patterns of cognitive aging. In humans and other animals, including dogs, cognitive abilities, such as learning and memory, change throughout aging (Craik and Bialystok 2006; Bizon and Woods 2009; Harada et al. 2013; Chapagain et al. 2018). However, for some cognitive processes, dogs may even provide a better model for human cognition than rodents and nonhuman primates, potentially due to convergent evolution between humans and dogs (Miklósi et al. 2004; Hare and Tomasello 2005; Hare 2017; MacLean et al. 2017). For millennia, humans have selected dogs for both behavioral (i.e., herding, hunting) and physical traits (Ostrander et al. 2017; Parker et al. 2017), contributing to the extensive diversity seen across modern breeds. While the association between domestic dog cognition and other life history traits (e.g., age) remains largely unexplored, there is evidence that absolute brain size is associated with breed differences in executive function (Horschler et al. 2019) – a cognitive domain responsible for inhibitory control, mental flexibility, and decision-making (Alvarez and Emory 2006; Jurado and Rosselli 2007).

Executive functions typically include inhibition (i.e., self-control and selective memory), working memory, and cognitive flexibility (Diamond 2013). In humans, executive function, learning, and long-term memory have

largely been found to increase in early life and decrease in late life (Craik and Bialystok 2006; Harada et al. 2013; but see Verhaeghen 2011). Other cognitive abilities (e.g., vocabulary and general knowledge) increase steadily throughout life (i.e., linearly) or increase rapidly and then plateau (i.e., resembling a positive logarithmic curve) (Harada et al. 2013). Similar to humans, domestic dogs experience changes to critical cognitive functions across life (Chapagain et al. 2018). Recent studies from laboratory and pet dogs have demonstrated that learning, memory, and cognitive functions under executive control decrease in older dogs (Adams et al. 2000; Tapp et al. 2003; Szabó et al. 2016; Wallis et al. 2016). Older dogs also show greater variability in the extent of cognitive decline with age (Adams et al. 2000). One source of this variability may be lifelong behavioral training, which has been associated with greater sustained and selective attention in older dogs (Chapagain et al. 2017). Although domestic dogs exhibit age-related cognitive changes, we still know very little about how cognition changes with age, in large part due to sample size: collecting data from enough very young and very old dogs has been challenging (Szabó et al. 2016). To date, most studies of dog cognitive aging have focused on one breed or a small number of breeds, which, due to the limited variability in life history within individual breeds, has limited our ability to examine associations between cognitive aging and physiological pace of aging. Consequently, the extent to which cognitive changes throughout aging are associated with life history traits that covary with physiological pace of aging (as measured by average breed lifespan) remains unknown.

Here, we investigated the associations between lifespan and cognitive traits in dogs, in order to test the hypothesis that animals with faster life histories also exhibit earlier onset of and/or more rapid cognitive decline. We addressed two questions using a cross-sectional dataset of more than 4,000 dogs from 66 breeds collected from participants of the Dognition project, a citizen-science initiative in which owners perform simple cognitive tests with their dogs at home (Stewart et al. 2015). First, we tested how cognition changes across the lifespan of domestic dogs. To date, many studies of dog cognition have modeled cognition as a linear process throughout the lifespan, yet data from humans, apes, and several within-breed studies of domestic dogs suggest the likelihood of non-linear changes across development and senescence (Craik and Bialystok 2006; Harada et al. 2013; Wallis et al. 2014; Manrique and Call 2015). Second, we tested if and how a key life history trait, expected breed lifespan, affected the trajectory of cognition across the lifespan. We explicitly tested two alternative hypotheses: i) *truncation*: that all breeds have similar cognitive trajectories throughout aging with larger breeds having a limited period of cognitive

decline (Fig. 1a), and ii) *compression*: that changes in cognitive abilities scale with lifespan such that larger dogs have a compressed (i.e., accelerated) cognitive trajectory (Fig. 1b).

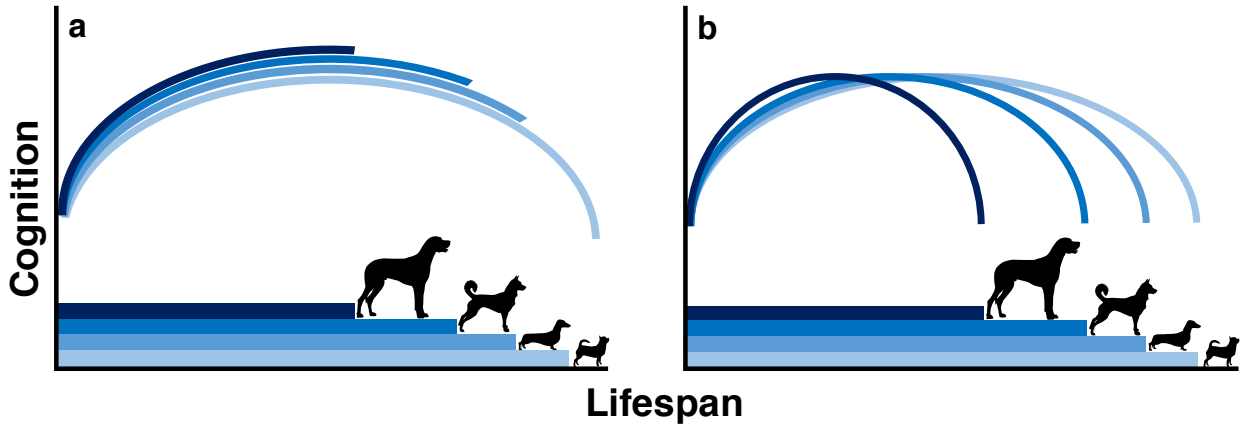

Fig. 1 Alternative models of cognitive aging in dogs. a Schematic of the truncation hypothesis in which larger and smaller dog breeds have similar cognitive trajectories throughout aging. Under this hypothesis, large dog breeds experience limited cognitive decline because they typically die before the more precipitous cognitive decline experienced by longer-lived, smaller breeds. **b** The compression hypothesis in which cognitive performance scales with lifespan, such that larger breeds will have an accelerated cognitive trajectory.

Methods

Data sources

Cognitive performance data were collected from *Dognition.com*, a citizen science website which provides users with video instructions for completing simple cognitive experiments at home with their dogs. Owners entered data into the website by answering simple questions about their dog's behavior during the cognitive tests (e.g., which location did your dog approach?). Importantly, results from citizen scientists using Dognition recapitulate results from professional scientists working in controlled laboratory settings (Stewart et al. 2015). Here, we restricted our analysis to data collected prior to April 2018 from purebred dogs with known sex, age, reproductive alteration status (i.e., spayed/neutered vs. intact), and breed (n= 4,419). Dogs in the study represented 66 breeds and ranged in age from < 1 to 14.2 years with a mean age of 4.78 years (standard deviation ± 3.13; Supplemental Fig. 1). To ensure representative sampling, only breeds with 10 or more individuals were retained for analysis (Supplemental Table 1). We used data from purebred dogs to ensure that we could estimate mean breed lifespan and to control for relatedness among breeds based on breed-averaged genotypic data (Parker et al. 2017; Supplemental

Table 2). We used estimates of mean breed lifespan from Jones et al. (2008; Supplemental Table 3). Because recent studies have found behavioral modifications correlated with reproductive alteration (Hart 2001; Mongillo et al. 2017; Scandurra et al. 2019), we also included reproductive alteration status as a covariate in all models.

We included data from nine cognitive tasks measuring diverse processes involving aspects of executive function, such as memory, reasoning, decision making, self-control, as well as measures of social cognition (Stewart et al. 2015; Horschler et al. 2019; Table 1). Sample size varied across tasks due to participant attrition across the series of experiments. We focused our analyses on tasks involving executive function as it is one of the cognitive domains most susceptible to effects of aging (Jurado and Rosselli 2007). Seven of the Dognition tasks involved an object-choice paradigm in which the dog had to choose one of two possible options, across a series of trials (range=1-6, mode=4; Table 1). One of the other two tasks was the eye contact task, in which the owner held a piece of food up to their face and recorded the time until the dog broke eye contact (up to 90 seconds). This task was designed as a measure of dog's social engagement. In the remaining task, the owner set a treat before the dog, instructed the dog not to take a treat, and recorded the time until the dog took the treat (up to 90 seconds) while the owner i) was visibly watching the dog, ii) had their back turned to the dog, or iii) faced the dog with their eyes closed (detailed in Stewart et al. 2015). Although originally developed as a measure of social cognition (sensitivity to cues about the human's visual perspective), recent analyses have focused on the executive function component of this task, which requires dogs to delay gratification (Horschler et al. 2019). Following this approach, we considered the latency to take the forbidden treat as a measure of executive function in our analyses. To summarize performance in this task, we performed a principal component analysis on the latencies to take the treat across conditions. This analysis yielded one principal component which explained 88% of the variance and is subsequently referred to as 'delay of gratification'. The Dognition battery also includes a contagious yawning task which we did not include because preliminary analyses showed minimal evidence for contagious yawning in this sample.

Table 1 Description of cognitive tasks, cognitive processes the task was designed to test, number of trials conducted per task, number of individuals included in analysis, and number of breeds included in analysis

Task	Description	Cognitive processes	Trials	Total dogs	Total breeds
Eye contact	The owner holds a treat to their face and records if and when the dog breaks eye contact within 90 seconds.	Social engagement	3	4359	65
Arm pointing	The owner places one treat to their right and left, points to one treat location, and records the location the dog first approaches.	Social cognition/ communication	6	4367	65
Foot pointing	The owner places one treat to their right and left, extends their foot toward one treat location, and records the location the dog first approaches.	Social cognition/ communication	6	4071	63
Delay of gratification		Inhibition/self-control	6	2826	51
Watching condition	The owner places the treat in front of the dog and verbally commands the dog not to take the treat. The owner records the duration of time until the dog takes the treat, up to 90 seconds.		2	2826	51
Closed eyes condition	Same as above, with the owner closing their eyes.		2	2826	51
Turned back condition	Same as above, with the owner turning their back.		2	2826	51
Memory vs. pointing	In view of the dog, the owner places a treat under one of two cups, then proceeds to point to the other cup. The owner records which location the dog first approaches.	Bias for information from memory vs. communication	6	2346	48
Memory vs. smell	Allowing the dog to see, the owner places a treat under one of two cups, then blocks the dog's view while switching the position of the treat. The owner records which location the dog first approaches.	Bias for information from memory vs. olfaction	4	2187	47
Delayed memory	In full view of the dog, the owner places a treat under one of two cups and then waits 60, 90, 120, and 150 seconds (across four trials) before releasing the dog. Then the owner records which location the dog first approaches.	Short-term memory/ sustained attention	4	2124	47
Inferential reasoning	The owner appears to place treats under two cups, while only baiting one. The owner raises the empty cup to show it is empty and records which location the dog first approaches.	Inferential reasoning/ reasoning by exclusion	4	1737	42
Physical reasoning	Blocking the dog's view, the owner places two pieces of folded paper on the floor. The owner places a treat under one paper so that the paper is elevated by the treat while the other paper is flat and records which location the dog first approaches.	Physical causality/ inferential reasoning	4	1654	40

Statistical Analysis

To address the questions of i) how cognitive performance changes across domestic dog lifespan (Equations 1, 2, and 3) and ii) whether cognition scales with mean breed lifespan (Equations 3 and 4), we compared the fit of all four mixed effects models for each of the seven tasks with a binomial response and ii) the two linear response variables (eye contact and the principal component scores reflecting delay of gratification; Supplemental Tables 4, 5). Because many cognitive abilities in humans exhibit a negative quadratic relationship (an inverted U-shape) with age (in particular those associated with executive processes), while others tend to increase throughout life or increase quickly during development and then plateau (Craik and Bialystok 2006; Harada et al. 2013; Wallis et al. 2014), we tested if cognitive performance followed these trajectories by modeling age as a quadratic, linear, and logarithmic predictor (Supplemental Table 4).

---

(1) Linear trajectory: $Cognitive\ measure \sim sex\ +\ reproductive\ alteration\ +\ age\ +\ mean\ breed\ lifespan$

(2) Logarithmic trajectory: $Cognitive\ measure \sim sex\ +\ reproductive\ alteration\ +\ log(age)\ +\ mean\ breed\ lifespan$

(3) Quadratic trajectory (additive): $Cognitive\ measure \sim sex + reproductive\ alteration + age + age^2 + mean\ breed\ lifespan$

(4) Quadratic trajectory (interactive): $Cognitive\ measure \sim sex\ +\ reproductive\ alteration\ +\ age \times mean\ breed\ lifespan\ +\ age^2 \times mean\ breed\ lifespan$

Equations 1, 2, 3, and 4 Equations 1, 2, and 3 represent hypothesized trajectories of cognitive aging, based on previously described patterns of cognitive aging. Equations 3 and 4 represent the truncation and compression hypotheses

In all models, the age and mean breed lifespan predictors were mean centered and scaled to a standard deviation of one. Age and mean breed lifespan were in units of years and therefore one order of magnitude larger than the predictors of sex and reproductive alteration. Scaling the predictors of age and mean breed lifespan made them similar in magnitude to the predictors of sex and reproductive alteration, facilitating interpretation of the model results (Harrison et al. 2018). All models of the quadratic trajectory included orthogonal linear and quadratic predictors of age. Mixed-effects models of the seven binomial measures were carried out using the 'PQLseq' package, which implements the mixed modeling framework MACAU in the R environment (Lea et al. 2015; Sun et al. 2019). This allowed us to model a binomial outcome variable (i.e., number of times dog chose the left cup out of 6) while controlling for background genetic similarity among the breeds, which was calculated from a recent genomic analysis of 150,067 SNPs in 1,346 dogs representing 161 breeds (Parker et al. 2017; Supplemental Table

2). The eye contact and delay of gratification measures were modeled controlling for breed relatedness using the 'EMMREML' package (Akdemir and Okeke 2015) in the R environment. Only breeds for which we had both cognitive and genetic data were included in our analyses (Supplemental Table 1). Model fits were compared using Akaike information criterion (AIC; Akaike 1974). To test the sensitivity of our models, we also repeated these analyses excluding overrepresented breeds, which were breeds which each constituted over 5% of the dataset (Supplemental Table 6). Five breeds fit this criterion (Australian Shepherds, Border Collies, German Shepherd Dogs, Golden Retrievers, and Labrador Retrievers) and together comprised over 45% of the dataset. For models of the three tasks involving gesture following (arm pointing, foot pointing, and memory vs. pointing), we included behavioral training history as a predictor in the truncation and compression models to ensure that our results were not confounded by the correlation between dog size and training history (training history was rated on a scale of 1 [none] – 4 [substantial]; $r_s = 0.12$, $p < 0.001$; Supplemental Table 7; Horschler et al. 2019).

Delayed memory task

We considered the delayed memory task the clearest test of basic memory because other tests involving memory measured preferences and biases, where memory was pitted against other information sources (e.g., memory of treat location vs. owner's pointing, memory of treat location vs. scent of the treat). Although designed and interpreted as a measure of memory, it is possible that the delayed memory task also reflects variation in sustained attention, since the hiding locations were not out of the dog's view during the delay. However, unlike traditional sustained attention tasks, there was no cue provided at the end of the delay, and thus subjects would most likely have been reliant on memory to motivate their search for food at the baited location. We modeled all trials from this task to test the truncation and compression hypotheses, however, we focused our analyses on the 150 second trial as this trial was the longest time delay and likely the most cognitively challenging. Importantly, the results of the 60, 90, and 120 second delayed memory trials were very similar to the 150 second trial (Supplemental Table 8).

Results

Cognition across the lifespan

For all tasks, the best models (ΔAIC > 2) included the quadratic predictor of age, compared to linear or logarithmic, meaning that cognitive performance followed the expected inverted U-shaped trajectory – increasing in early life and declining in late life (Figs. 2, 3; Supplemental Fig. 2; Supplemental Table 4). Although the best models included quadratic functions of age, the coefficient for the quadratic term was significant in only six tasks (eye contact, delayed memory, memory vs. pointing, memory vs. smell, and inferential reasoning tasks, as well as the delay of gratification score; Fig. 2, Fig. 3; Supplemental Tables 4, 5, 8). Models without a significant age^2 term (arm pointing, foot pointing, and physical reasoning tasks) showed an increase in cognitive performance throughout aging (Supplemental Table 5).

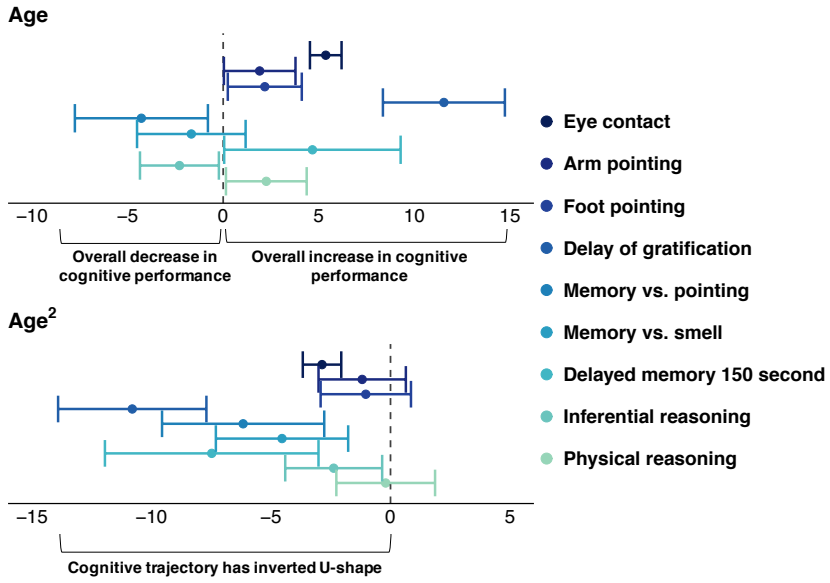

Fig. 2 Age has both linear and quadratic associations with cognitive function. Effect sizes and estimated confidence intervals ($beta \pm 1.96 \times SE$) of age and age^2 predictor variables for the additive (truncation) models for each cognitive task. Estimated confidence intervals that do not cross the line of null effect (x = 0) are statistically significant. For ease of interpretation and visualization, and to keep all variables on a similar scale, we converted the beta for the eye contact task to minutes.

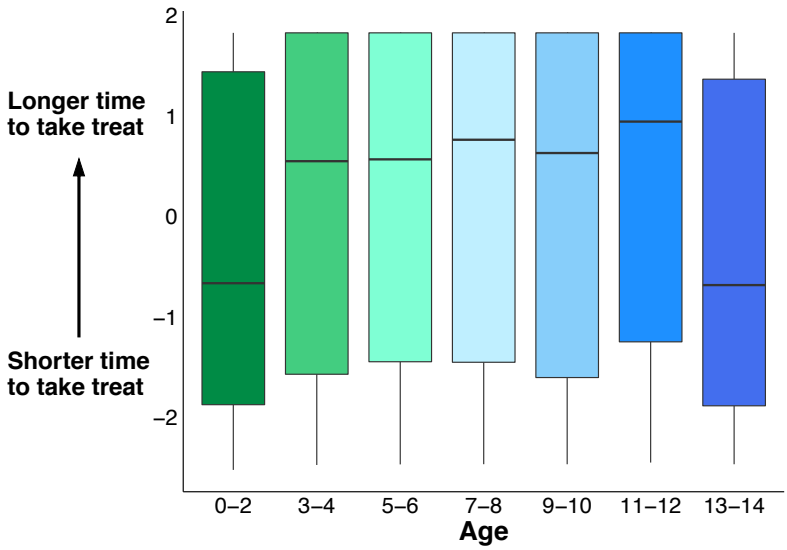

Fig. 3 Self-control changes with age. Delay of gratification principal component 1 values for 2-year age groups. The delay of gratification task measures the time until the dog takes a treat (latency) under conditions of the owner watching, closing their eyes, and turning their back. Increasing y-axis values indicate greater performance in prolonging gratification (i.e., increased latency to take the treat).

Truncation vs. compression models

Models testing the truncation hypothesis fit the data better than or as well as models of the compression hypothesis for seven of the nine tasks (Table 2; Supplemental Table 5). The two tasks for which the model of the compression hypothesis had a better model fit were the eye contact task and delay of gratification score. However, neither of these models had significant interactions with mean breed lifespan, between age and mean breed lifespan, or between age^2 and mean breed lifespan. For models of the compression hypothesis, only the arm pointing (β = 2.196, SE = 0.996, p = 0.027, n = 4367) and foot pointing tasks (β = 2.017, SE = 1.028, p = 0.049, n = 4071) showed significant interaction effects between age^2 and mean breed lifespan, while the memory vs. pointing task (β = 0.087, SE = 0.042, p = 0.037, n = 2346) had a significant effect of mean breed lifespan in models of the truncation and compression hypotheses. These associations would support the compression hypothesis; however, interactive models of these tasks did not fit the data better than additive models representing the truncation hypothesis (ΔAIC < 2; Table 2; Supplemental Table 5). Our sensitivity analyses that excluded overrepresented breeds generally recapitulated results of the comparison between truncation and compression hypothesis models (Supplemental Table 6). In these analyses, fewer tasks had significant effects of age and age^2, likely due to reduced power, however the results were very similar to analyses with the entire dataset and did not suggest that our results were being driven by

breeds that were overrepresented in the data. While we focused our analyses on the 150 second delayed memory trial, we evaluated how age affected cognitive performance across all delayed memory trials by modeling delay-specific accuracies in young (0-5 years), middle-aged (6-10 years), and old dogs (11+ years). Comparing the slope of the delay function, we found that dogs 11 years and older performed lower across all delayed memory trials (Supplemental Fig. 3).

Table 2 Comparing the fit of models of the truncation hypothesis and the compression hypothesis for each cognitive task. Lower AIC value indicates a better model fit. ΔAIC > 2 is considered a difference in model fit. The numbers in bold denote a difference in model fit between truncation and compression models

Task	ΔAIC of truncation hypothesis models and compression hypothesis models (compression – truncation)	Model with better fit
Eye contact	**-13.0**	compression hypothesis
Arm pointing	1.2	no difference
Foot pointing	-0.3	no difference
Delay of gratification	**-7.5**	compression hypothesis
Memory vs. pointing	0.1	no difference
Memory vs. smell	0.8	no difference
Delayed memory 150 second	-0.2	no difference
Inferential reasoning	**2.4**	truncation hypothesis
Physical reasoning	1.7	no difference

Gesture following

We observed associations between predictors involving breed-mean lifespan for the three tasks involving gesture following (arm pointing, foot pointing, and memory vs. pointing), supporting the compression hypothesis, although model fit did not differ substantially between models of the truncation and compression hypothesis. Additionally, in all models of gesture following, the age coefficient indicated increases in performance with aging, rather than late-life deterioration of cognitive performance, suggesting that these associations are not likely to support accelerated cognitive deterioration in faster-aging breeds. To ensure that our results were not confounded by the correlation between dog size and training history, we included training as a predictor in the truncation and compression models for all gesture following models. The proportion of dogs in each category of training history was similar between intact and spayed and neutered individuals, males and females, and across dogs of all ages (in one-year age groups). Effects of breed lifespan were reduced to statistically indistinguishable from zero when we included training history in the models of gesture following tasks (arm pointing [$mean\ breed\ lifespan \times age^2$]: β

= -0.64, SE = 0.915, p = 0.485, n = 1105; foot pointing [$mean\ breed\ lifespan \times age^2$]: β = 0.275, SE = 0.936, p = 0.769, n = 1057; memory vs. pointing [mean breed lifespan]: β = 0.071, SE = 0.083, p = 0.394 n = 720; Supplemental Table 7). However, because not all owners reported their dog's training history – resulting in reduced power for this analysis – we could not rule out the possibility that this reduction in significance was due to a smaller sample size. We therefore compared this analysis to an analysis of the same subsample excluding training history as a predictor (Supplemental Table 7) and found that the effects of mean breed lifespan were not significant.

Associations of reproductive alteration vary across gesture following tasks

Reproductive alteration was associated with decreased gesture following throughout aging (Fig. 4; arm pointing: β = -0.117, SE = 0.039, p < 0.01, n = 4367; memory vs. pointing: β = 0.379, SE = 0.097, p < 0.001, n = 2346; Supplemental Table 5). After controlling for training history in analyses of the arm pointing and memory vs. pointing tasks, reproductive alteration was still significantly associated with decreased gesture following (arm pointing: β = -0.272, SE = 0.073, p < 0.001, n = 1105; memory vs. pointing: β = 0.527, SE = 0.164, p < 0.01, n = 720), indicating that spayed or neutered animals were less likely to follow social cues from their owner, even after controlling for training history (Supplemental Table 7).

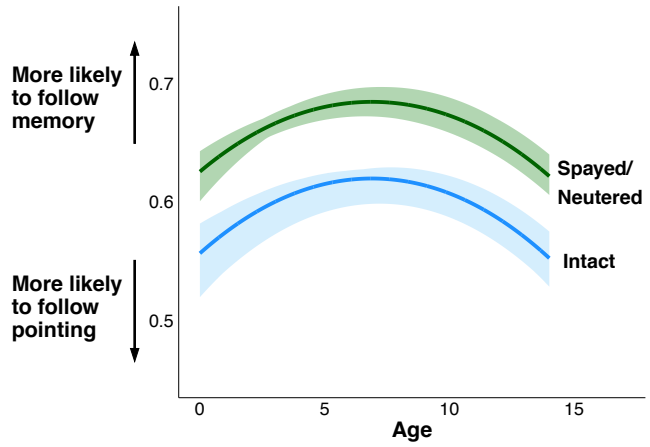

Fig. 4 Gesture following differs between intact and spayed and neutered dogs. Predicted cognitive trajectory for the memory vs. pointing task throughout aging (years) of an average dog in the dataset whether spayed or neutered (green) or intact (blue), with bootstrapped 95% confidence intervals.

Sex differences

In the eye contact task, males maintained eye contact with the experimenter longer than females ($\beta = 2.26$, SE = 0.738, $p = 0.002$, $n = 4359$), but this effect size was small (males held eye contact for an average of 2.26 seconds longer than females). In the delayed memory task, males were more likely than females to locate a treat after the 150 second delayed memory trial ($\beta = 0.204$, SE = 0.101, $p = 0.043$, $n = 2124$), but not any other delayed memory trial; again this effect was small, but statistically significant (males had 22% higher odds of choosing the cup with the treat). After performing our sensitivity analyses by excluding overrepresented breeds, males still showed longer social engagement in the eye contact task ($\beta = 2.323$, SE = 1.008, $p = 0.021$, $n = 2318$) but sex differences for the 150 second delayed memory trial were no longer significant.

Discussion

We investigated age-related changes in dog cognition and found that all cognitive measures changed across the lifespan, with most measures following a clear negative quadratic trajectory across the lifespan. For each of the nine cognitive tasks we evaluated, models with a quadratic term for age better fit the data than linear and logarithmic terms and six of these cognitive tasks showed a distinct inverted U-shape across aging (Fig. 2; Supplemental Fig. 2; Supplemental Tables 4, 5), indicating that a broad suite of cognitive processes in domestic dogs increase in early life, peak in midlife, and decrease in late life. Additionally, we found that cognitive performance in tasks testing physical reasoning and the propensity to follow owners' pointing gestures (without competing sources of information) increase throughout aging.

Tasks directly testing memory and self-control were the clearest tests of executive function and had particularly robust quadratic curves throughout aging (Fig. 2.; Fig. 3.; Supplemental Table 5). In humans, executive function follows a similar negative quadratic trajectory throughout the lifespan and is one of the cognitive domains most susceptible to aging. Declines in executive function greatly impact daily life by reducing cognitive performance in domains such as decision making, memory, and self-control (Jurado and Rosselli 2007; Alvarez and Emory 2006; Bizon and Woods 2009; Harada et al. 2013). Similar declines have been reported in nonhuman primate and rodent models (Moore et al. 2006; Rodefer and Nguyen 2008; Beas et al. 2013), and recently described for domestic dog attention (Wallis et al. 2014). Our findings extend these similarities to dogs across a range of cognitive

processes, thus building on previous laboratory work with dogs (Milgram et al. 1994; Head et al. 2001; Tapp et al. 2003) and advancing companion dogs as a useful model for human cognitive aging.

To assess associations between cognition and aging, we tested models representing what we have termed the 'truncation hypothesis', in which all dogs have similar cognitive trajectories, and the 'compression hypothesis', in which the timing of decline is accelerated in shorter-lived breeds. Models representing the truncation hypothesis fit the data better than or as well as models representing the compression hypothesis across seven of the nine cognitive tasks (Table 2; Supplemental Table 5). The two tasks for which models representing the compression hypothesis fit the data better than models representing the truncation hypothesis did not have significant associations of mean breed lifespan or between mean breed lifespan and linear or quadratic terms of age. Additionally, all models representing the compression hypothesis lacked significant interactions between age and mean breed lifespan after controlling for training history. Thus, we conclude that there is not sufficient evidence for the compression hypothesis, and that these results most strongly support the truncation hypothesis. Together, our results suggest that all dog breeds, regardless of average breed lifespan or rate of physiological aging, exhibit similar cognitive aging trajectories such that larger dogs may experience a limited cognitive decline at the end of their shorter lives.

Although the pace of physiological aging varies with lifespan, there is evidence that the age of onset of senescence does not differ among breeds, except, perhaps, in very large breeds (Kraus et al. 2013). If general onset of senescence is similar among breeds, larger breeds will tend to have an abnormally shortened senior period, while smaller breeds will likely undergo a protracted decline. Our findings indicate a similar pattern in cognitive performance and are concordant with recent work finding similar prevalence of canine dementia across breeds of varying size (Salvin et al. 2010, 2012). However, Kraus et al. (2013) suggest that large breeds physiologically deteriorate rapidly, which we did not detect for cognitive aging. Together, these results may suggest that the pathways which influence cognitive aging may be partially decoupled from those which affect the pace of physiological aging. While further investigation is clearly warranted, these findings have important implications for dog owners considering the quality of life during the senior period in terms of both cognitive and physiological health.

We also observed effects of reproductive alteration on tasks involving responses to pointing gestures. Intact dogs were more likely than spayed and neutered dogs to follow owners' cues across two tasks involving arm pointing even after controlling for training history (Supplemental Table 7). These findings are consistent with results

from a recent study that demonstrated reduced tendency of gonadectomized female dogs to follow human pointing gestures compared to intact females (Scandurra et al. 2019). Neutering increases food motivation and decreases metabolic rate, which can lead to lower energy levels and increased risk of obesity (Duffy and Serpell 2006; German 2006). It is therefore possible that neutered dogs had a greater motivation to obtain the food than intact dogs and were less attentive to the cue given by the owner. It is unclear how sex hormones alter cognition and behavior in dogs, however, there is some evidence that intact male dogs may exhibit slower cognitive decline than neutered males (Hart 2001) which may be due to neuroprotective activity of sex hormones (Zárate et al. 2017). Additionally, our findings demonstrated few and inconsistent sex-related differences in cognitive performance. Sex was significantly associated with performance on two measures, duration of eye contact, in which male dogs held slightly longer eye contact than females, and the 150 second delayed memory trial, in which males had a greater propensity than females to remember treat location after this time delay (although this effect was not detected for the sensitivity analyses with reduced sample size). Sex differences in dog cognition have been reported across a variety of measures including looking times in violation of expectation tasks, gaze at human faces following oxytocin administration, and speed and accuracy in spatial memory tasks (Müller et al. 2011; Nagasawa et al. 2015; Mongillo et al. 2017). However, these studies found that female dogs tended to show longer looking times compared to males, and better performance on spatial memory, effects in the opposite direction to those we observed. Given the inconsistency across studies, it will be important for future research to assess the robustness of sex differences on these measures, as well as specific factors that may determine the nature of these effects (Miller and Halpern 2014).

One limitation of this study stems from a lack of very old dogs in our sample. We had relatively few dogs of very old age: dogs aged 11 and older comprised 5% of our dataset. We observed greater variation in cognitive performance in older dogs, particularly among the oldest dogs in the study. For many tasks, the performance of the oldest aged dogs in our study ranged greatly, often spanning the full spectrum of the dependent variable's range. The relatively small number of very old dogs means that assessing cognitive performance in this group is more susceptible to the influence of a small number of individuals. Future studies further establishing how cognition changes and varies among this demographic would be valuable. We suspect that the limited number of very old dogs may result from a selection bias in which owners of older, potentially highly impaired dogs, may have been less likely to pursue participation in these activities. Thus, active recruitment of the oldest dogs will be an important priority for future research. While collecting self-reported data from dog owners enabled the relatively large sample

size of this study, we had variation in the reporting of information such as training history, which decreased power to detect effects of aging and possible associations with mean breed lifespan within this group. It will be important to generate larger datasets in the future that can include other potentially relevant covariates. We also collected data from dog owners at a single time point which limited the degree to which we could evaluate individual variation in cognitive performance throughout aging. Lastly, the cognitive assessment we used included diverse tasks, but the particular cognitive processes measured by each specific task were not unambiguous.

Due to extraordinary intraspecific phenotypic diversity, dogs present a unique model for investigating how age-related traits vary with cognition across the lifespan. Our findings suggest that age-related changes in executive function in domestic dogs follow patterns similar to those in humans and provide insight regarding the relationships (or lack thereof) between life history and cognitive trajectories in a species characterized by extensive intraspecific diversity. An important priority for future work will be to determine whether dogs and humans share similar aging trajectories in other cognitive domains such as long-term memory, cognitive processing speed, and episodic-like memory. Using consistent and readily deployable cognitive assessments, such as the ones presented here, future studies could evaluate longitudinal changes in cognitive performance of the same cohort of dogs across various timepoints to gain a finer grained understanding of dog cognitive aging.

References

1. Adams B, Chan A, Callahan H, Milgram NW (2000) The canine as a model of human cognitive aging. Prog Neuro-Psychopharmacol & Biol Psychiat 24:675–692
2. Akaike H (1974) A new look at the statistical model identification. IEEE Trans Automat Contr 19:716–723. doi: 10.1109/TAC.1974.1100705
3. Akdemir D, Okeke UG (2015) EMMREML: Fitting mixed models with known covariance structures. https://cran.r-project.org/package=EMMREML R package version 3.1
4. Alvarez JA, Emory E (2006) Executive function and the frontal lobes: A meta-analytic review. Neuropsychol Rev 16:17–42. doi: 10.1007/s11065-006-9002-x
5. Austad S. (2010) Animal size, metabolic rate, and survival, among and within species. In: Wolf NS (ed) The comparative biology of aging. Springer, Dordrecht, pp 27–41
6. Bartke A (2017) Somatic growth, aging, and longevity. npj Aging Mech Dis 3:1–6. doi: 10.1038/s41514-017-0014-y
7. Beas BS, Setlow B, Bizon JL (2013) Distinct manifestations of executive dysfunction in aged rats. Neurobiol Aging 34:2164–2174
8. Bizon JL, Woods AG (2009) Animal models of human cognitive aging. Humana Press
9. Chapagain D, Range F, Huber L, Virányi Z (2018) Cognitive aging in dogs. Gerontology 64:165–171. doi: 10.1159/000481621
10. Chapagain D, Virányi Z, Wallis LJ, et al (2017) Aging of attentiveness in border collies and other pet dog breeds: The protective benefits of lifelong training. Front Aging Neurosci 9:1–14. doi: 10.3389/fnagi.2017.00100
11. Craik FIM, Bialystok E (2006) Cognition through the lifespan: Mechanisms of change. Trends Cogn Sci

10:131–138. doi: 10.1016/j.tics.2006.01.007
12. Diamond A (2013) Executive functions. Annu Rev Psychol 64:135–168. doi: 10.1146/annurev-psych-113011-143750
13. Duffy DL, Serpell JA (2006) Center for the Interaction of Animals and Society, School of Veterinary Medicine, University of Pennsylvania Non-reproductive Effects of Spaying and Neutering on Behavior in Dogs Proceedings of the Third International Symposium on Non-Surgical Contracepti. In: Proceedings of the Third International Symposium on Non-Surgical Contraceptive Methods for Pet Population Control
14. Fan R, Olbricht G, Baker X, Hou C (2016) Birth mass is the key to understanding the negative correlation between lifespan and body size in dogs. Aging (Albany NY) 8:3209–3222. doi: 10.18632/aging.101081
15. Fick LJ, Fick GH, Li Z, et al (2012) Telomere length correlates with life span of dog breeds. Cell Rep 2:1530–1536. doi: 10.1016/j.celrep.2012.11.021
16. Galis F, Van Der Sluij I, Van Dooren TJM, et al (2007) Do large dogs die young ? J Exp Zool (Molecular Dev Evol 308:119–126. doi: 10.1002/jez.b
17. German AJ (2006) The growing problem of obesity in dogs and cats. Am Soc Nutr 1940–1946
18. Harada CN, Love MCN, Triebel K (2013) Normal cognitive aging. Clin Geriatr Med 29:737–752. doi: 10.1016/j.cger.2013.07.002
19. Hare B (2017) Survival of the friendliest: Homo Sapiens evolved via selection for prosociality. Annu Rev Psychol 68:155–185. doi: 10.1146/annurev-psych-010416-044201
20. Hare B, Tomasello M (2005) Human-like social skills in dogs? Trends Cogn Sci 9:439–444. doi: 10.1016/j.tics.2005.07.003
21. Harrison XA, Donaldson L, Correa-Cano ME, et al (2018) A brief introduction to mixed effects modelling and multi-model inference in ecology. PeerJ 1–32. doi: 10.7717/peerj.4794
22. Hart BL (2001) Effect of gonadectomy on subsequent development of age-related cognitive impairment in dogs. J Am Vet Med Assoc 219:51–56
23. Head E, William Milgram N, W.Cotman C (2001) Neurobiological models of aging in the dog and other vertebrate species. In: Functional Neurobiology of Aging. pp 457–468
24. Healy K, Guillerme T, Cooper N, et al (2014) Ecology and mode-of-life explain lifespan variation in birds and mammals. Proc R Soc B Biol Sci 281:20140298–20140298. doi: 10.1098/rspb.2014.0298
25. Hoffman JM, Creevy KE, Franks A, et al (2018) The companion dog as a model for human aging and mortality. Aging Cell 17:. doi: 10.1111/acel.12737
26. Horschler DJ, Hare B, Call J, et al (2019) Absolute brain size predicts dog breed differences in executive function. Anim Cogn. doi: 10.1007/s10071-018-01234-1
27. Jones P, Chase K, Martin A, et al (2008) Single-nucleotide-polymorphism-based association mapping of dog stereotypes. Genetics 179:1033–1044. doi: 10.1534/genetics.108.087866
28. Jurado MB, Rosselli M (2007) The elusive nature of executive functions: A review of our current understanding. Neuropsychol Rev 17:213–233. doi: 10.1007/s11065-007-9040-z
29. Kraus C, Pavard S, Promislow DEL (2013) The size–life span trade-off decomposed: Why large dogs die young. Am Nat 181:492–505. doi: 10.1086/669665
30. Lea AJ, Tung J, Zhou X (2015) A flexible, efficient binomial mixed model for identifying differential DNA methylation in bisulfite sequencing data. PLoS Genet 11:1–31. doi: 10.1371/journal.pgen.1005650
31. MacLean EL, Herrmann E, Suchindran S, Hare B (2017) Individual differences in cooperative communicative skills are more similar between dogs and humans than chimpanzees. Anim Behav 126:41–51. doi: 10.1016/j.anbehav.2017.01.005
32. Manrique HM, Call J (2015) Age-dependent cognitive in flexibility in great apes. Anim Behav 102:1–6. doi: 10.1016/j.anbehav.2015.01.002
33. Metcalfe NB, Monaghan P (2003) Growth versus lifespan : perspectives from evolutionary ecology. 38:935–940. doi: 10.1016/S0531-5565(03)00159-1
34. Miklósi Á, Topál J, Csányi V (2004) Comparative social cognition: What can dogs teach us? Anim Behav 67:995–1004. doi: 10.1016/j.anbehav.2003.10.008
35. Milgram NW, Head E, Weiner E, Thomas E (1994) Cognitive functions and aging in the dog: acquisition of nonspatial visual tasks. Behav Neurosci 108:57–68. doi: https://doi.org/10.1037/0735-7044.108.1.57
36. Miller DI, Halpern DF (2014) The new science of cognitive sex differences. Trends Cogn Sci 18:37–45. doi: 10.1016/j.tics.2013.10.011
37. Mongillo P, Scandurra A, Aniello BD, Marinelli L (2017) Effect of sex and gonadectomy on dogs' spatial performance. Appl Anim Behav Sci 191:84–89. doi: 10.1016/j.applanim.2017.01.017
38. Moore TL, Killiany RJ, Herndon JG, et al (2006) Executive system dysfunction occurs as early as middle-

age in the rhesus monkey. Neurobiol Aging 27:1484–1493. doi: 10.1016/j.neurobiolaging.2005.08.004
39. Müller CA, Mayer C, Dörrenberg S, et al (2011) Female but not male dogs respond to a size constancy violation. Biol Lett 689–691. doi: 10.1098/rsbl.2011.0287
40. Nagasawa M, Mitsui S, En S, et al (2015) Oxytocin-gaze positive loop and the coevolution of human-dog bonds. Sci Reports 348:
41. Ostrander EA, Wayne RK, Freedman AH, Davis BW (2017) Demographic history, selection and functional diversity of the canine genome. Nat Rev Genet 18:705–720. doi: 10.1038/nrg.2017.67
42. Parker HG, Dreger DL, Rimbault M, et al (2017) Genomic analyses reveal the influence of geographic origin, migration, and hybridization on modern dog breed development. Cell Rep 19:697–708. doi: 10.1016/j.celrep.2017.03.079
43. Rodefer JS, Nguyen TN (2008) Naltrexone reverses age-induced cognitive deficits in rats. Neurobiol Aging 29:309–313. doi: 10.1016/j.neurobiolaging.2006.10.005
44. Salvin HE, Mcgreevy PD, Sachdev PS, Valenzuela MJ (2010) Under diagnosis of canine cognitive dysfunction: A cross-sectional survey of older companion dogs. Vet J 184:277–281. doi: 10.1016/j.tvjl.2009.11.007
45. Salvin HE, McGreevy PD, Sachdev PS, Valenzuela MJ (2012) The effect of breed on age-related changes in behavior and disease prevalence in cognitively normal older community dogs, Canis lupus familiaris. J Vet Behav 7:61–69
46. Scandurra A, Alterisio A, Di Cosmo A, et al (2019) Ovariectomy impairs socio-cognitive functions in dogs. Animals 9:. doi: 10.3390/ani9020058
47. Stewart L, Rodriguez K, Call J, et al (2015) Citizen science as a new tool in dog cognition research. PLoS One 10:e0135176. doi: 10.1371/journal.pone.0135176
48. Sun S, Zhu J, Mozaffari S, et al (2019) Heritability estimation and differential analysis of count data with generalized linear mixed models in genomic sequencing studies. Bioinformatics 35:487–496. doi: 10.1093/bioinformatics/bty644
49. Szabó D, Gee NR, Miklósi Á (2016) Natural or pathologic? Discrepancies in the study of behavioral and cognitive signs in aging family dogs. J Vet Behav Clin Appl Res 11:86–98. doi: 10.1016/j.jveb.2015.08.003
50. Tapp PD, Siwak CT, Estrada J, et al (2003) Size and reversal learning in the beagle dog as a measure of executive function and inhibitory control in aging. Learn Mem 10:64–73. doi: 10.1101/lm.54403
51. Verhaeghen P (2011) Aging and executive control: Reports of a demise greatly exaggerated. Curr Dir Psychol Sci 20:174–180. doi: 10.1177/0963721411408772
52. VonHoldt BM, Pollinger JP, Lohmueller KE, et al (2010) Genome-wide SNP and haplotype analyses reveal a rich history underlying dog domestication. Nature 464:898–902. doi: 10.1038/nature08837
53. Wallis LJ, Range F, Müller CA, et al (2014) Lifespan development of attentiveness in domestic dogs: Drawing parallels with humans. Front Psychol 5:. doi: 10.3389/fpsyg.2014.00071
54. Wallis LJ, Virányi Z, Müller CA, et al (2016) Aging effects on discrimination learning, logical reasoning and memory in pet dogs. Age (Omaha) 38:1–18. doi: 10.1007/s11357-015-9866-x
55. Zárate S, Stevnsner T, Gredilla R (2017) Role of estrogen and other sex hormones in brain aging. Neuroprotection and DNA repair. Front Aging Neurosci 9:1–22. doi: 10.3389/fnagi.2017.00430

Chapter 2

Natural disaster and immunological aging in a nonhuman primate

Marina M. Watowich[1], Kenneth L. Chiou[2,3], Michael J. Montague[4], Cayo Biobank Research Unit, Noah D. Simons[7], Julie E. Horvath[8,9,10,11], Angelina V. Ruiz-Lambides[12], Melween I. Martínez[12], James P. Higham[13,14], Lauren J. N. Brent[15], Michael L. Platt[4,5,6], Noah Snyder-Mackler[2,3]

[1] Department of Biology, University of Washington; Seattle, WA, 98195 USA.
[2] Center for Evolution and Medicine, Arizona State University; Tempe, AZ, 85281 USA.
[3] School of Life Sciences, Arizona State University; Tempe, AZ, 85281 USA.
[4] Department of Neuroscience, Perelman School of Medicine; University of Pennsylvania, Philadelphia, PA 19104, USA.
[5] Department of Psychology, School of Arts and Sciences; University of Pennsylvania, Philadelphia, PA 19104, USA.
[6] Marketing Department, Wharton School of Business; University of Pennsylvania, Philadelphia, PA 19104, USA.
[7] Department of Evolutionary Anthropology, Duke University; Durham, NC 27708, USA.
[8] Department of Biological and Biomedical Sciences, North Carolina Central University; Durham, NC 27707, USA.
[9] Research and Collections Section, North Carolina Museum of Natural Sciences; Raleigh, NC 27601, USA.
[10] Department of Biological Sciences, North Carolina State University; Raleigh, NC 27695, USA.
[11] Department of Evolutionary Anthropology, Duke University; Durham, NC 27708, USA.
[12] Caribbean Primate Research Center, Unit of Comparative Medicine, University of Puerto Rico; San Juan, PR 00936, USA.
[13] Department of Anthropology, New York University; New York, NY 10003, USA.
[14] New York Consortium in Evolutionary Primatology; New York, NY, 10016 USA.
[15] Centre for Research in Animal Behaviour, University of Exeter; Exeter EX4 4QG, UK.

Abstract

Weather-related disasters are increasing in frequency and severity, leaving survivors to cope with ensuing mental, financial, and physical hardships. This adversity can exacerbate existing morbidities, trigger new ones, and increase the risk of mortality–features that are also characteristic of advanced age–inviting the hypothesis that extreme weather events may accelerate aging. To test this idea, we examined the impact of Hurricane Maria and its aftermath on immune cell gene expression in large, age-matched, cross-sectional samples from free-ranging rhesus macaques (*Macaca mulatta*) living on an isolated island. A cross-section of macaques were sampled 1-4 years before (n = 435) and one year after (n = 108) the hurricane. Hurricane Maria was significantly associated with differential expression of 4% of immune-cell-expressed genes, and these effects were correlated with age-associated alterations in gene expression. We further found that individuals exposed to the hurricane had a gene expression profile that was, on average, 1.96 years older than individuals that were not–roughly equivalent to an increase in 7-8 years of a human life. Living through an intense hurricane and its aftermath was associated with expression of key immune genes, dysregulated proteostasis networks, and greater expression of inflammatory immune cell-specific marker genes. Together, our findings illuminate potential mechanisms through which the adversity unleashed by extreme weather

and potentially other natural disasters might become biologically embedded, accelerate age-related molecular immune phenotypes, and ultimately contribute to earlier onset of disease and death.

Introduction

Survivors of extreme adverse events, such as natural disasters, have increased incidence of cardiovascular diseases and chronic low-grade inflammation (1–6). At the molecular level, severe hardship can also alter immune cell gene expression (7–9) and advance hallmarks of aging such as prematurely aging T cell populations (10) and accelerating epigenetic aging (11–13). While everyone ages, not everyone ages at the same rate, and individuals of the same chronological age can have dramatic differences in the onset or severity of age-related diseases (14–16). Characteristic changes in age-associated phenotypes are known as biological aging. The difference between biological and chronological age (i.e., age acceleration or deceleration) is associated with morbidity and mortality in humans (17, 18), can be manipulated through experimental interventions in non-human primates and mice (19, 20), and can change throughout the life course due to environmental exposures (e.g., smoking) (21, 22). Age acceleration can be measured using biological clocks, which can quantify the difference between biological and chronological age (17, 18). The prevalence of shared morbidities as a result of extreme adversity and aging invites the hypothesis that exposures to adversity may accelerate aging (11, 12, 23, 24). Indeed, adversity associated with traumatic-stress (e.g., war) or environmental disasters, like wildfire smoke, can increase inflammatory markers, indicating that premature immune aging may be a particularly salient mechanism by which disasters translate into disease (7, 12, 25–27). At the molecular level, environmental conditions can induce persistent gene regulatory changes that affect gene transcription for many years, a mechanism through which adversity and other experiences may become biologically embedded and mechanistically explain lasting immune changes (28–33). Despite these tantalizing links, prior studies of adversity and aging acceleration have typically lacked biological measures in the same population prior to the adverse event, and almost exclusively investigated violence- and deprivation-related adversity (e.g., war, abuse). Thus, whether aged molecular phenotypes extend to natural disasters like extreme weather events (e.g., hurricanes, floods, tornados) remains unknown.

Hurricane Maria, the most destructive hurricane recorded in the history of Puerto Rico, made landfall in Puerto Rico on September 20, 2017 as a category 4 hurricane. One kilometer off the southeastern coast of Puerto Rico lies Cayo Santiago, a 15.2-hectare island home to a population of 1,800 free-ranging rhesus macaques that

have been studied for decades. Cayo Santiago was the first part of Puerto Rico hit and thus bore the full force of Hurricane Maria. The storm severely damaged homes and infrastructure across the Puerto Rican mainland and destroyed most of the vegetation, freshwater cisterns, and research structures on Cayo Santiago (Figure 1A, 1B, 1C) (34). The Cayo Santiago field station is an ideal system for studying the immune consequences of aging and environmentally-induced adversity for several reasons. First, rhesus macaques share many behavioral and biological features with humans, including aging phenotypes. However, the rhesus macaque lifespan is approximately one-quarter of the human lifespan (35), permitting effective sampling of a significant portion of the aging process in just a few years. Third, macaques on Cayo Santiago are provisioned with food and water–even in the immediate aftermath of the hurricane–thus controlling for nutritional disruptions that might additionally affect the aging process (36–38).

To test how Hurricane Maria influenced immune cell gene regulation and aging, we leveraged our collection of peripheral blood samples and detailed demographic data (Dataset S1) from age-matched cross-sectionally sampled subsets of the Cayo Santiago rhesus macaque population annually in the four years prior to Hurricane Maria (n = 435) and one year after (n = 108) Hurricane Maria (Figure 1D). We hypothesized that exposure to the hurricane would recapitulate molecular changes associated with the natural process of aging.

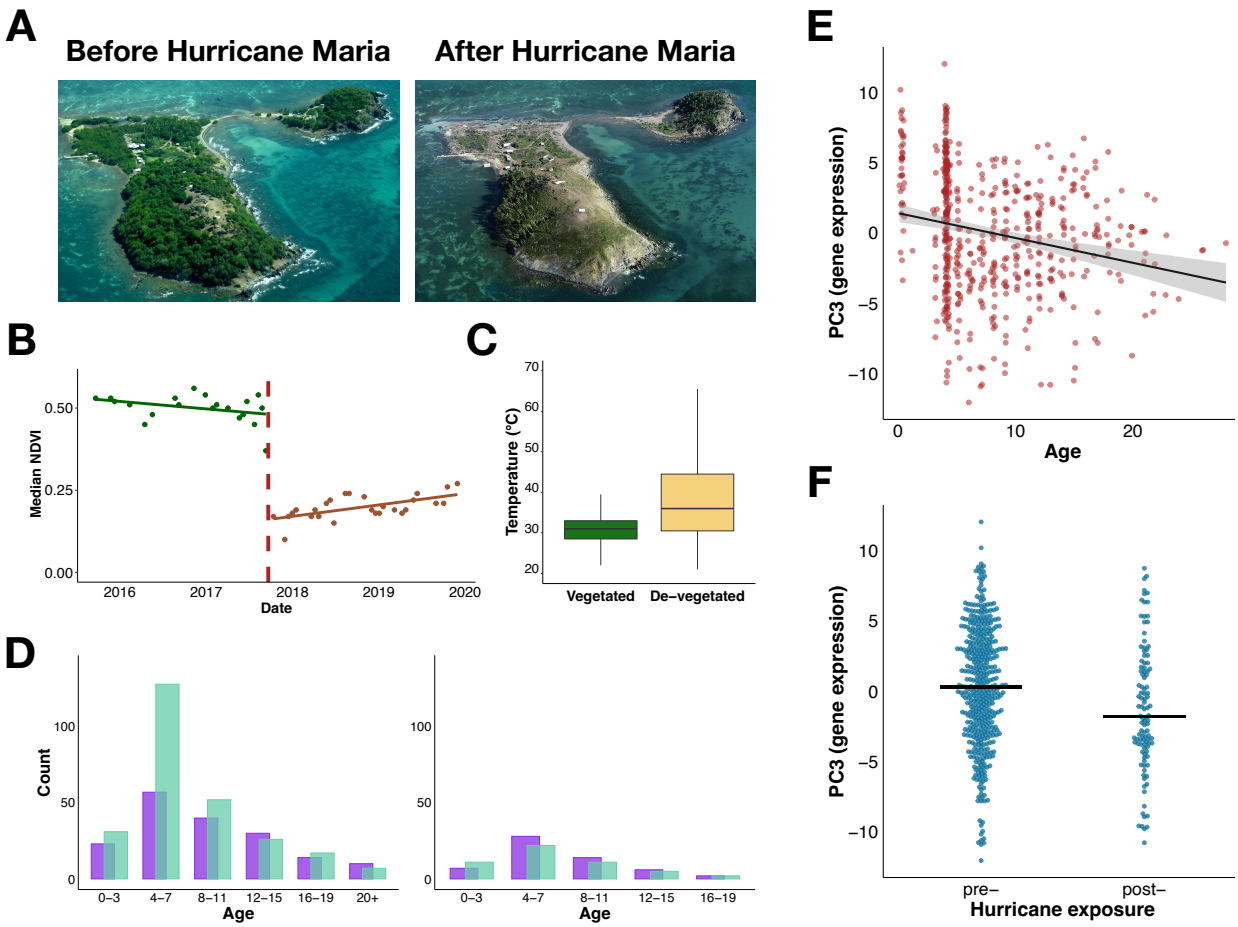

Figure 1. Hurricane Maria caused severe destruction to Cayo Santiago and was associated with altered immune cell gene regulation. (**A**) Hurricane Maria struck the island of Cayo Santiago on September 20, 2017, causing severe devastation to the vegetation and substantial remodeling of the environment. Aerial photographs show Cayo Santiago in August 2008 (left) and January 2020 (right). Photos reused with permission of Joyce Cohen, WOM Productions, and Michelle Skrabut La Pierre. (**B**) Vegetation, as measured by normalized difference vegetation index (NDVI), decreased by 63% due to the storm (t-test, $p = 3.7 \times 10^{-25}$). (**C**) Temperature in areas that lost vegetation due to Hurricane Maria (i.e., de-vegetated) were significantly warmer than areas still vegetated after the storm (t-test, $p < 1 \times 10^{-10}$). (**D**) Peripheral whole blood was collected cross-sectionally from the rhesus macaque population on Cayo Santiago island approximately annually 1–4 years before (n = 435) and one year after (n = 108) Hurricane Maria struck the island. Animals sampled post-hurricane were an average of 0.89 years younger than animals sampled pre-hurricane (median age pre-hurricane = 6.94, median age post-hurricane = 6.05, t-test of means p-value = 1.16×10^{-3}). (**E**) PC3 of global gene expression captures the shared effects between increasing age ($\beta = -0.19$, $p = 8.96 \times 10^{-8}$) and (**F**) exposure to Hurricane Maria ($\beta = -1.79$, $p = 9.12 \times 10^{-5}$) on immune gene expression. PC3 explains 3.4% of the overall variance in gene expression.

Results

Age-associated immune cell gene expression patterns

We first quantified how chronological age was associated with immune cell gene expression. As expected, chronological age was strongly associated with immune cell gene regulation. Age was significantly associated with the first and third principal components of gene expression, which explained 55.2% and 3.4% of the variance, respectively (PC1: age $\beta = -0.39$, $p = 0.005$, Figure S1; PC3: age $\beta = -0.19$, $p = 8.96 \times 10^{-8}$, Figure 1E). At the level of individual genes, we found that 16% of the 7009 detectably expressed genes were significantly associated with chronological age (n genes = 1131, FDR < 10%, Dataset S2, in a model controlling for Hurricane Maria exposure, sex, and RNA quality, n = 543). Genes more highly expressed in older animals were enriched for biological processes associated with inflammation (Benjamini-Hochberg corrected $p_{BH} = 5.72 \times 10^{-5}$) and innate immune system activity (e.g., negative regulation of lymphocyte mediated immunity, $p_{BH} = 0.005$) (Dataset S3). Transcription factor binding site analysis identified that these genes were putatively under control of transcription factors (TFs) in the bZip protein family (e.g., AP-1, Fosl2, JunB) as well as TFs NFkB-p65 and NR5A2 (FDR < 5%), which are both implicated in cytokine production and inflammatory diseases (39, 40) (Dataset S4). By contrast, genes more highly expressed in younger animals were enriched for biological processes associated with translation ($p_{BH} = 1.86 \times 10^{-23}$) and immunoglobulin production ($p_{BH} = 0.108$) (Dataset S5). We did not find significant evidence for any sex differences in aging. We also examined non-linear age-related changes in gene expression using autoregressive integrated moving average (ARIMA) models (41) and detected 1246 genes with non-zero trends that clustered into five aging trajectories (Figure S2). Clusters 1, 2, and 3 changed linearly across aging (i.e., increasing, decreasing) and 62.9% (n = 656) of genes in these clusters overlapped with genes detected by our linear modeling approach. Notably, genes in clusters 4 and 5 exhibited non-linear trajectories with increasing age. Genes in cluster 4 followed an inverted U-shape trajectory across the lifespan (increase in mid-life and decrease in late life), while cluster 5 genes exhibited a U-shaped trajectory (decrease in mid-life and increase in late life). Cluster 5, in particular, included several important immune genes such as *CCL5* and *CD4*, which encode for the T cell chemoattractant CCL5, expressed by activated T cells, and protein CD4 that is critical in the antigen detection

process for regulatory and helper T cell subsets, suggesting that expression of these key immune genes reaches a nadir in midlife, but rapidly increase in late life.

Exposure to a natural disaster is associated with altered immune cell gene expression

We next evaluated whether experiencing Hurricane Maria was associated with differences in immune cell gene expression. Exposure to Hurricane Maria was significantly associated with PC3 (β = -1.79, p = 9.12 x 10^{-5}) (Figure 1F) and, at the gene level, differential expression in 4% of genes (n = 260, FDR < 10%). We found no sex differences in the gene expression response to Hurricane Maria. Genes more highly expressed in animals sampled after Hurricane Maria (n = 54) were implicated in inflammation (e.g., positive regulation of IL-8 production, p_{BH} = 0.052) (Dataset S6). Genes with reduced expression in animals sampled after Hurricane Maria (n = 206) were involved in translation (p_{BH} = 2.58 x 10^{-6}), chaperone cofactor-dependent protein refolding (p_{BH} = 5.75 x 10^{-2}), and processes suggestive of a decrease in adaptive immune activity (e.g., regulation of T cell differentiation, p_{BH} = 0.096) (Dataset S7). Genes with reduced expression in animals sampled after Hurricane Maria were putatively controlled by HSF1 (FDR < 5%) (Dataset S8), the central TF of the heat shock response. Together, downregulation of translation and protein folding activity suggest a disruption to protein folding networks that promote proteostasis– the loss of which is a hallmark of aging (13, 42). Specifically, *HSC70/HSPA8*, a constitutively expressed component of the HSP70 family, exhibited the strongest association with exposure to Hurricane Maria. Expression of *HSC70* was 2x lower after Hurricane Maria (β = -1.03, se β = 0.09, FDR = 1.02 x 10^{-24}). Decreased *HSC70* activity may exacerbate cardiovascular diseases (43, 44) and Alzheimer's Disease (45, 46), which are both age-related diseases that are more prevalent in survivors of severe adversity (1, 6). Further, among the 260 genes differentially expressed between animals sampled before and after Hurricane Maria, gene-gene coexpression networks were disproportionately disrupted for genes associated with the heat shock response. Seven gene pairs were differentially correlated before versus after Hurricane Maria (FDR < 10%). These pairs were composed of 11 unique genes, meaning that several genes were represented in multiple pairs. Five of these 11 genes were involved in the heat shock response, an overrepresentation compared to the background rate among hurricane-associated genes,

underscoring that the heat shock response is particularly disrupted in individuals that experienced Hurricane Maria (binomial test, $p = 6.97 \times 10^{-4}$).

Exposure to a natural disaster broadly recapitulates gene expression differences associated with aging

We quantified the extent to which the effects of age and exposure to the hurricane on immune cell gene expression were similar in two ways. First, 40% of the 260 hurricane-associated genes were also significantly associated with age (n = 104), which is 2.5x more than expected by chance (Fisher's Exact Test OR = 3.7, $p = 4.06 \times 10^{-21}$) (Figure 2, Dataset S2). Moreover, these 104 genes were significantly more likely to exhibit alterations in expression that were consistent with the prediction that exposure to the hurricane was akin to increases in chronological age. In other words, we found strong and significant concordance in the hurricane and aging effects in these 104 genes: 84.6% of the genes (n = 88) significantly associated with age and the hurricane had higher expression with both aging and exposure to Hurricane Maria or lower expression with both aging and hurricane exposure (binomial test, $p = 3.18 \times 10^{-13}$) (Figure 2). Second, we quantified if the expression of genes were similarly associated with hurricane exposure and aging in both magnitude and direction. Across all genes, the effects of aging and exposure to Hurricane Maria were significantly positively correlated ($r = 0.23$, $p = 1.33 \times 10^{-84}$) (Figure 2). The strength of this correlation increased more than two-fold when we limited to genes that were more strongly associated with aging and the hurricane (genes with FDR < 10% for both age and Hurricane Maria: $r = 0.58$, $p = 1.05 \times 10^{-10}$) (Figure S3). Importantly, effects of the hurricane and aging persisted when we controlled for potential covariates of body condition, wound presence, and sampling condition (see Methods section *Testing other sources of transcriptional variation*).

Genes with lower expression levels in samples from animals that experienced the hurricane and in older individuals suggested a disruption to protein folding processes (e.g., proteostasis, $p_{BH} = 5.94 \times 10^{-5}$) and telomerase activity ($p_{BH} = 0.02$) (Dataset S9). Genes with reduced expression in samples after Hurricane Maria and with older age were enriched for the TF HSF1 binding site (FDR = 0.005) (Dataset S10). Further implicating the heat shock response pathway, we found that genes coding for molecular chaperones that aid in protein folding and protein degradation (i.e., ubiquitination) overwhelmingly had lower expression in samples from older individuals and those that experienced Hurricane Maria (Figure 3A). In fact, genes involved in molecular chaperoning and ubiquitination were among the most perturbed (Figure 3A, Figure S4), comprising 9 of the top 10 most affected by the hurricane

(Dataset S2). Decreased molecular chaperone activity leads to protein misfolding and aggregation, decreased clearing of disabled proteins from the cell via ubiquitination, and is implicated in many age-related diseases (Figure 3B, Figure S4) (47–49). Together, these data suggest that exposure to Hurricane Maria may increase protein misfolding and contribute to the onset and progression of age-associated diseases.

Only 16 genes were associated with the hurricane and aging in opposing directions (meaning that they were up-regulated with aging and down-regulated following Hurricane Maria; Figure 2). Genes in this group included

IRF1, *CCL5*, *PRF1*, *GSTP1*, which are integral to the aging process, yet may represent a signature of an environmental stress-specific response that differs in direction from age-related processes.

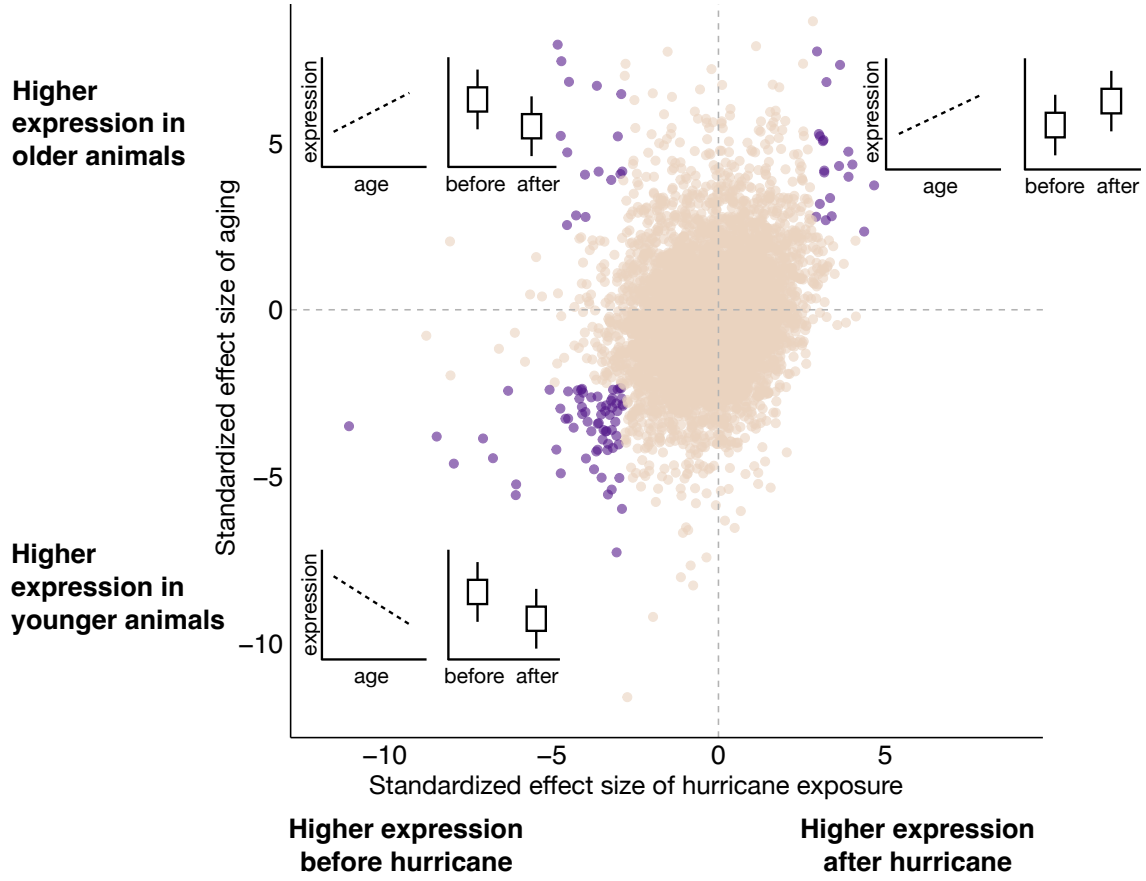

Figure 2. Similar effects of Hurricane Maria and aging on immune cell gene expression. The standardized effect sizes of experiencing Hurricane Maria on immune gene expression are positively correlated with standardized effect sizes of aging on immune gene expression ($r = 0.23$, $p = 1.33 \times 10^{-84}$). Genes that are significantly associated (FDR < 10%) with aging and Hurricane Maria correlate even more strongly ($r = 0.58$, $p = 1.05 \times 10^{-10}$). Genes significantly associated with both effects are colored purple. Inset plots show schematics of the gene expression differences represented in each quadrant.

Lastly, we tested whether animals exposed to Hurricane Maria had immune cell expression profiles consistent with signatures of accelerated aging. To do so, we used human transcriptional age predictors that have been successfully applied by our group to predict age from gene expression in rhesus macaques (35, 50). We hypothesized that samples after the hurricane would have older biological age predictions, which might be indicative of accelerated biological aging in these animals. Reproductively mature adult animals that experienced Hurricane

Maria had gene expression profiles that were, on average, 1.96 years biologically older than adults sampled before Hurricane Maria (in a linear model of predicted age controlling for chronological age and hurricane exposure, p

= 3.0 x 10^{-4}; Figure 3C). When scaled to the human lifespan, immune gene expression of adults who experienced the hurricane was equivalent to an age acceleration of 7-8 years.

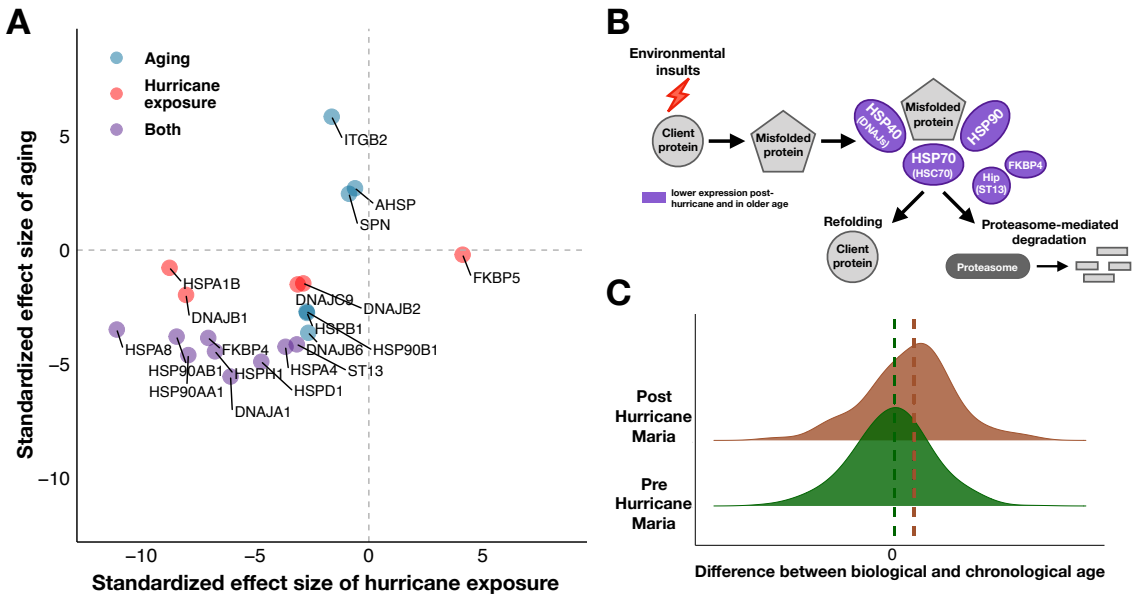

Figure 3. Hurricane Maria disrupted genes involved in protein homeostasis and was associated with accelerated gene expression aging. (**A**) Aging and experiencing Hurricane Maria were associated with reduced expression of key molecular chaperone proteins. Genes shown were differentially expressed with aging and/or hurricane exposure (FDR < 10%). (**B**) Molecular chaperone proteins in the protein homeostasis pathway that were significantly associated with the hurricane and aging. These proteins promote proper folding of client proteins and clear terminally misfolded proteins from the cell. (**C**) Predicted biological ages based on gene expression profiles for pre-hurricane (green) and post-hurricane (brown) samples. Post-hurricane samples have a predicted biological age that is, on average, 1.96 years greater than their chronological age (p = 0.0003).

Aging and exposure to natural disaster are both associated with higher expression of innate immune cell marker genes

Immune cell composition changes across the lifespan and could therefore be reflected in the transcriptome. To examine age or hurricane-associated differences in immune cell composition, we used immune cell marker genes identified from single-cell RNA-sequencing (Dataset S11). Overall, cell-specific markers of canonical anti-inflammatory immune cells had lower expression in older individuals and those that experienced the hurricane, while markers of myeloid-derived cells associated with the inflammatory response had higher expression (Figure 4A, 4B). Our findings are consistent with known changes in cell populations across aging and also demonstrate that experiencing Hurricane Maria recapitulated age-associated differences at the level of immune cell composition. Specifically, granulocyte, classical (CD14+) monocyte, non-classical monocyte (CD14-), NK cell, and cytotoxic T cell marker genes were more highly expressed with aging, while helper T cell and B cell marker genes were more lowly expressed ($p_{BH} < 0.05$). Animals exposed to Hurricane Maria had greater expression of classical monocyte marker genes and lower expression of helper T cell marker genes than individuals that did not experience the hurricane ($p_{BH} < 0.05$) (Figure 4B).

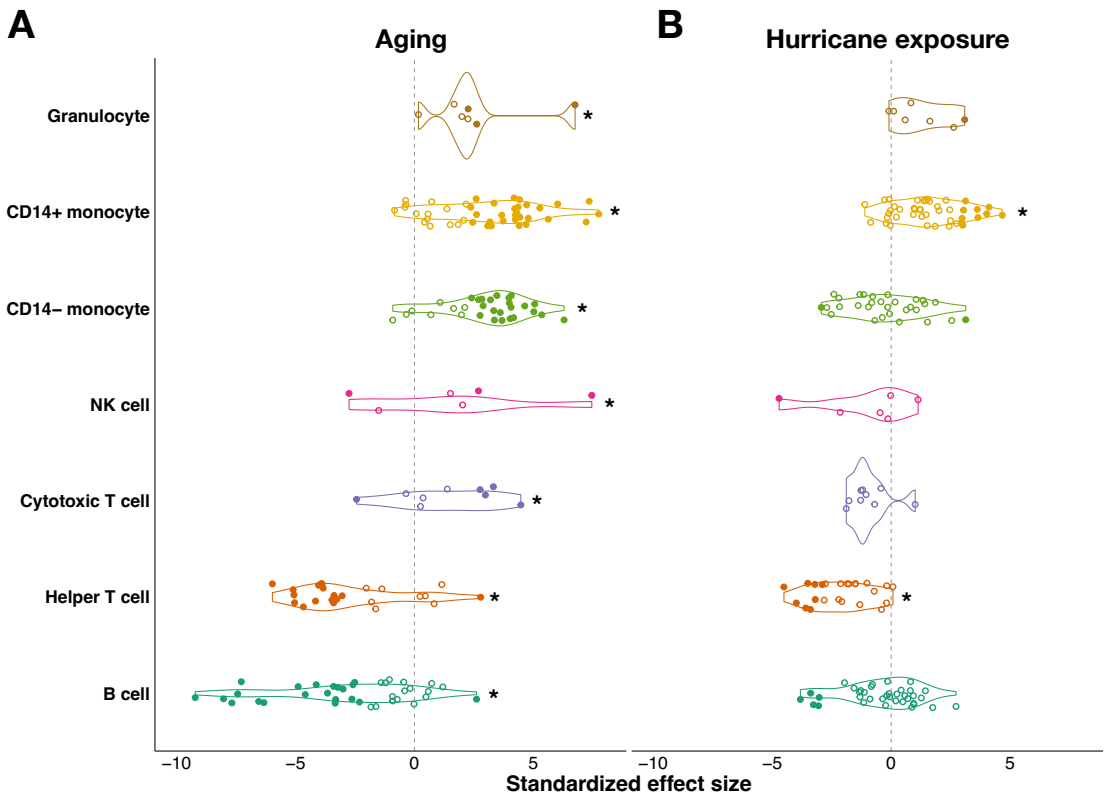

Figure 4. Aging and experiencing Hurricane Maria were associated with broadly similar immune cell marker gene expression. Shaded points represent marker genes that were significantly differentially expressed (FDR < 10%) across aging (**A**) and Hurricane Maria (**B**). Open points represent marker genes that were not significantly associated with the effect of aging or hurricane exposure. Asterisks denote cell types for which differentially expressed marker genes were either positively or negatively enriched ($p_{BH} < 0.05$).

Discussion

Here, we leveraged a rare natural experiment on a cross-section of animals sampled either before or after experiencing a major hurricane. Our findings suggest that differences in immune cell gene expression in individuals exposed to an extreme natural disaster were in many ways similar to the effects of the natural aging process. Further, we observed evidence for accelerated biological aging in samples collected after animals experienced Hurricane Maria. This adds yet another factor to the growing list of adverse experiences that can alter immune gene expression, disrupt protein homeostasis networks, and appear to accelerate markers of biological aging. Importantly, we identify a critical mechanism–immune cell gene regulation–that may explain how adversity, specifically in the context of natural disasters, may ultimately 'get under the skin' to drive age-associated disease onset and

progression. Indeed, the leukocyte transcriptome was, on average, 1.96 years older in animals that experienced Hurricane Maria compared to those that did not, corresponding to predicted biological age acceleration of approximately 7-8 human years. These alterations were also not short-lived: we detected the hurricane-associated differences in immune cell gene expression one year after the event. Together, our findings support the idea that the peripheral immune system is altered following an extreme adverse event and may help to explain how natural disasters increase morbidity and mortality rates.

The most salient result associated with aging and in animals that experienced Hurricane Maria were lower levels of expression of genes associated with the heat shock response and molecular chaperone activity. Canonically, the heat shock response (HSR) is activated in response to heat stress, UV radiation, infection, and other acute environmental stressors, yet we observed substantial downregulation in HSR genes despite the extensive loss of shade and temperature increase across Cayo Santiago. Activation of the heat shock response induces molecular chaperones to assist in protein folding and guide misfolded and aggregate proteins towards degradation pathways (51, 52). Components of the HSR involved in protein homeostasis, known as proteostasis networks, decrease throughout aging (51), which leads to greater incidence of the protein misfolding and aggregation implicated in many diseases (e.g., Huntington's disease, Alzheimer's Disease, and ALS). Our results indicate that aging and experiencing Hurricane Maria were both associated with lower levels of molecular chaperone gene expression. Thus, the hurricane-associated downregulation of the HSR may indicate dysregulation of proteostasis networks and contribute to observed disease susceptibility in survivors of extreme adversity.

Notably, several components of the heat shock response are also directly involved in the glucocorticoid response (53–55), which is activated in response to external stressors and well-documented to be disrupted by adverse experiences (56). Specifically, greater expression of *FKBP5* following Hurricane Maria may indicate increased FKBP51, which is implicated in aberrant stress responses and glucocorticoid resistance following adversity (53–58). These findings add to the increasing evidence that the aberrant GC responses frequently observed in human survivors of extreme adversity may be mechanistically driven by disruptions to *FKBP5* at the genomic or epigenomic level and extend to survivors of natural disasters (29, 59, 60).

Changes in gene expression at the bulk tissue level are also sensitive to changes in the relative cell proportions in the tissue. We leveraged this fact and found that adaptive immune-associated cell-marker genes (e.g., helper T cells) were more lowly expressed, while inflammatory innate immune cell-marker genes (e.g., classical

monocytes) were more highly expressed in samples from animals exposed to Hurricane Maria. Additionally, we observed a general pattern of greater expression of markers of pro-inflammatory cells in animals sampled after Hurricane Maria (Figure 4B). The fact that hurricane exposure broadly recapitulates age-associated changes in key immune cell marker genes adds to recent studies in humans finding 'aged' T cell composition (10). Chronic pro-inflammatory immune activity is characteristic of older populations, leading to the suggestion that upregulation of pro-inflammatory immune cells, and their associated activity (e.g., inflammatory cytokines), may be a mechanism by which severe adversities contribute to morbidity and premature mortality (3, 8, 10, 61).

Our study centered on understanding the effects of a major natural disaster, which included both the effects of the hurricane itself as well as its aftermath. It is difficult, and potentially not necessary, to disentangle the initial event from the aftermath because the devastating repercussions of severe natural disasters contribute to their extreme nature and are enduring sources of adversity. Due to the opportunistic nature of our study, the available samples from 2018 were from a single social group. It is therefore possible that the animals sampled after the hurricane differed from the pre-hurricane samples in ways that may confound our results. We thus carefully examined all potential confounds we could measure (body condition, wound presence, and sampling conditions), and found that the hurricane and aging effects persisted despite any influence from these covariates (see Methods section *Testing other sources of transcriptional variation).*

Our study relied on opportunistic sampling surrounding an extremely unpredictable event, which is accompanied by some limitations in our study design. The cross-sectional, rather than longitudinal, nature of our study means that we were unable to measure aging rates within the same individuals either before or after the hurricane. This design therefore limits our ability to disentangle aging effects from cohort effects. However, the age-associated results we identified recapitulate those found in studies of humans and other closely related species (35), suggesting that any cohort effects are likely small. Importantly, because age and hurricane exposure are not correlated in our study, we are able to disentangle their effects on immune gene expression as animals before and after the hurricane were drawn from similar age distributions–with the only difference being that animals sampled in 2018 experienced Hurricane Maria. Nevertheless, future work would benefit from longitudinal studies that can more accurately quantify within-individual changes in age and in the face of a natural disaster.

Notably, we did not find evidence that the observed immune disruption in animals that experienced Hurricane Maria varied by sex, contrary to expectations from human studies (62–64). However, it has been

suggested that heightened morbidity and mortality observed in human females after natural disasters may be due to socio-cultural constraints rather than biological differences (65, 66). Since we did not find that sex moderated immune responses to environmental devastation in rhesus macaques, our findings support the idea that sociocultural constraints placed on human females, rather than conserved biological differences, contribute to the observed health disparity human females face after natural disasters.

We observed heterogeneity in animals' gene expression after Hurricane Maria that was not explained by any variables we tested. Lack of social support both following adversity and throughout aging is associated with increased disease risk (67–69). Additionally, it is increasingly recognized that gene expression is highly responsive to social constraints and that social stress can drive broadly similar immune modifications to the stress response in humans and non-human primates (70–72). The effects of sociality can be highly context-specific but, broadly, socially stressed individuals would be expected to have an exacerbated response to extreme adversity. However, in this system, animals that were most socially isolated before the storm adjusted their social milieu the most after the storm (34), suggesting social flexibility might buffer these individuals from the effects of the hurricane yet obscure predictions about which individuals might be most socially stressed. Future studies should investigate the extent to which social factors, such as social dominance, integration, and flexibility, influence immune gene regulation and cell composition following natural disaster.

In conclusion, we find support for the hypothesis that environmental adversity and the natural aging process were associated with broadly similar disruptions in peripheral immune regulation. While the biological costs of adversity are becoming increasingly clear, our findings encourage efforts to develop a thorough understanding of the modifiers of aging and adversity, which may provide rapidly realized mitigation of detrimental immune system effects for populations that have experienced extreme adversity.

Materials and Methods

Study subjects and experimental design

Data were collected from rhesus macaques (*Macaca mulatta*) on the island of Cayo Santiago, a long-term field site where animals have been continuously monitored between 1938 and 2018. Animals are individually identified by tattoos and ear notches. Whole blood samples, body weight measurements, and identification of the presence of wounds were collected during the annual trap-and-release period. Trapping of animals on Cayo Santiago

occurs annually, approximately 1-3 months before the breeding season, between October to February, to minimize interference with the reproductive season. Specifically, before the annual trap-and-release period in years 2013, 2014, 2015, 2016, and 2018, age and sex-matched individuals were selected for biological sampling as part of other ongoing studies. When Hurricane Maria struck in 2017, we took advantage of the rare opportunity to sample part of the population in 2018 when conditions allowed. Thus, while different animals were sampled each year, they were broadly age and sex-matched across each year and across the hurricane (Fig. 1D). Additionally, because natural disasters are difficult to predict, to have pre- and post-hurricane samples, this project took advantage of samples collected for other ongoing projects.

Although Hurricane Maria was an extreme weather event, mortality in the population was relatively limited in the wake of the storm–only 2.75% of the population died in the immediate aftermath of the storm (Figure S5A). Notably, there was no differential survival based on sex or age in the year after the storm, as the average age of death within one year of Hurricane Maria did not differ from the average age of death in the 2 decades prior to the storm ($p = 0.13$). This supports recent findings of no overall increase in mortality has been found after the 3 previous major hurricanes to hit Cayo Santiago (Hurricanes Hugo in 1989, Georges in 1998, and Maria in 2017) (73).

Blood sampling

Whole blood was drawn from sedated rhesus macaques by veterinary staff. A 2.5 mL blood sample was collected in PAXgene® Blood RNA Tubes (PreAnalytiX GmbH) and stored at room temperature for 2-4 hours before being transferred to 4°C for 24 hours and finally to -80°C for long term storage until RNA extraction. Before Hurricane Maria, we collected 435 blood samples from 357 animals from December 2013–December 2016 (median age of 6.94 years; n females = 174, n males = 261), and sampled 108 animals after Hurricane Maria from October–December 2018 (median age = 6.05 years; n females = 57, n males = 51). Detailed metadata for each sample can be found in Dataset S1. As part of ongoing population management, a subset of the animals sampled in 2016 were captured on Cayo Santiago and transported to the Sabana Seca Field Station (n = 95) where the same procedure was performed. Due to the limited infrastructure on the island of Cayo Santiago and as part of the same population management, animals sampled in 2018 (n = 108) were also sampled at Sabana Seca.

RNA extraction, sequencing, and data preprocessing

RNA for 499 samples was extracted using the MagMAX for Stabilized Blood Tubes RNA Isolation Kits (ThermoFisher) and RNA from 48 samples was extracted using the PAXgene Blood RNA Kit IVD (Qiagen) following the standard protocols for each procedure. RNA quality (RQN) was quantified using AATI Fragment Analyzer. RNA sequencing libraries were prepared using 50ng of total RNA and following a recently developed 3'-biased protocol, TM3'Seq (74). Libraries were amplified with 16 PCR cycles. All other procedures followed the published protocol or manufacturer recommendations. Libraries were combined in equimolar quantities and sequenced on an Illumina NovaSeq S2 flowcell (R1 was 25bp and R2 was 80bp to capture the cDNA transcript) to an average read depth of 3.5 million reads per sample. We mapped cDNA reads to the *Macaca mulatta* reference assembly Mmul_10 using kallisto (75) (average mapping rate = 71.1%).

Read count normalization

Prior to normalization, we removed reads mapping to seven genes encoding hemoglobin and ribosomal RNA subunits which together comprised 54% of all mapped reads. We aggregated expression levels at the level of the gene, since 3'-seq cannot accurately assign reads to all alternative transcripts of a gene. We removed lowly expressed genes with fewer than 3.28 transcripts per million, the value that most evenly split the distributions of lowly expressed genes and highly expressed genes, resulting in 7,009 detectibly expressed genes for downstream analyses (https://github.com/mwatowich/Natural-disaster-accelerates-immune-aging). Read counts were normalized using the *voom* function from the limma package in the R environment (76) which normalizes counts overall to account for between-sample variation by estimating the mean-variance relationship of the log-counts among all samples.

Vegetation and temperature analyses

We measured how the vegetation on Cayo Santiago changed following Hurricane Maria by quantifying normalized difference vegetation index (NDVI) from Landsat 8 satellite images available on Sentinel-hub EO-Browser from approximately 2 years before and 2 years after Hurricane Maria. NDVI measures the density of greenness in a given area and is the most commonly used remote sensing measure of greenness (77). To elucidate how temperatures across the island had been altered by the extensive vegetation loss due to Hurricane Maria, we installed remote temperature sensors 0–2 meters from the ground in areas with (i) vegetation cover before and after

Hurricane Maria ("vegetated") and (ii) vegetation cover before Hurricane Maria that lost vegetation cover after the storm ("de-vegetated") (Figure 1C). Temperature sensors were installed after Hurricane Maria and were active from June–August 2018 and April 2019 to present. Detailed methods are described in Testard et al. (34)

Modeling the effects of age and Hurricane Maria on gene expression

We carried out statistical analyses in the R version 4.0.2 environment unless otherwise specified. To evaluate global trends in gene expression variation, we performed a principal component analysis on the correlation matrix of normalized gene expression values. We used R package EMMREML (78) to employ a mixed modeling approach to quantify the effects of age, sex, and exposure to Hurricane Maria on gene expression while controlling for effects of RNA quality (RQN), which was quantified during RNA library preparation, and relatedness between individuals. Kinship was estimated using ANGSD and ngsRelate (79) from mapped 3'seq bam files. Data from all 543 samples were included in these models. Genes that passed an FDR threshold of 10% were considered to be differentially expressed. q values were calculated using the R qvalue package (80).

Modeling interactions between sex and age and Hurricane Maria on gene expression

As prior research has identified sex differences in how the immune system ages (81) and how different sexes respond to adversity (62, 65, 82), we tested whether the sexes differed in their responses to aging and Hurricane Maria by modeling an interaction between sex and chronological age and, in a separate model, sex and hurricane exposure. Only three genes passed our FDR of 10% for an interaction between sex and age and no interaction effects of sex and hurricane exposure passed our FDR of 10%.

Temporal trends in age-related gene expression

To further investigate how gene expression changed with increased age, we used an autoregressive moving average (ARIMA) model adapted from Marquez et al. 2020 (81). This approach determines the best-fitting ARIMA model for each gene as a function of age and selects the models that exhibit gene expression trajectories that are significantly different from random fluctuations across age (41). We controlled for batch effects of RNA quality on gene expression by using a partial residual gene expression matrix calculated by subtracting the residuals of RNA quality (quantified by our linear modeling approach) from our normalized gene expression matrix. We limited our

analysis to adults (> 3 years, n = 505), as infant gene expression often strongly differed from adults, decreasing our ability to effectively group genes based on temporal trajectories occurring throughout the majority of animals' lifespan. Finally, we grouped gene trajectories by calculating a distance matrix of the correlation of predicted values across aging.

Enrichment analyses

To identify biological processes that were enriched in genes differentially expressed with chronological age and exposure to Hurricane Maria, we conducted Gene Ontology (GO) enrichment analysis using the R package *topGO* (83). We used the *weight01* algorithm to conduct Fisher's Exact Tests. To investigate GO enrichment in genes associated with age, we compared genes that significantly increased in expression across age (from the results of our linear model) to a background of all other genes. We then repeated this analysis for differentially expressed genes that had significantly lower expression in older individuals. We repeated these analyses for genes significantly up- and down-regulated in samples collected before and after Hurricane Maria. To characterize enrichment of biological functions in genes associated with both age and Hurricane Maria, we compared differentially expressed genes that had i) greater expression in older and hurricane-exposed individuals, ii) lower expression in older and hurricane-exposed individuals (Dataset S9), and iii) greater expression in older individuals but lower expression in hurricane-exposed individuals against a background of all other genes in the dataset. There were no genes that passed an FDR threshold of 10% that were more lowly expressed in older and more highly expressed in hurricane-exposed individuals, thus we did not perform an enrichment test on this subset of genes.

To characterize putative gene regulatory mechanisms, we tested for enrichment of transcription factor binding motifs within 2 kb upstream and downstream of transcription factor start sites of genes significantly associated with aging and Hurricane Maria using the program HOMER (84). We use all other genes in our dataset as the background set of genes for this test. We searched for known vertebrate transcription factor binding motifs and report all transcription factor motifs that passed an FDR threshold of 10%. We tested the same subsets of genes differentially expressed with aging, Hurricane Maria, and shared effects as our GO enrichment analyses.

Transcriptomic clock

To test whether samples collected after Hurricane Maria were predicted to have accelerated biological ages, we predicted ages of the animals in our dataset from their normalized gene expression profiles using human transcriptomic age predictors (50). This approach predicts transcriptomic age via weighted scores for each gene multiplied by scaled normalized gene expression data. To calculate this metric, we used genes that overlapped between the Peters dataset and our dataset (matched using Ensembl homolog annotations from biomaRt (85, 86). Peters et al. performed a meta-analysis using a discovery and replication dataset to produce more strongly supported markers. The number of overlapping genes between our dataset and the meta-analysis was limited and we therefore used markers from their discovery dataset that overlapped with genes in our dataset that were highly associated with aging (FDR < 1%) for a total of 321 genes.

Using the transcriptomic age predictor and equation provided by Peters et al. (50), we predicted the chronological ages of animals in our dataset from their gene expression data. We estimated the predictor (Z) using equation 1 (below) on our normalized gene expression matrix.

$$Z = \sum_{i} x_{v(i)} \hat{b}_{R(i)}$$

Predictions of biological age did not control for sex, as we did not detect sex effects on gene expression. After predicting chronological age from normalized gene expression, we scaled the predictions to the age distribution in our sample population using equation 2 (below).

$$SZ = \mu_{age} + (Z - \mu_Z) \times \frac{\sigma_{age}}{\sigma_Z}$$

There was a significant correlation between scaled predictions and chronological age among the pre-hurricane samples (r = 0.42, p= 7.12 x 10^{-19}). To determine the extent to which experiencing Hurricane Maria moderated predicted age, we modeled the scaled predictions as a function of chronological age and exposure to Hurricane Maria. We first predicted transcriptomic ages of sexually mature adults (> 1 years) for similar reasons as in our ARIMA modeling approach and found that biological age was 1.96 years older on average in samples after Hurricane Maria (p = 0.0003). This effect was slightly weaker but still significant when we predicted biological age with all genes in our dataset that were associated with age at an FDR of < 10% (n = 838; β = 1.64, p = 0.003). To test whether results held when we included infants, we performed the analysis again including samples from all animals (< 1 years) and found that biological age was an average of 1.1 years older in samples from after Hurricane Maria (p = 0.03).

Testing other sources of transcriptional variation

We tested whether body condition, presence of wounds, or sampling condition moderated the differential gene expression we observed in samples after Hurricane Maria, as we hypothesized that each may be a potential confound in our analysis. These effects were modeled using the previously described linear model (gene expression as a function of age, exposure to Hurricane Maria, sex, RQN, and estimated kinship) and including the additional covariate. None of these variables significantly altered the effects of the hurricane on gene expression.

We hypothesized that animals after the hurricane might have poorer body condition due to vegetation loss and adversity related to social changes following the hurricane, however we found no difference in body condition in individuals sampled before or after the hurricane (Wilcoxon rank sum test: $p = 0.09$; Figure S5B). Body condition was calculated using a loess regression of body weight controlling for age, sex, and location where weight was recorded (i.e., sampling locations with different scales). At the gene-level, only 2 genes passed an FDR threshold of 10% with body condition.

We expected that the immune-related differences in gene expression we observed following Hurricane Maria may have been driven by wounds which might be more prevalent following the hurricane or might have healed more slowly if animals had other, undetected infections. We tested whether the absence or presence of a wound (e.g., open cuts, broken fingers, etc.) affected gene expression and found that no genes passed a liberal false discovery rate of 20% (n animals with wound data = 203).

A subset of animals in our study were trapped on Cayo Santiago and transported to an inland facility where the biological sampling took place, this included 95 animals in 2016 that were part of an ongoing population management and all animals in 2018 because research infrastructure on Cayo Santiago was still destroyed at the time. Because of this potential confound with the hurricane, we tested whether effects of the hurricane were similar in the entire sample (n = 543) and in only off-island sampled animals from 2016 and 2018 (n = 203) using the same modeling framework controlling for age, sex, RNA quality, and kinship. The effect of the hurricane on gene expression was highly correlated between the smaller sample (off-island blood drawn, n = 203) and the main model (n = 543) among all genes (Pearson's $r = 0.54$, $p < 1 \times 10^{-16}$) and those that passed an FDR of 15% for both models ($n = 45$, $r = 0.75$, $p = 3.71 \times 10^{-9}$). Further, hurricane and age-associated effects on gene expression were also still

correlated in the same direction in the models with the reduced sample size ($r = 0.17$, $p = 7.4 \times 10^{-49}$) among all genes and those that passed an FDR of 15% for both effects ($n = 57$, $r = 0.59$, $p = 1.52 \times 10^{-6}$).

Characterizing gene-gene relationships

To characterize whether relationships between gene pairs were altered by Hurricane Maria, we quantified correlations between pairs of genes differentially expressed with Hurricane Maria using 'correlation by individual level product' (87). We used gene expression values that controlled for residuals of RNA quality, sex, and aging. To test whether a given pair of genes was differentially correlated in samples before Hurricane Maria versus samples from after the hurricane, we first scaled gene expression residuals within each group (pre-hurricane, post-hurricane)(87). Next, we multiplied normalized gene expression values for each gene in the pair and used the EMMREML package to fit this vector of products as a function of exposure to Hurricane Maria, while controlling for kinship. To test whether genes that were in differentially correlated pairs across Hurricane Maria were more likely to be involved in the heat shock response than by chance, we tested for enrichment using a binomial test with a background rate of all genes with a Gene Ontology term name involving "heat shock", genes encoding for HSP subunits, and genes encoding for DNAJ subunits (17 of 230 hurricane-associated genes).

Marker gene enrichment tests

We characterized whether and how immune cell marker genes were associated with aging and Hurricane Maria exposure. We identified immune cell-specific marker genes from single-cell sequencing data of rhesus macaque peripheral blood mononuclear cells (PBMCs). Single-cell RNA sequencing data were generated from two adult female rhesus macaques from the large breeding colonies at Yerkes National Primate Research Center. For each individual, PBMCs were isolated with density gradient centrifugation and cells were captured on a 10X Genomics Chromium controller. Sequencing libraries were prepared using Chromium Single-Cell 3' v2 chemistry according to the manufacturer's specifications. Libraries were sequenced on an S2 flow cell on an Illumina NovaSeq 6000. Resulting reads were mapped to the MacaM v7 reference genome (88) (including mitochondrial and intronic sequences) with –count function in CellRanger v.3.0.2 (89). Individuals were demultiplexed based on standing genetic variation and doublets were removed with demuxlet (90) using the following parameters: --tag-group CB --tag-UMI UB --field GT --geno-error 0.05 --doublet-prior 0.076 --min-uniq 30 --min-snp 5. Count matrices were

filtered to include only cells with at least 200 genes expressed and only genes expressed in at least 3 cells with Seurat v3 (91). The resulting count matrices included ~14k genes and ~2.3k cells per individual. Marker genes were identified using the Seurat (91) and monocle3 (92–95) packages in the R environment. One hundred and forty-nine genes passed a specificity threshold of 0.1 and sensitivity threshold of 0.1 (Dataset S11).

As our bulk RNA sequencing data were generated from peripheral whole blood, which likely contains pertinent immune cells types beyond those in PBMCs, we also characterized granulocyte marker genes published in Palmer et al. 2006 (96), which identified canonical granulocyte marker genes from human peripheral blood samples. We expect that the majority of granulocyte marker genes in our dataset are specific to neutrophils, since they comprise the vast majority of granulocytes in primates. We used a subsampling approach to test whether marker genes for each cell type changed significantly with increased aging or hurricane exposure. Specifically, we constructed a null distribution of median standardized effect sizes by resampling all standardized effect sizes and considered marker genes significantly perturbed if the marker genes' median standardized beta fell outside of Bonferroni corrected confidence intervals of 0.18% and 99.82%.

References

1. J. A. Sumner, *et al.*, Trauma Exposure and Posttraumatic Stress Disorder Symptoms Predict Onset of Cardiovascular Events in Women. **132**, 251–259 (2016).
2. I. C. Passos, *et al.*, Inflammatory markers in post-traumatic stress disorder: A systematic review, meta-analysis, and meta-regression. *The Lancet Psychiatry* **2**, 1002–1012 (2015).
3. R. von Känel, *et al.*, Evidence for low-grade systemic proinflammatory activity in patients with posttraumatic stress disorder. *J. Psychiatr. Res.* **41**, 744–752 (2007).
4. J. A. Sumner, *et al.*, Cross-Sectional and Longitudinal Associations of Chronic Posttraumatic Stress Disorder With Inflammatory and Endothelial Function Markers in Women. *Biol. Psychiatry* **82**, 875–884 (2017).
5. H. Gola, *et al.*, Posttraumatic stress disorder is associated with an enhanced spontaneous production of pro-inflammatory cytokines by peripheral blood mononuclear cells. *BMC Psychiatry* **13** (2013).
6. K. Kario, B. S. McEwen, T. G. Pickering, Disasters and the heart: A review of the effects of earthquake-induced stress on cardiovascular disease. *Hypertens. Res.* **26**, 355–367 (2003).
7. M. S. Breen, *et al.*, Differential transcriptional response following glucocorticoid activation in cultured blood immune cells: a novel approach to PTSD biomarker development. *Transl. Psychiatry* **9** (2019).
8. M. S. Breen, *et al.*, Gene networks specific for innate immunity define post-traumatic stress disorder. *Mol. Psychiatry* **20**, 1538–1545 (2015).
9. A. O'Donovan, *et al.*, Transcriptional control of monocyte gene expression in post-traumatic stress disorder. *Dis. Markers* **30**, 123–132 (2011).
10. A. E. Aiello, *et al.*, PTSD is associated with an increase in aged T cell phenotypes in adults living in Detroit. *Psychoneuroendocrinology* **67**, 133–141 (2016).
11. R. Yang, *et al.*, A DNA methylation clock associated with age-related illnesses and mortality is accelerated in men with combat PTSD. *Mol. Psychiatry* (2020) https:/doi.org/10.1038/s41380-020-0755-z.
12. E. J. Wolf, *et al.*, Traumatic stress and accelerated DNA methylation age: A meta-analysis. *Psychoneuroendocrinology* **92**, 123–134 (2018).
13. C. López-Otín, M. A. Blasco, L. Partridge, M. Serrano, G. Kroemer, The Hallmarks of Aging. *Cell* **153**, 1194–1217 (2013).

14. E. Pihl, T. Jürimäe, Relationships between body weight change and cardiovascular disease risk factors in male former athletes. *Int. J. Obes.* **25**, 1057–1062 (2001).
15. C. Ikejima, *et al.*, Prevalence and causes of early-onset dementia in japan: A population-based study. *Stroke* **40**, 2709–2714 (2009).
16. J. C. Eisenmann, G. J. Welk, M. Ihmels, J. Dollman, Fatness, fitness, and cardiovascular disease risk factors in children and adolescents. *Med. Sci. Sports Exerc.* **39**, 1251–1256 (2007).
17. G. Hannum, *et al.*, Genome-wide Methylation Profiles Reveal Quantitative Views of Human Aging Rates. *Mol. Cell* **49**, 359–367 (2013).
18. S. Horvath, DNA methylation age of human tissues and cell types. *Genome Biol.* **14** (2013).
19. J. A. Mattison, *et al.*, Caloric restriction improves health and survival of rhesus monkeys. *Nat. Commun.* **8**, 1–12 (2017).
20. A. Sziráki, A. Tyshkovskiy, V. N. Gladyshev, Global remodeling of the mouse DNA methylome during aging and in response to calorie restriction. *Aging Cell* **17** (2018).
21. R. Peto, *et al.*, Smoking, smoking cessation, and lung cancer in the UK since 1950: Combination of national statistics with two case-control studies. *Br. Med. J.* **321**, 323–329 (2000).
22. R. R. Wing, *et al.*, Benefits of modest weight loss in improving cardiovascular risk factors in overweight and obese individuals with type 2 diabetes. *Diabetes Care* **34**, 1481–1486 (2011).
23. N. Snyder-Mackler, M. Somel, J. Tung, Shared signatures of social stress and aging in peripheral blood mononuclear cell gene expression profiles. *Aging Cell* **13**, 954–957 (2014).
24. J. B. Lohr, *et al.*, Is Post-Traumatic Stress Disorder Associated with Premature Senescence? A Review of the Literature. *Am J Geriatr Psychiatry* **23**, 709–725 (2015).
25. P. F. Kuan, *et al.*, Cell type-specific gene expression patterns associated with posttraumatic stress disorder in World Trade Center responders. *Transl. Psychiatry* **9**, 1–11 (2019).
26. M. Jergović, *et al.*, Patients with posttraumatic stress disorder exhibit an altered phenotype of regulatory T cells. *Allergy, Asthma Clin. Immunol.* **10**, 43 (2014).
27. C. Black, *et al.*, Early life wildfire smoke exposure is associated with immune dysregulation and lung function decrements in adolescence. *Am. J. Respir. Cell Mol. Biol.* **56**, 657–666 (2017).
28. A. Minelli, C. Magri, E. Giacopuzzi, M. Gennarelli, The effect of childhood trauma on blood transcriptome expression in major depressive disorder. *J. Psychiatr. Res.* **104**, 50–54 (2018).
29. P. O. McGowan, *et al.*, Epigenetic regulation of the glucocorticoid receptor in human brain associates with childhood abuse. *Nat. Neurosci.* **12**, 342–348 (2009).
30. D. Mehta, *et al.*, Childhood maltreatment is associated with distinct genomic and epigenetic profiles in posttraumatic stress disorder. *Proc. Natl. Acad. Sci. U. S. A.* **110**, 8302–8307 (2013).
31. M. Uddin, *et al.*, Epigenetic and immune function profiles associated with posttraumatic stress disorder. *Proc. Natl. Acad. Sci. U. S. A.* **107**, 9470–9475 (2010).
32. L. Cao-Lei, *et al.*, DNA methylation signatures triggered by prenatal maternal stress exposure to a natural disaster: Project ice storm. *PLoS One* **9** (2014).
33. M. J. Girgenti, R. S. Duman, Transcriptome Alterations in Posttraumatic Stress Disorder. *Biol. Psychiatry* **83**, 840–848 (2018).
34. C. Testard, *et al.*, Rhesus macaques build new social connections after a natural disaster. *Curr. Biol.*, 1–11 (2021).
35. K. L. Chiou, *et al.*, Rhesus macaques as a tractable physiological model of human ageing. *Phil. Trans. R. Soc. B* **375** (2020).
36. S. D. Hursting, J. A. Lavigne, D. Berrigan, S. N. Perkins, J. C. Barrett, Calorie Restriction, Aging, and Cancer Prevention: Mechanisms of Action and Applicability to Humans. *Annu. Rev. Med.* **54**, 131–152 (2003).
37. L. K. Heilbronn, E. Ravussin, Calorie restriction and aging: Review of the literature and implications for studies in humans. *Am. J. Clin. Nutr.* **78**, 361–369 (2003).
38. E. W. Tobi, *et al.*, DNA methylation signatures link prenatal famine exposure to growth and metabolism. *Nat. Commun.* **5** (2014).
39. C. Giuliani, I. Bucci, G. Napolitano, The role of the transcription factor Nuclear Factor-kappa B in thyroid autoimmunity and cancer. *Front. Endocrinol. (Lausanne).* **9**, 1–8 (2018).
40. I. Cobo, *et al.*, Transcriptional regulation by NR5A2 links differentiation and inflammation in the pancreas. *Nature* **554**, 533–537 (2018).
41. P. J. Brockwell, R. A. Davis, *Introduction to Time Series and Forecasting*, 2nd Ed. (Springer-Verlag, 2002).
42. C. López-Otín, G. Kroemer, Hallmarks of Health. *Cell* **184**, 33–63 (2021).

43. M. J. Ranek, M. J. Stachowski, J. A. Kirk, M. S. Willis, The role of heat shock proteins and co-chaperones in heart failure. *Philos. Trans. R. Soc. B Biol. Sci.* **373** (2018).
44. R. L. Jan, *et al.*, Extracellular heat shock protein HSC70 protects against lipopolysaccharide-induced hypertrophic responses in rat cardiomyocytes. *Biomed. Pharmacother.* **128**, 110370 (2020).
45. P. N. Silva, *et al.*, Analysis of HSPA8 and HSPA9 mRNA expression and promoter methylation in the brain and blood of Alzheimer's disease patients. *J. Alzheimer's Dis.* **38**, 165–170 (2014).
46. J. Dou, *et al.*, Targeting Hsc70-based autophagy to eliminate amyloid β oligomers. *Biochem. Biophys. Res. Commun.* **524**, 923–928 (2020).
47. J. Anckar, L. Sistonen, Regulation of HSF1 function in the heat stress response: Implications in aging and disease. *Annu. Rev. Biochem.* **80**, 1089–1115 (2011).
48. J. Li, J. Labbadia, R. I. Morimoto, Rethinking HSF1 in Stress, Development, and Organismal Health. *Trends Cell Biol.* **27**, 895–905 (2017).
49. G. Kim, *et al.*, The heat shock transcription factor Hsf1 is downregulated in DNA damage-associated senescence, contributing to the maintenance of senescence phenotype. *Aging Cell* **11**, 617–627 (2012).
50. M. J. Peters, *et al.*, The transcriptional landscape of age in human peripheral blood. *Nat. Commun.* **6** (2015).
51. L. J, M. R.I., The Biology of Proteostasis in Aging and Disease. *Annu Rev Biochem* **84**, 435–464 (2015).
52. R. I. Morimoto, Cell-nonautonomous regulation of proteostasis in aging and disease. *Cold Spring Harb. Perspect. Biol.* **12**, 1–20 (2020).
53. M. Criado-Marrero, *et al.*, Hsp90 and FKBP51: Complex regulators of psychiatric diseases. *Philos. Trans. R. Soc. B Biol. Sci.* **373** (2018).
54. A. S. Zannas, T. Wiechmann, N. C. Gassen, E. B. Binder, Gene-Stress-Epigenetic Regulation of FKBP5: Clinical and Translational Implications. *Neuropsychopharmacology* **41**, 261–274 (2016).
55. M. Bekhbat, S. A. Rowson, G. N. Neigh, Checks and balances: The glucocorticoid receptor and NFκB in good times and bad. *Front. Neuroendocrinol.* **46**, 15–31 (2017).
56. D. B. O'Connor, J. F. Thayer, K. Vedhara, Stress and Health: A Review of Psychobiological Processes. *Annu. Rev. Psychol.* **72**, 663–688 (2021).
57. G. E. Miller, *et al.*, A Functional Genomic Fingerprint of Chronic Stress in Humans: Blunted Glucocorticoid and Increased NF-κB Signaling. *Biol Psychiatry* **64**, 266–272 (2008).
58. S. Cohen, *et al.*, Chronic stress, glucocorticoid receptor resistance, inflammation, and disease risk. *Proc. Natl. Acad. Sci. U. S. A.* **109**, 5995–5999 (2012).
59. G. Turecki, M. Meaney, Effects of the social environment and stress on glucocorticoid receptor gene methylation: a systematic review. *Biol Psychiatry* **79**, 87–96 (2016).
60. V. T. Cunliffe, The epigenetic impacts of social stress: How does social adversity become biologically embedded? *Epigenomics* **8**, 1653–1669 (2016).
61. A. Sommershof, *et al.*, Substantial reduction of naïve and regulatory T cells following traumatic stress. *Brain. Behav. Immun.* **23**, 1117–1124 (2009).
62. G. M. H. Marres, L. P. H. Leenen, J. De Vries, P. G. H. Mulder, E. Vermetten, Disaster-related injury and predictors of health complaints after exposure to a natural disaster: An online survey. *BMJ Open* **1** (2011).
63. F. H. Norris, *et al.*, 60,000 disaster victims speak : Part I . an empirical review of the empirical literature, 1981-2001. *Psychiatry* **65**, 207–239 (2002).
64. M. Uddin, L. Sipahi, J. Li, K. C. Koenen, Sex differences in DNA methylation may contribute to risk of PTSD and depression: A review of existing evidence. *Depress Anxiety.* **3**, 1151–1160 (2013).
65. E. Neumayer, T. Plümper, The gendered nature of natural disasters: The impact of catastrophic events on the gender gap in life Expectancy, 1981-2002. *Ann. Assoc. Am. Geogr.* **97**, 551–566 (2007).
66. P. T.T, S. R. Sundari, Sex differentials in the risk factors of post traumatic stress disorder among tsunami survivors in Tamil Nadu, India. *Asian J. Psychiatr.* **23**, 46–50 (2016).
67. J. Cook, V. Simiola, Trauma and aging. *Curr. Psychiatry Rep.* **20** (2018).
68. J. Holt-Lunstad, T. B. Smith, J. B. Layton, Social relationships and mortality risk: a meta-analytic review. *PLoS Med.* **7**, e1000316 (2010).
69. J. Holt-Lunstad, T. B. Smith, M. Baker, T. Harris, D. Stephenson, Loneliness and Social Isolation as Risk Factors for Mortality: A Meta-Analytic Review. *Perspect. Psychol. Sci.* **10**, 227–237 (2015).
70. N. Snyder-Mackler, *et al.*, Social status alters immune regulation and response. *Science (80-.).* **354**, 1041–1046 (2016).
71. G. E. Miller, *et al.*, Greater inflammatory activity and blunted glucocorticoid signaling in monocytes of chronically stressed caregivers. **41**, 191–199 (2014).
72. S. W. Cole, *et al.*, Social regulation of gene expression in human leukocytes. *Genome Biol.* **8** (2007).

73. D. O. Morcillo, U. K. Steiner, K. L. Grayson, A. V. Ruiz-Lambides, R. Hernández-Pacheco, Hurricane-induced demographic changes in a non-human primate population: Demographic effects of hurricanes. *R. Soc. Open Sci.* **7** (2020).
74. L. F. Pallares, S. Picard, J. F. Ayroles, Tm3'Seq: A tagmentation-mediated 3' sequencing approach for improving scalability of RNAseq experiments. *G3 Genes, Genomes, Genet.* **10**, 143–150 (2020).
75. N. L. Bray, H. Pimentel, P. Melsted, L. Pachter, Near-optimal probabilistic RNA-seq quantification. *Nat. Biotechnol.* **34**, 525–527 (2016).
76. M. E. Ritchie, *et al.*, limma powers differential expression analyses for RNA-sequencing and microarray studies. *Nucleic Acids Res.* **43**, e47 (2015).
77. N. P. Robinson, *et al.*, A Dynamic Landsat Derived Normalized Difference Vegetation Index (NDVI) Product for the Conterminous United States. *Remote Sens.* **9** (2017).
78. D. Akdemir, U. G. Okeke, EMMREML: Fitting mixed models with known covariance structures. *https://cran.r-project.org/package=EMMREML.*, R package version 3.1 (2015).
79. T. S. Korneliussen, A. Albrechtsen, R. Nielsen, ANGSD: Analysis of Next Generation Sequencing Data. *BMC Bioinformatics* **15**, 1–13 (2014).
80. J. Storey, A. Bass, A. Dabney, D. Robinson, qvalue: Q-value estimation for false discovery rate control (2020).
81. E. J. Márquez, *et al.*, Sexual-dimorphism in human immune system aging. *Nat. Commun.* **11** (2020).
82. E. W. Tobi, *et al.*, DNA methylation differences after exposure to prenatal famine are common and timing- and sex-specific. *Hum. Mol. Genet.* **18**, 4046–4053 (2009).
83. A. Alexa, J. Rahnenfuhrer, topGO: Enrichment Analysis for Gene Ontology (2020).
84. H. S, B. C, S. N, B. E, E. Al., Simple Combinations of Lineage-Determining Transcription Factors Prime cis-Regulatory Elements Required for Macrophage and B Cell Identities. *Mol Cell* **38**, 576–589 (2010).
85. S. Durinck, P. Spellman, B. E, W. Huber, Mapping identifiers for the integration of genomic datasets with the R/Bioconductor package biomaRt. *Nat. Protoc.* **4**, 1184–1191 (2009).
86. S. Durinck, *et al.*, BioMart and Bioconductor: a powerful link between biological databases and microarray data analysis. *Bioinformatics* **21**, 3439–3440 (2005).
87. A. Lea, *et al.*, Genetic and environmental perturbations lead to regulatory decoherence. *Elife* **8** (2019).
88. A. V. Zimin, *et al.*, A new rhesus macaque assembly and annotation for next-generation sequencing analyses. *Biol. Direct* **91** (2014).
89. G. X. Zheng, *et al.*, Massively parallel digital transcriptional profiling of single cells. *Nat. Commun.* **8**, 1–12 (2017).
90. H. M. Kang, *et al.*, Multiplexed droplet single-cell RNA-sequencing using natural genetic variation. *Nat. Biotechnol.* **36**, 89 (2018).
91. T. Stuart, *et al.*, Comprehensive integration of single-cell data. *Cell* **177**, 1888–1902 (2019).
92. C. Trapnell, *et al.*, The dynamics and regulators of cell fate decisions are revealed by pseudotemporal ordering of single cells. *Nat. Biotechnol.* **32**, 381–386 (2014).
93. X. Qiu, *et al.*, Reversed graph embedding resolves complex single-cell trajectories. *Nat. Methods* **14**, 979–982 (2017).
94. J. Cao, *et al.*, The single-cell transcriptional landscape of mammalian organogenesis. *Nature* **566**, 496–502 (2019).
95. L. McInnes, J. Healy, J. Melville, UMAP: Uniform manifold approximation and projection for dimension reduction. *arXiv* (2018).
96. C. Palmer, M. Diehn, A. A. Alizadeh, P. O. Brown, Cell-type specific gene expression profiles of leukocytes in human peripheral blood. *BMC Genomics* **7**, 1–15 (2006).

Chapter 3

Environmental adversity and aging are associated with immune gene regulation in a nonhuman primate

Marina M. Watowich[1,2,3], Elisabeth A. Goldman[6], Kenny L. Chiou[2,3], Christina Costa[7], Michael J. Montague[9], Rachel Petersen[12], Sam Patterson[7], Cayo Biobank Research Unit, Julie E. Horvath[14,15,16,17], Kirstin Sterner[6], Melween I. Martinez[18], Michael L. Platt[9,10,11], Lauren J.N. Brent[19], James P. Higham[7,8], Amanda J. Lea*[12,13], and Noah Snyder-Mackler*[2,3,4,5]

[1]Department of Biology, University of Washington; Seattle, WA, 98195 USA
[2]Center for Evolution and Medicine, Arizona State University; Tempe, AZ, 85281 USA
[3]School of Life Sciences, Arizona State University; Tempe, AZ, 85281 USA
[4]School of Human Evolution and Social Change, Arizona State University; Tempe, AZ, 85281 USA
[5]Neurodegenerative Disease Research Center, Arizona State University; Tempe, AZ, 85281 USA
[6]Department of Anthropology, University of Oregon, Eugene, OR, USA
[7]Department of Anthropology, New York University; New York, NY 10003, USA
[8]New York Consortium in Evolutionary Primatology; New York, NY, 10016 USA
[9]Department of Neuroscience, Perelman School of Medicine; University of Pennsylvania, Philadelphia, PA 19104, USA
[10]Department of Psychology, School of Arts and Sciences; University of Pennsylvania, Philadelphia, PA 19104, USA
[11]Marketing Department, Wharton School of Business; University of Pennsylvania, Philadelphia, PA 19104, USA
[12]Department of Biological Sciences, Vanderbilt University, Nashville, Tennessee, 37235, USA
[13]Child and Brain Development, Canadian Institute for Advanced Research, Toronto, Canada
[14]Department of Biological and Biomedical Sciences, North Carolina Central University; Durham, NC 27707, USA
[15]Research and Collections Section, North Carolina Museum of Natural Sciences; Raleigh, NC 27601, USA
[16]Department of Biological Sciences, North Carolina State University; Raleigh, NC 27695, USA
[17]Department of Evolutionary Anthropology, Duke University; Durham, NC 27708, USA
[18]Caribbean Primate Research Center, Unit of Comparative Medicine, University of Puerto Rico; San Juan, PR 00936, USA
[19]Centre for Research in Animal Behaviour, University of Exeter; Exeter EX4 4QG, UK

*Denotes joint last-authorship

Abstract

Aging is the greatest predictor of mortality and top risk factor for most non-communicable diseases. During aging, the immune system becomes increasingly dysregulated, which promotes disease development and progression. A similar process has been shown to occur in response to external challenges (e.g., social adversity, ecological challenges), yet it remains unclear whether environmental insults advance aging phenotypes via the same molecular pathways as primary immunological aging. To probe this question, we quantified peripheral immune cell genome-wide CpG methylation from a cross-sectional sample of free-ranging rhesus macaques living off the coast of Puerto Rico (n=571) that experience a variety of social

adversities in early life (e.g., maternal loss) and endured a major hurricane during our study. We found 78661 significant age-associated sites in total (31% of all sites tested). Age-associated hypermethylation occurred more frequently in areas of active gene regulation, while hypomethylation was enriched in putatively non-regulatory regions. Age-associated hypomethylation co-occurred with increased chromatin accessibility while hypermethylation showed the opposite trend, hinting at a coordinated, multi-level loss of epigenetic stability during aging. We detected 32048 CpG sites significantly associated with exposure to a severe hurricane, and these sites overlapped age-associated sites, most strongly in regulatory regions and most weakly in quiescent regions. Further, we found that 1) aging was associated with a hypomethylation of transposable elements (TEs) while environmental adversity was associated with increased TE methylation, 2) hypomethylation of quiescent regions with age was enriched for genes in several inflammation-related pathways, and 3) age-associated differential methylation had a stronger relationship with downstream gene expression than the effects of hurricane exposure. Together, our results suggest that environmental insults may contribute to aging-related molecular phenotypes in regions of active gene transcription, but that primary aging has specific signatures in non-regulatory regions.

Introduction

Aging is the greatest risk factor for disease and death, largely because of age-associated declines in physiological functioning and increased immune dysregulation throughout the lifespan (i.e., "immunosenescence"). Decreased functional capacity throughout the body and immunosenescence are the result of accumulated damage and the inability to comprehensively repair sustained damage (Gladyshev et al., 2021; López-Otín et al., 2013; Seale et al., 2022). Age-dependent damage occurs via "primary" and "secondary" aging. Primary aging is the inevitable accumulation of damage over time, while secondary aging is stochastic damage that can be exacerbated by environmental perturbation and disease (Holloszy, 2000; Seale et al., 2022). However, the extent to which these two types of aging are truly distinct and act along different pathways remains unclear (Seale et al., 2022).

Age-related deterioration occurs via a common set of molecular "hallmarks"–molecular phenotypes that generate damage, are part of the damage-control response, or emerge when damage accumulation surpasses repair (López-Otín et al., 2013). Epigenomic changes comprise one hallmark of aging that is often expected to be damage-generating but can also be part of the damage-repair response (Seale et al., 2022; Sriraman et al., 2020). For example, the progressive loss of cell- and tissue-specific epigenetic marks is expected to drive age-related loss of tissue and cellular specificity and function (Dmitrijeva et al., 2018; Thompson et al., 2010). Additionally, epigenetic marks, such as DNA methylation, can suppress deleterious genomic elements that contribute to molecular damage and immune dysregulation (i.e., transposable elements; TEs). As methylation patterns deviate from a healthy (i.e., typically young) state, deleterious elements are expected to become more active and generate or exacerbate existing damage. Specifically, TEs can cause double-stranded DNA breaks, promote genomic instability, and trigger the inflammatory response (Andrenacci et al., 2020; Chénais, 2022; De Cecco et al., 2019; Gorbunova et al., 2021), yet this can be alleviated by interventions that induce repressive epigenetic modifications and ultimately extend lifespan (Andrenacci et al., 2020; Gorbunova et al., 2021; Wood et al., 2016).

In addition to being involved in the aging process, DNA methylation is responsive to environmental stimuli and is therefore thought to be a key link between the environment, genome, and phenotype. For example, people exposed to a severe famine during early gestation had higher body mass index in mid- and late-life, as well as methylation profiles at several metabolic genes that were distinct from siblings who did not experience the famine *in utero*, suggesting that changes in DNA methylation patterns may be linked to downstream phenotypic outcomes (Tobi et al., 2014). Further, severe environmental adversities such as childhood abuse have been linked to an acceleration of molecular aging phenotypes at the level of the methylome, but many studies to date have focused on single epigenomic biomarkers, like composite epigenetic clocks, to examine differences between biological and chronological age, or examined methylation of candidate genes in pertinent pathways (i.e., glucocorticoid/stress response pathway) (Seale et al., 2022; Unternaehrer et al., 2012; Zannas et al., 2015). However, it remains largely unexplored how primary and secondary aging manifest at the level of individual loci throughout the genome, a level which can reveal gene regulatory pathways linked to primary

versus secondary aging (Seale 2022). For example, it remains unclear the extent to which environmental perturbations (i.e., secondary aging) induce similar effects on the aging methylome as primary aging, including the specificity of their genomic targets (i.e., location) and their potential to generate deleterious consequences. In short, is secondary aging a unique type of aging or solely an exacerbation of primary aging?

Here, we tested the extent to which primary and secondary aging act along distinct pathways and processes by probing the similarities between age-related and environmentally-induced changes in methylation. We did so using a long-term, free-ranging rhesus macaque study population (the macaques of Cayo Santiago), in which individuals are tracked longitudinally and experience naturally occurring environmental adversities during their lifetime. More specifically, we investigated primary and secondary aging on DNA methylation by assessing the impact of two adversities known to be associated with morbidities and mortality in primates and to have biological impacts on Cayo animals in particular: exposure to Hurricane Maria and experiencing maternal loss in the first four years of life (Tung et al., 2016; Watowich et al., 2022).

We leveraged peripheral blood samples and detailed demographic and behavioral data from a cross-sectional sample of Cayo Santiago rhesus macaques (n = 571) to address 3 goals. First, we described how DNA methylation levels vary across the lifespan to characterize the effects of primary aging on the methylome. Second, we tested for epigenetic signatures of several environmental insults and quantified the extent to which these signatures were distinct from or similar to signatures of aging. Third, we used transcriptomic data to probe the relationship between DNA methylation and gene expression. By characterizing how socioenvironmental adversities affect DNA methylation, and the extent to which they overlap or are distinct from aging-specific methylation changes, we can quantify how secondary aging may be distinct from or exacerbate primary aging phenotypes.

Results

Primary and secondary aging are associated with global immune cell hypomethylation

We first identified changes in DNA methylation associated with age, exposure to a severe hurricane, and maternal loss in a cross-sectional sample of animals spanning their natural lifespan (0.1-29 years). Our dataset contained 571 samples from 499 unique individuals (277 females, 222 males) sampled between 2011-2018 (Fig. 1A; Table S1). Of our 571 samples, 101 were from animals exposed to Hurricane Maria and 108 were from animals that had experienced the loss of a mother in the first four years of life. For 67 unique individuals we had repeated, longitudinal samples across 2 or more years (139 samples, 2-3 samples per individual). We used reduced representation bisulfite sequencing (RRBS) to characterize peripheral immune cell DNA methylation levels at 8.3 million sites across the rhesus macaque genome. After removing CpG sites that were invariably methylated, represented in fewer than 100 samples, and with <5 or >500x coverage, we retained 253,076 CpG sites across the genome for further analysis (information about retained sites is in Fig. 1B-C).

To identify CpG sites associated with chronological age, we took a binomial mixed-effects approach. We modeled DNA methylation levels at each CpG site as a function of chronological age, sex, and exposure to Hurricane Maria, while controlling for relatedness between individuals and technical effects. As expected, chronological age was associated with many differences in DNA methylation levels across the genome – 31% of tested CpG sites were significantly associated with age (n = 78661; FDR < 5%; Table S2). Consistent with prior studies in humans and other mammals, we identified ~4x as many sites that were less methylated (i.e., "hypomethylated") in older animals than sites that were more methylated with age (i.e., "hypermethylated"; n sites hypomethylated = 63931, n hypermethylated = 14730; Fig. 2A) (Jones et al., 2015). Exposure to Hurricane Maria was significantly associated with differential methylation of 32048 CpG sites (Table S2). Similarly to aging, the vast majority of these sites (~90%, n = 29234) were less methylated in animals sampled after the storm, while 2814 were hypermethylated in the post-storm sample (Fig. 2B). We also performed the same modeling approach including a covariate for whether individuals had experienced maternal loss in the first four years of life for 505 animals. Surprisingly, we did not find any sites significantly associated with maternal loss. However, we did observe a non-uniform distribution of p-

values across all CpG sites, such that low p-values were enriched, hinting that maternal loss may have an effect on a subset of CpG sites though not enough to pass our multiple hypothesis testing burden.

To confirm that the age-associated effects we observed showed effects consistent with those reported by previous studies, we tested whether our age-associated sites were more likely to overlap loci found to be significantly associated with aging from human EWAS studies. When we grouped proximate age-associated CpG sites into differentially methylated regions ("DMRs"; see Methods section *Defining DMRs*) and tested for overlap with age-associated EWAS sites, we indeed did observe significant enrichment of our age DMRs and age-related sites on both the 450K and EPIC arrays (450K: OR = 2.59, $p = 3.78 \times 10^{-27}$, OR = 3.29, $p = 5.86 \times 10^{-74}$).

Age and environmental exposure affect similar suites of CpG sites

Next, we quantified the extent to which the effects of age and hurricane exposure affected similar CpG sites in three ways. First, we asked whether age and adversity CpG sites were more likely to overlap than expected by chance and found that 37% of hurricane-associated CpG sites were also significantly associated with age, a significant enrichment between site-level effects (OR = 1.35, $p = 1.75 \times 10^{-124}$). Second, we also observed that age and hurricane effects were almost 2x more likely to overlap than expected by chance at the DMR-level (OR = 3.56, $p = 4.65 \times 10^{-168}$), with 51% of hurricane DMRs also being characterized as age DMRs (n = 1194). Third, we further probed the overlap of age and adversity effects by asking whether age-associated DMRs were more likely to overlap sites associated with adversity from human EWAS studies, and, conversely, if hurricane-associated DMRs were enriched for sites found to be associated with aging from human EWAS. Indeed, we found that age DMRs were more likely to overlap sites associated with childhood adversity (OR = 1.4, p = 0.01), and hurricane DMRs were more likely than expected to overlap sites associated with aging from human EWAS studies, both for the 450K and EPIC arrays (450K OR = 1.76, $p = 1.37 \times 10^{-8}$; EPIC OR = 1.69, $p = 1.23 \times 10^{-11}$).

Effects of primary and secondary aging co-occur but have divergent signatures

Aging is associated with hypermethylation of active regulatory states and loss of methylation in quiescent regions

We next tested whether sites associated with age and hurricane exposure were more likely to occur in particular regions of the genome, based on the direction of effect. Here, we tested genomic regions including gene bodies, promoters, CpG islands, CpG shores, and unassigned regions (i.e., not otherwise categorized), as well as chromatin states based on ChromHMM states from human peripheral blood mononuclear cells. Consistent with previous observations, hypermethylated age-associated CpG sites were more likely to fall in regions of active transcription, including CpG islands, promoters, gene bodies, enhancers, and regions annotated as active transcription start sites (TSS) according to their histone profiles, trends that were recapitulated at the DMR level (Fig. 2C; CpG islands: OR = 7.44, $p < 10^{-25}$, promoters: OR = 1.97, $p = 2.55 \times 10^{-134}$, gene bodies: OR = 1.44, $p = 1.12 \times 10^{-97}$, enhancers: OR = 1.15, $p = 3.52 \times 10^{-3}$, active TSS: OR = 1.83, $p = 1.77 \times 10^{-35}$; Tables S3 and S4).

Hypomethylated age-associated sites were more likely to fall in putatively non-regulatory or weakly regulatory regions, such as regions annotated as weak repressed polycomb, weak transcription, genic enhancers, unassigned regions, and–overwhelmingly–quiescent regions (weak repressed polycomb: OR = 1.05, $p = 2.59^{-5}$, weak transcription: OR = 1.06, $p = 9.51 \times 10^{-5}$, genic enhancers: OR = 1.11, $p = 2.62 \times 10^{-2}$, unassigned: OR = 1.67, $p < 10^{-25}$, quiescent regions: OR = 1.83, $p < 10^{-25}$; Fig. 2C; Table S3). Strikingly, over 40% of age-associated sites were located in quiescent regions (n = 34551) and 94% of these were hypomethylated. Quiescent regions are putatively non-regulatory regions that are devoid of the histone modifications and constitutively highly methylated (Hoffman et al., 2013). The loss of methylation in constitutively highly methylated regions is hypothesized to enable increased activity of deleterious elements and contribute to immune dysregulation with aging (Jones et al., 2015; Seale et al., 2022). We hypothesized that age-associated hypomethylated sites in quiescent regions may be in or near genes implicated in immune dysregulation and found that genes hypomethylated in quiescent regions were enriched for positive regulation of apoptotic processes ($p = 1.8 \times 10^{-3}$), interferon-gamma production ($p = 8.77 \times 10^{-3}$), negative regulation of cell migration ($p = 3.72 \times 10^{-3}$), negative regulation of cytokine production ($p = 8.19 \times 10^{-3}$), and inflammatory processes ($p = 4.46 \times 10^{-03}$; Table S5).

Environmental adversity is associated with hypomethylation in active regulatory states and hypermethylation in quiescent regions

While hurricane-associated CpG sites were globally hypomethylated–as were age effects–the genomic regions in which differential methylation occurred were strikingly different. Sites hypomethylated in post-hurricane samples were enriched in nearly all areas of the genome associated with active transcription and gene regulation, such as promoters, enhancers, gene bodies, and areas near TSS, and were only depleted in quiescent regions, weak repressed polycomb, and regions not otherwise annotated (Fig. 2D; Table S6). Approximately half of hypermethylated CpG sites in the post-hurricane samples were located in quiescent regions ($n = 1288$, $OR = 1.28$, $p = 6.33 \times 10^{-11}$). Hypermethylated hurricane-associated sites were also enriched in genomic regions associated with strong and weak transcription, and regions not otherwise annotated (strong transcription: $OR = 1.49$, $p = 1.46 \times 10^{-9}$, weak transcription: $OR = 1.29$, $p = 2.21 \times 10^{-5}$, unassigned: $OR = 1.21$, $p = 1.5 \times 10^{-6}$; Fig. 2D; Table S6). Hurricane DMRs were enriched in similar genomic regions as single sites (Table S7).

Age and adversity effects overlap in active regulatory regions

We next tested where age and hurricane effects were most likely to overlap and found substantial enrichment in areas associated with active gene regulation. Specifically, sites significantly associated with age and hurricane exposure were more likely to overlap in enhancers, gene bodies, promoters, CpG shores and islands, as well as chromatin states associated with strong and weak transcription and near bivalent/poised TSS (Fig. 3A; Table S8). Age and hurricane effects were less likely to overlap in quiescent and heterochromatin regions, as well as weak repressed polycomb complexes (Fig. 3A; Table S8).

Correlation between primary and secondary age effects

Following our observation that primary and secondary age effects co-occurred in particular genomic regions with greater frequency than expected, we next asked whether these effects were differently correlated amongst regions. Specifically, we quantified the correlation among adversity effects and chronological age. We expected that the effects of the two adversities, hurricane exposure and maternal loss, would generally be more correlated to each other than with age. Among all sites, the effects of hurricane exposure were moderately correlated with those of maternal loss ($r = 0.13$, $p < 10^{-100}$), and slightly negatively correlated with those of age ($r = -0.07$, $p = 7.48 \times 10^{-275}$).

The effects of maternal loss were slightly associated with those of age ($r = 0.03$, $p = 3.88 \times 10^{-50}$). As we hypothesized, the correlation between the effects of adversities was generally higher than the correlation of either adversity with age and this trend was generally consistent across all genomic regions and chromatin states, suggesting that the effects of secondary aging may be more similar to each other than to primary aging (Fig. 3B; Table S9).

Primary and secondary aging have distinct signatures in repetitive elements

One mechanism that has been suggested to partially explain immunosenescence and dysregulation with aging is increased activity of deleterious elements; this is particularly true for genomic regions that are constitutively highly methylated and become less methylated with age, putatively reducing epigenetic suppression of deleterious elements. Thus, we investigated whether age-associated hypomethylated sites were enriched in or near (+/-50kb) TEs, which could potentially indicate a pathway for greater TE activation with aging. TEs were enriched in putatively non-regulatory regions, including quiescent regions, heterochromatin, and chromatin states associated with weak transcription. We found that sites in TEs were more likely to be significantly associated with aging than expected ($OR = 1.24$, $p = 1.64 \times 10^{-110}$). Consistent with prior studies, age-associated CpG sites in TEs were more likely to be hypomethylated than expected ($OR = 1.69$, $p < 10^{-25}$); this effect was even stronger when we limited our test to only significantly age-associated sites ($OR = 5.41$, $p < 10^{-25}$; Fig. 4A).

Hurricane-associated CpG sites were less likely to overlap TEs than expected by chance ($OR = 0.63$, $p = 1.21 \times 10^{-275}$). Hurricane-associated sites in TEs were less likely to be hypomethylated after the hurricane ($OR = 0.56$, $p < 10^{-25}$) and, in fact, were more likely to be hypermethylated ($OR = 1.51$, $p = 7.39 \times 10^{-26}$). Notably, while hypomethylated age-associated CpG sites were more likely than expected to overlap TEs, age-associated sites that were also significantly associated with Hurricane Maria were less likely to overlap TEs than expected by chance ($OR = 0.81$, $p = 1.80 \times 10^{-25}$), suggesting the age-associated changes in TEs may be signatures of primary, but not secondary, aging.

Age-associated methylation is coordinated with other epigenetic modifications

DNA methylation is one of several epigenetic modifications that can impact gene regulation. To better understand how changes in DNA methylation coordinated with other epigenomic modifications, we used data generated from independent datasets. First, we asked whether age and hurricane-associated sites were enriched within or outside of regions of accessible chromatin, generated from rhesus macaque PBMCs (Snyder-Mackler et al., 2019). Hypermethylated age-associated sites were more likely to be located in areas of accessible chromatin (OR = 1.62, $p = 6.47 \times 10^{-65}$), while hypomethylated sites were depleted in accessible chromatin regions (OR = 0.57, $p = 2.51 \times 10^{-192}$; Fig. 4A). Fitting with our chromatin state enrichment analysis, hypomethylated hurricane-associated sites were more likely to overlap in regions of open chromatin (OR = 1.74, $p = 1.58 \times 10^{-156}$), while hypermethylated sites were not statistically enriched.

Like other epigenetic modifications, chromatin conformation changes with age (Márquez et al., 2020). DNA methylation and chromatin conformation can alter the structure and relative accessibility of the genome to molecules (e.g., transcription factors). However, it remains relatively unknown the extent to which changes in these two epigenetic regulatory mechanisms act independently or overlap–either to compound or negate one another–to alter genome accessibility during aging. We therefore investigated the extent to which differential methylation overlapped age-dependent changes in chromatin accessibility identified in humans (Márquez et al., 2020). Hypermethylated age-associated CpGs were nearly two-times more likely to be in regions of chromatin that closed with aging (OR = 3.52, $p = 3.71 \times 10^{-132}$; Fig. 4A), suggesting that previously accessible chromatin becomes less active with age due to twin processes of methylation and heterochromatin formation. Interestingly, in no genomic regions that we tested was there a depletion of hypermethylation and closing chromatin, demonstrating that these processes co-occur consistently in all areas of the genome we tested. Conversely, sites significantly hypomethylated with aging were more likely to be in chromatin regions that became more accessible with aging (OR = 1.35, $p = 1.82 \times 10^{-9}$; Fig. 4A). Together, our results suggest that age-associated changes in these two epigenetic modifications are highly correlated across the genome and, given their extensive coordination, these effects may compound and exacerbate dysregulation accrued during aging.

Age and environmental adversity affect broadly similar biological pathways

To investigate how age-associated differential methylation may putatively alter gene expression during aging, we first performed gene set enrichment analyses of the effects of age and hurricane exposure. We performed these tests at the DMR-level as DMRs are expected to have more regulatory influence than single CpG sites. First, we asked whether genes in or within 50kb of hypomethylated age DMRs were enriched for particular biological pathways, compared to a background of nonsignificant and hypermethylated age DMRs. Hypomethylation would canonically predict upregulation of gene expression and, interestingly, hypomethylated age DMRs trended towards enrichment of inflammatory pathways, including the interferon alpha and gamma responses, IL-6/JAK/STAT3 signaling, inflammatory response, complement cascade, MYC targets V2, and TNFa signaling via NFkB (Table S10), though no gene sets passed a false discovery rate threshold of 5%. Conversely, genes in and near hypermethylated age DMRs–in which more methylation would canonically predict downregulation of gene expression–trended to be enriched for genes in the peroxisome pathway, p53 pathways, DNA repair, MYC targets V1, unfolded protein response, PI3K/Akt/mTOR, and the G2/M DNA damage checkpoint pathways, which are pathways often associated with repair processes and age-related immune dysregulation, although no processes passed a false discovery rate threshold of 5% (SI Table S10).

Next, we asked whether hurricane DMRs were enriched for specific biological pathways and found that, while not significant, hallmarks associated with inflammation (i.e., interferon responses, IL-6 signaling) were enriched with hypomethylated DMRs (SI Table S11). Enrichment of hypermethylated hurricane DMRs was less clear, as there were so few, but were trended to be associated with reactive oxygen clearance and developmental pathways (SI Table S11). Third, we asked whether age and hurricane gene set enrichment results were correlated. We found moderate correlation and that more hallmarks than expected were affected in the same direction by age and hurricane ($r = 0.38$, $p = 0.01$; $OR = 4.61$, $p = 0.03$; Fig. 4B), suggesting that age and hurricane exposure may broadly affect similar biological pathways.

Age and hurricane effects are putatively regulated by distinct transcription factors

To understand whether certain regulatory networks were potentially affected by aging, we investigated whether age-associated methylation near DMRs were enriched for particularly regulatory factors. We tested whether hypo- and

hypermethylated DMRs were enriched for different transcription factor binding site (TFBS) motifs. Strikingly, hypomethylated DMRs were enriched for motifs of TFs associated with inflammation and the oxidative stress response (Fig. 4C). For example, hypomethylated DMRs were enriched for Bach1, a major regulator of the oxidative stress response, NFE2L2, which partially regulates the NLRP3 inflammasome in conjunction with c-Jun, and five members of the AP-1 complex (JUND, JUN, MAFK, FOS, and FOSL2), which is increasingly recognized to contribute to age-related inflammation (Fig. 4C) (Garces de los Fayos Alonso et al., 2018). Hypermethylated age DMRs were enriched for several TFs in the ZBTB family, which is implicated in development and lineage commitment, and NRF1, which activates expression of metabolic genes and cell growth, as well as several zinc finger proteins (Cassandri et al., 2017; Cheng et al., 2021). Interestingly, ZBTB33 was also enriched among hypermethylated age DMRs. *ZBTB33* encodes the transcriptional regulator Kaiso, which can promote histone deacetylation and heterochromatin formation, mechanisms proposed to suppress gene expression of inflammation, cell proliferation, and apoptosis (Chen et al., 2015).

DMRs hypomethylated in post-hurricane samples were enriched for 3 transcription factors in the CEBP family, which play an important role in the inflammatory response and myeloid differentiation, regulate acute-phase cytokine genes, and can have an antiproliferative effect on T-cells (Fig. 4D). As there were few hypermethylated hurricane DMRs, we tested hypomethylated DMRs against hypermethylated DMRs and DMRs not significantly associated with the hurricane, to increase the background set, which likely lowers our power to detect differences between hypo and hypermethylated DMRs. The transcription factors enriched for hypermethylated and background hurricane DMRs appeared to have less specificity in their function, but included three members of the MEF2 family, which is involved in cell and tissue differentiation and proliferation (Fig. 4D) (Pon & Marra, 2015).

DNA methylation and regulation of expression of nearby genes

To further disentangle the extent to which DNA methylation regulated age-related gene expression in peripheral immune blood cells, we performed three complementary analyses. First, we tested whether age-associated differentially methylated CpG sites were more likely to be in or within 50kb of genes that are differentially expressed with each effect. Second, we asked whether the effects of age at single CpG sites were associated with effects of age-associated gene expression. Third, we narrowed our investigation to CpG sites in promoter regions

and tested whether the correlation between CpG site methylation and gene expression was stronger for CpG sites in promoter regions than sites in other regions. Fourth, we investigated whether the distance of promoter CpG sites to transcription start sites correlated with age-associated gene expression effects. We then performed these analyses for the effects of hurricane exposure.

We first asked whether age-associated CpG sites were more likely to fall in genes associated with aging from our gene expression study, compared to genes not detectably expressed in whole blood (see Methods *Effects of DNA methylation on gene expression*; Watowich et al., 2022). Fitting with our genome-wide analysis, our first analysis showed that hypermethylated sites were more likely to fall in or within 50kb of blood-expressed genes (OR = 1.3, $p = 2 \times 10^{-55}$) while hypomethylated sites were less likely (OR = 0.82, $p = 1.51 \times 10^{-96}$). Our second analysis revealed that the effects of age at the single CpG site level were negatively correlated with effects of age on gene expression, as canonically expected. This negative relationship was observed among (i) all gene-CpG pairs (i.e., CpG sites within 50kb of a gene, $r = -0.02$, $p = 9.26 \times 10^{-27}$) and more strongly among (ii) CpG site-gene pairs that were both significantly associated with age ($r = -0.068$, $p = 1.064 \times 10^{-11}$). Third, we investigated whether the relationship between effects of age at single CpGs in promoters (i.e., 2kb upstream of TSS) were even more strongly correlated with the expression of downstream genes. As expected, the effects of age at CpG sites within promoters were more negatively correlated with gene expression of the nearby gene than among all sites, as expected, ($r = -0.1$, $p = 4.4 \times 10^{-13}$) and this effect was even stronger among promoter CpG site-genes pairs where the site and gene were both significantly associated with age ($r = -0.34$, $p = 2.87 \times 10^{-7}$; Fig. 4B). Fourth, we investigated whether promoter CpG sites closer to TSS of genes were more strongly correlated than more distal promoter CpG sites. Indeed, the association between age effects of CpG sites and downstream genes was strongest for sites closest to TSS (Fig. 5). For example, CpGs significantly associated with age and within 500 base pairs of age-associated gene TSS were more strongly correlated ($r = -0.65$, $p = 3.11 \times 10^{-7}$; Fig. 4C) than CpGs between 0-1000bp from TSS ($r = -0.43$, $p = 0.02$). We observed the same trend among promoter CpG-gene pairs that were not significantly age-associated, although correlations between site-gene pairs were slightly weaker.

We then probed the relationship between methylation and expression for the effects of hurricane exposure. First, we found that hurricane-associated sites were more likely to fall in and near (+/- 50kb) genes expressed in whole blood

(OR = 1.5, p = 1.59 x 10^{-242}). Further, hurricane-associated CpG sites were more likely to fall in or near genes also significantly associated with hurricane exposure (OR = 1.11, p = 1.89 x 10^{-3}; hurricane-associated genes determined from mixed-effects linear models detailed in (Watowich et al., 2022) and passing a FDR < 10%). Second, hurricane-associated sites also showed the expected negative relationship with gene expression when we tested all site-gene pairs (r = -0.0048, p = 0.04) and pairs for which the CpG site and gene were significantly associated with hurricane exposure (r = -0.08, p = 8.30 x 10^{-3}). We did not observe a statistically significant relationship for hurricane-associated sites within promoter regions and the expression of downstream genes.

Cell type heterogeneity

Immune cell composition changes with aging and may be reflected in DNA methylation levels, which can vary across cell types. To assess whether and how immune cell populations differed across the lifespan in our study population, we modeled immune cell proportions from a subset of samples for which we had data from blood smears (n = 32). Although our sample was under-powered to detect significant effects, all blood cell populations changed with age in the expected direction. Specifically, the percent of monocytes, neutrophils, and eosinophils trended towards increasing in older animals, while the percent of lymphocytes trended towards decreasing in older animals (Fig. S1). Basophils made up less than 0.7% of observed cells in any animal, and thus we do not report their age-related trend. To test the extent to which cell population differences affected our results, we compared models with and without controlling for cell percentages, among the samples for which we had cell counts and found that the effects of age and sex were highly correlated between the two methods (age: r = 0.83, p < 10^{-25}; sex: r = 0.90, p < 10^{-25}).

Within-individual DNA methylation changes reflect cross-sectional estimates

While our dataset consists largely of cross-sectional samples, we did have 67 animals that were sampled at at least two time points during our data collection, allowing us to ask whether results of our cross-sectional analyses recapitulated intra-individual DNA methylation changes across aging. We performed these analyses at the DMR level as we expect that the coordinated methylation changes in DMRs is likely more stable at two time points than that of single sites. The effects of age from the cross-sectional analysis (i.e., standardized beta of age) was correlated

with the proportion of our repeated samples that showed increased methylation with aging (n individuals = 67, r = 0.32, $p = 5.38 \times 10^{-117}$; Fig. 6A). Effects of exposure to Hurricane Maria from the cross-sectional analysis was also correlated with intra-individual methylation levels in animals sampled before versus after the storm (n individuals = 23, r = 0.21, $p = 1.19 \times 10^{-24}$; Fig. 6B). We then extended this analysis to our gene expression dataset and also observed a moderate correlation between within-sample longitudinal changes in gene expression and effect sizes from the cross-sectional model (Fig. S2; SI *Within-individual gene expression changes reflect cross-sectional estimates*).

Discussion

The extent to which primary and secondary aging act along the same molecular pathways to generate similar or distinct damage remains unresolved. Here we find that, at the level of the methylome, environmental adversities largely overlap with age-associated effects in areas of active gene regulation but diverged in putatively less-regulatory regions. Broadly, we observed a substantial overlap between the effects of aging and hurricane exposure in enhancers, promoters, and gene bodies, but a divergence in quiescent and heterochromatin regions. Further, secondary and primary age effects were generally more correlated in areas contributing to active gene regulation, and less correlated in putatively non-regulatory regions. Primary aging effects were largely concentrated in quiescent and heterochromatin regions, in which there was extensive hypomethylation in older individuals, consistent with prior studies (Jones et al., 2015). Hurricane-associated sites were also extensively hypomethylated but were concentrated in areas associated with active gene regulation. While we did not observe significant effects of maternal loss, the overall effects of maternal loss on methylation were moderately correlated with those of hurricane exposure, particularly in areas of active gene regulation. The correlation between these two environmental adversities was consistently greater than either with aging, suggesting that signatures of secondary aging are more similar to one another than primary aging, providing further evidence that primary aging has signatures distinct from secondary aging. Additionally, our results reveal that DNA methylation may be responsive to extreme natural disasters and their aftermath. However, future studies should test the extent to which differential methylation persists or attenuates following severe natural disaster, and whether this varies across genomic regions and chromatin states.

Interestingly, we observed two potential primary age-specific damage generating pathways. First, we found that quiescent chromatin states were overwhelmingly more likely to be hypomethylated with age than expected by chance. Hypomethylated sites were also in and nearby genes involved in inflammatory pathways, suggesting potential derepression of these genes with age. Further, we observed coordinated loss of methylation and greater chromatin accessibility with aging, hinting at the possibility of derepression of two epigenetic modifications in tandem and greater activation of deleterious elements. Secondly, we found that TEs were far more likely to be hypomethylated with aging, but not hurricane exposure, potentially reflecting a damage-generating pathway specific to intrinsic age-effects. Consistent with prior studies, we observed TEs across the genome were hypomethylated with aging, suggesting that the epigenetic landscape becomes more permissible for TE mobilization (Andrenacci et al., 2020; Gorbunova et al., 2021). We observed broad hypermethylation of TEs in animals exposed to Hurricane Maria, a surprising result given that adverse conditions are generally expected to reduce epigenetic silencing capacity and that TE activation may be an adaptive mechanism that can increase genetic variability (Pappalardo et al., 2021). However, epigenetic-level changes in TE methylation following stressful events is not well-understood and appears to be highly context-specific depending on the adversity and the element type (Horváth et al., 2017; Pappalardo et al., 2021). For example, human neuroblastoma cells exhibited hypermethylation of LINE-1 elements when treated with morphine–which can induce oxidative stress–for short periods of time, but hypomethylation of LINE-1 elements when exposed for longer periods of time (Trivedi et al., 2014). The timing of when methylation changes following adversities is currently not well-understood and is likely to be highly context specific. Thus, it is possible that the global hypermethylation of TEs we observe is a time-dependent response and potentially an induced repair mechanism.

Our findings also support gene regulatory effects of promoter methylation on downstream gene expression, particularly for the effects of age. CpG sites in promoter regions associated with age were much more strongly correlated with gene expression than non-age-associated CpG sites or sites outside of promoter regions. CpG sites closer to TSS tended to be more strongly associated with aging and also more highly correlated with downstream methylation, suggesting that sites close to the TSS exert a greater influence on gene expression.

Surprisingly, we detected only slight effects of early life adversity on DNA methylation. However, nearly all juveniles were removed from our analysis, lowering our power to detect effects which may attenuate over time. While strong effects of maternal loss and social competition on survival have been found in other primate systems, these have largely been observed in systems without food provisioning, and animals on Cayo Santiago may be buffered from extreme early life hardship by provisioned resources (Tung et al., 2016; Zipple et al., 2021). Further, our study had several limitations. Methylation patterns vary between cell types and will likely be affected by changes in cell composition. In this study, we were unable to fully disentangle cell-intrinsic methylation changes from changes in cell composition, yet we found that cell composition changed as expected with aging in this population. Previously, we have previously found that immune cell-specific marker genes in animals sampled after Hurricane Maria showed generally similar patterns to those of age, suggesting that the hurricane and aging had similar effects on cell composition (Watowich et al., 2022). Yet, future studies should measure cell-specific methylation levels to fully characterize the extent to which methylation changes are specific to cell type.

While our study was largely cross-sectional, approximately one quarter of our samples were from animals repeatedly sampled at least a year apart. Among both the DNA methylation and gene expression datasets, we found moderate correlation of mean differences in methylation from the cross-sectional models and intra-individual changes in methylation and gene expression levels. While longitudinal sampling designs remain the gold-standard for detecting age-related changes, our results highlight that cross-sectional designs should not be discounted and are valuable in their ability to allow investigators to disentangle age and cohort effects.

In conclusion, we find that a novel environmental perturbation–surviving a major hurricane–was associated with DNA methylation patterns broadly similar to those of primary aging in genomic regions associated with active gene regulation, but diverged in putatively non-regulatory regions, suggesting damage-generating pathways specific to primary aging. While environmental insults leading to secondary aging can be detrimental and advance disease-progression, our findings suggest that secondary and primary aging partially, but do not fully, overlap. Therefore, it may be possible to both disentangle how secondary aging advances immune dysregulation to inform strategies to mitigate negative consequences for survivors of extreme environmental hardships and also to simultaneously reduce

deleterious effects of both primary and secondary aging by identifying moderators of aging that affect areas in which primary and secondary aging overlap.

Methods

Study Subjects and Experimental Design

Whole blood and behavioral data were collected from rhesus macaques (*Macaca mulatta*) on the island of Cayo Santiago, a long-running field site where animals have been continually studied since the site's inception in 1938. Whole blood samples and information about the animal's body condition and weight are collected during the annual trap and release period on Cayo Santiago, which occurs approximately 1-3 months before the breeding season. Age and sex-matched individuals were identified for biological sampling before the trapping period each year. Our study drew on samples collected from 2010-2018, although animals were not sampled in 2017, as Hurricane Maria devastated the island's infrastructure weeks before the trapping period was scheduled. When conditions allowed, we resumed biological sampling in 2018, with the aim of collecting samples from animals age and sex-matched to pre-hurricane samples. More details on biological sampling collection is in Watowich et al. 2022 (Watowich et al., 2022).

Blood Sampling

For this study we generated the DNA methylation dataset from samples of peripheral whole blood samples collected annually from 2010-2016 and in 2018. Veterinary staff drew whole blood from sedated animals into one 3mL BD Vacutainer® EDTA tube. Blood in the EDTA tube was immediately refrigerated for ~1-3 hours before transport to the Puerto Rican mainland and long-term storage in -80°C. From 2014-2016, we collected 470 blood samples from 421 animals (median age of 9.09 y; n females = 260, n males = 210). After Hurricane Maria, in 2018, 101 animals were sampled (median age = 7.17 y; n females = 56, n males = 45). Detailed metadata for each sample in the DNA dataset can be found in Table S1.

The RNA dataset was generated from whole blood collected into a 2.5mL PAXgene Blood RNA Tube (PreAnalytiX GmbH) in years 2014-2016, and in 2018. From 2014-2016, we collected 435 blood samples from 357 animals (median age of 6.94 y; n females = 174, n males = 261). In 2018, 108 animals were sampled (median age = 6.05 y; n

females = 57, n males = 51). For a detailed description of the RNA dataset blood sampling and handling, see (Watowich et al., 2022). In 2016, as part of ongoing population management, a subset of animals were transported from Cayo Santiago to the Sabana Seca Field Station where the standard blood collection procedure was performed (DNA dataset: n = 89, RNA dataset: n = 95). As infrastructure was limited on Cayo Santiago following Hurricane Maria, and as part of the ongoing population management strategy, animals sampled in 2018 were sampled at Sabana Seca Field Station (DNA dataset: n = 100, RNA dataset: n = 108).

Behavioral Data Collection and Generation

Since 1956, observers have updated demographic records daily. These records include dates of birth and death, sex, maternal and sire identification, and individual dispersal between social groups. We used historical demographic records to assess individual exposure to forms of early life adversity (Tung et al., 2016). An individual was considered to experience maternal loss if their mother died (including natural death and permanent removal from the population) before the individual reached 4 years of age.

DNA/RNA Extraction and Sequencing and Data preprocessing

To generate the DNA methylation dataset, DNA was extracted from whole blood at the University of Washington, Seattle in 2019 using the QIAamp Fast DNA Tissue Kit (QIAGEN). CpG methylation was measured using reduced representation bisulfite sequencing (RRBS) from an input of 300 ng of DNA. Detailed methods for the generation of the DNA methylation dataset can be found in Chiou 2020 (Chiou et al., 2020). Briefly, we used the EZ-96 DNA Methylation-Lightning MagPrep kit (Zymo Research) to perform the RRBS bisulfite conversion, and then libraries were ligated with unique dual index sequencing primers and amplified with 16 cycles of PCR.

Detailed methods of the generation of the RNA dataset are in Watowich et al. 2022 (Watowich et al., 2022). RNA extraction was performed using the MagMAX for Stabilized Blood Tubes RNA Isolation Kits (Thermo Fisher) (n = 499) and the PAXgene Blood RNA Kit IVD (Qiagen) (n = 48), using standard procedures. RNA quality number (RQN) was quantified using AATI Fragment Analyzer. We used a three-prime RNA sequencing approach, TM3'SEq, to generate RNA sequencing libraries from 50ng of total RNA and amplified libraries with 16 PCR

cycles (Pallares et al., 2020). For both RNA-seq and RRBS libraries, libraries were combined in equimolar quantities and sequenced on an Illumina NovaSeq S2 flowcell.

RRBS reads were trimmed using Trim Galore! and reads were mapped to the rhesus macaque reference genome (Mmul_10). Methylated and total counts were extracted using Bismark (Krueger & Andrews, 2011). Sites with complete data in fewer than 100 individuals (17%) and sites with median methylation greater than 90% or less than 10% (i.e., hyper/hypomethylated) were removed, resulting in over 250,000 variably methylated CpG sites from across the genome for further analysis. For the RNA-seq reads, we mapped cDNA reads to the Mmul_10 assembly using kallisto (Bray et al., 2016). As sequencing was performed on whole blood, we removed reads mapping to seven genes encoding hemoglobin and ribosomal RNA subunits. As 3'seq does not assign reads as the transcript-level, reads were aggregated at the gene-level. We filtered out lowly expressed reads (<3.29 transcripts per million), resulting in 7009 detectably expressed genes. We normalized read counts with the voom function from the limma package in the R environment (4.0.2) (Ritchie et al., 2015) (https://github.com/mwatowich/ Natural-disaster-and-immunological-aging-in-a-nonhuman-primate).

Modeling the Effects of Age and Adversity on DNA Methylation

CpG methylation was modeled using a binomial mixed modeling framework, to model methylated and total counts as a function of age, Hurricane Maria exposure, sex, and controlling for relatedness and technical effects of DNA extraction batch. The model of early life effects used the same framework and controls for relatedness and batch effects. Modeling was performed using MACAU implemented in the PQLseq package in R (Lea et al., 2015; A. S. Sun et al., 2018; S. Sun et al., 2019). The kinship matrix was generated using the --kinship function in KING from VCF files generated from RRBS reads (Manichaikul et al., 2010). For each main variable modeled (i.e., age, Hurricane Maria exposure), percent variance explained was calculated using the following equation:

$$beta(x)^2 * var(x) \,/\, (((beta(y)^2 * var(y)) + (beta(n..)^2 * var(n..))) + sigma2)$$

Defining DMRs

Regions of multiple CpGs that act in a coordinated manner–differentially methylated regions–are expected to be more functionally relevant and impactful on gene regulation than single CpG sites (Lea et al. 2016). We defined

differentially methylated regions as regions with higher than expected CpG density and coordinated methylation patterns. To identify DMRs, we focused on 'focal' CpG sites (FDR < 5%) for our variable of interest (i.e., age) and scanned for (i) strictly significant (FDR < 5%), (ii) loosely significant (FDR < 10%), and (iii) all other CpGs within +/-2000bp of the focal site. We then performed 10 permutations for each variable of interest to determine the median number of loosely significant CpGs significantly within DMRs by random chance (Lea et al., 2016). For example, the median number of CpGs that passed a relaxed threshold (FDR<10%) for permutations of age-associated values was 3. We retained DMRs that had more than the median number of CpGs associated with the variable of interest at the relaxed threshold significance threshold determined by the permutations. Further, DMRs were removed if fewer than 75% of the effect sizes for all CpGs in the DMR or CpGs that were significant at the relaxed threshold were in the same direction. DMRs were merged if they overlapped. The effect size attributed to the DMR was the median effect size of all CpG sites within the DMR. We annotated whether DMRs intersected with different chromatin states and regulatory regions in the same way as single CpG sites. Code to generate DMRs is available on Github (https://github.com/mwatowich/aging_hurricane_DNAm).

We identified 5009 DMRs associated with age and removed 3 that were longer than 10000 base pairs, as these were 13x less dense than DMRs shorter than then thousand base pairs, leaving 5006 age DMRs. Age DMRs showed a similar distribution of hypo- to hypermethylation as single sites (n hypermethylated age DMRs = 3659, n hypermethylated = 1347). Age DMRs contained a median of 6 CpG sites, a median of 5 CpGs associated with age at a relaxed threshold (FDR < 10%), a median of 4 CpGs associated with age at a stringent threshold (FDR < 5%). We also quantified 2349 DMRs associated with hurricane exposure. Hurricane DMRs also followed the distribution of effect sizes we observed at the single-site level, with 2327 being hypomethylated in hurricane-exposed animals and 22 being hypermethylated. Hurricane DMRs contained a median of 7 CpG sites, a median of 5 at a relaxed FDR threshold of 10%, and a median of 4 that passed a strict FDR threshold of 5%.

Genome Region and Chromatin State Enrichment

First, we annotated CpG sites by determining whether they fell within gene bodies. We used the rhesus macaque Ensembl Gene list downloaded via biomaRt in the R environment (4.0.2) for gene coordinates and intersected these with our CpG sites using bedtools intersect function (Cunningham et al., 2022; Durinck et al., 2005, 2009; Quinlan

& Hall, 2010). Each annotation intersection was performed via bedtools intersect unless otherwise specified. We annotated CpGs as within promoter regions of genes if they fell within 2 kilobases upstream of the TSS. CpG islands were determined using UCSC Genome Browser's CpG island track for rhesus macaque (Karolchik D et al., 2004; Kent et al., 2002). We defined CpG shores as 2kb on either side of CpG islands. Chromatin states were downloaded from the Roadmap Epigenomics Project ChmmModels of human primary mononuclear cells (Epigenome ID E062; E062_15_coreMarks_hg38lift_dense.bed. We used the web browser-based liftOver tool to lift coordinates for human PBMC chromatin states to the macaque mmul10 genome, using preset mapping parameters (Ernst & Kellis, 2012; Kent et al., 2002).

Chromatin Accessibility Enrichment

Accessible chromatin regions were determined by calling peaks in ATAC-seq data generated in rhesus macaque PBMCs, as specified in Snyder-Mackler 2019 (Snyder-Mackler et al., 2019). Further, we annotated regions of opening and closing chromatin by lifting over coordinates of regions characterized in human PBMCs by Marquez et al. 2020 to the coordinates of the Mmul_10 genome (Márquez et al., 2020). We included all regions that were found by Marquez et al. to be differentially accessible and showing the same direction of effect (i.e., both opening) in both males and females, as well as regions differentially accessible in males or females (i.e., opening in males, not significant in females).

Repetitive Element Enrichment

To annotate CpG sites within transposable elements, we used the RepeatMasker annotation track from UCSC's Genome Browser database for the mmul10 genome (Karolchik D et al., 2004; Kent et al., 2002). We determined whether CpGs were within TEs using bedtools' intersect function (Quinlan & Hall, 2010). To characterize whether TEs in the rhesus genome were conserved or relatively young, we compared the rhesus macaque and olive baboon (*Papio anubis*) repeat tracks (a closely related species with a well-annotated genome) by lifting over repeat track coordinates from rhesus to baboon coordinates. Repeated elements that mapped successfully to the baboon genome were considered "conserved", while repeated elements that did not lift over successfully (i.e., only in rhesus) were considered evolutionary "young".

Gene set enrichment

We performed several gene set enrichment analyses. First, we asked whether age or hurricane DMRs were more likely to be enriched for certain gene set enrichment analysis (GSEA) 'hallmarks'. As GSEA is a rank-ordered comparison, we used gene sets including both DMRs and background DMRs, ranked by median effect size of CpGs in the region.

We also investigated whether genes in quiescent chromatin states near hypomethylated CpG sites were enriched for any biological processes. We first associated genes with hypomethylated CpG sites by determining if the hypomethylated sites were within or +/-50kb of a gene. We eliminated any duplicated matches and also retained only genes detectibly expressed in the blood (i.e., in our RNAseq dataset described in Watowich et al., 2022). The background gene set for this investigation included genes that overlapped or were within 50kb of sites not hypomethylated in quiescent regions, essentially genes near all other CpG sites in our analysis. We then compared the two gene sets using gene ontology analysis via the TopGO package in the r environment with the 'weight01' algorithm and Fisher's exact test of biological processes (Alexa & Rahnenfuhrer, 2020).

EWAS Enrichment

For the following functional enrichment analyses, we focused our analysis on the DMR-level rather than the level of single CpG sites. First, we asked whether age-associated DMRs were more likely to be in regions known to be differentially methylated with aging from human EWAS studies. CpG sites associated with aging and top age-related diseases were extracted from the EWAS Atlas (National Genomics Data Center) (Li et al., 2019; Xiong et al., 2022). We added +/- 50bp to the CpG site coordinates from the 450K and EPIC array probes to enable better conversion between genomes and used liftOver–with standard mapping parameters–to convert coordinates to the mmul10 genome (Kent et al., 2002; Quinlan & Hall, 2010). We intersected the converted EWAS probe regions with CpG sites from our analysis and used Fisher's Exact Tests to test for enrichment.

Transcription Factor Binding Site Enrichment

We performed transcription factor binding site enrichment analysis of DMRs using monaLisa in the R environment (version 4.1.2). For the analysis of age effects, we compared hypomethylated DMRs to hypermethylated DMRs. For

the analysis of hurricane effects, we compared hypomethylated DMRs to non-significant and hypermethylated DMRs because there were so few (n = 22) hypermethylated hurricane DMRs. Sequences from the rheMac10 genome were extracted from DMR regions using getSeq from the BSgenome package (Pages, H, 2022). Transcription factor binding site position weight matrices for vertebrates were downloaded from Jaspar 2020 (Fornes et al., 2020).

Correlation Between Cross-Sectional Analysis and Repeated Sample Methylation Levels

To determine whether samples obtained from the same individual over time recapitulated trends found from our cross-sectional analyses, we determined the frequency that repeated samples were in the same direction as expected from the cross-sectional study results. We determined the proportion of methylation for repeated samples for each age-associated DMR and subtracted the proportion methylated at the oldest time points from that of the youngest. We performed this analysis at the DMR-level as we expected that DMR methylation would be more stable than single CpG sites. For each DMR, we calculated the percent of individuals with a positive difference in proportion of methylation between oldest and youngest time points. Pearson's correlation tests were used to test the association between the percent of individuals with a positive change (more methylation when older) and the standardized betas for a given variable from the models of cross-sectional samples. We performed this analysis for age-associated DMRs and Hurricane Maria-associated DMRs to understand whether outcomes from longitudinal and cross-sectional analyses were correlated for these different types of effects. We also performed the same analysis for our gene expression dataset, subtracting gene expression levels in older repeated samples from those in the younger sample for the same individual.

Effects of DNA Methylation on Gene Expression

To characterize the relationship between DNA methylation and gene expression, we first characterized global trends in the relationship between methylation and expression by examining the correlation between standardized betas of different variables of interest (i.e., age) from the cross-sectional models of DNA methylation and gene expression from the complete datasets. We considered genes to be differentially expressed with age and hurricane exposure if they passed a false discovery rate threshold of 10%, using the methods from Watowich et al. 2022, which describes our complementary RNAseq dataset.

Cell Type Heterogeneity Enrichment

For a subset of the individuals in our DNA methylation dataset (n = 32), we had blood smears that were made at the time blood was drawn for our methylation dataset. High-resolution scans of each blood smear slide were uploaded to Zooniverse, a web platform in which citizen scientists can assist researchers in data collection. Volunteers on Zooniverse enrolled in our project (Monkey Health Explorer) and completed a certification and test in identifying blood immune cell types including neutrophils, lymphocytes, monocytes, eosinophils, and basophils. Once 15 volunteers had analyzed each image, we considered the image "completed". When discrepancies in cell type classification occurred between volunteers, a trained researcher would determine the final classification or, occasionally, the cell would be removed from the analysis. To ensure large enough quantities of cells to confidently ascertain cell proportions, we retained only samples with at least 90 white blood cells classified for our final analysis. We modeled the percent of each immune blood cell type as a function of age and sex using the R function "lm" from the stats package in the R environment.

Next, to test the extent to which our results might be influenced by changes in cell proportions across aging, we compared the results of age and sex effects from models controlling and not controlling for immune cell percentages. Among the 32 animals for which we had cell count data, we modeled DNA methylation using the same binomial mixed model framework we used for the main model of the full dataset (n = 543) we discuss above. We modeled DNA methylation as a function of age, sex, while controlling for technical effects and kinship. In one model set we included percent of neutrophils, lymphocytes, monocytes, and eosinophils, and in the other set we did not. We did not include basophil percentages as there is practically no variation between individuals (range = 0% to 0.67%). We did not include the effect of Hurricane Maria exposure in the models as all blood smear slides in this analysis were made during a single trapping season (2015). We then compared the standardized effect sizes of age and sex effects from the two model sets for the 178,470 sites that overlapped between (i.e., converged) both model sets. Further, we tested whether the model controlling for cell type percentage produced more significant results than the model not controlling for cell type percentage. We found both produced 7 sites significantly associated with age at a relaxed threshold (FDR < 20%). The model not controlling for cell type only produced 2 significant sex-associated sites, while the model controlling for cell type produced 7 (FDR < 20%), possibly suggesting that not

controlling for cell type might result in more conservative results in our dataset though we note that this analysis is very under-powered compared to the full dataset.

Data Availability

DNA methylation and RNA sequencing reads are available in the National Center for Biotechnology Information Short Read Archive (DNAm: PRJNA610241; RNA: PRJNA715739) (*ID 715739 - BioProject - NCBI*, n.d.).

Acknowledgements

We sincerely thank the Caribbean Primate Research Center for maintaining the Cayo Santiago population and for helping collect invaluable long-term biological, social, and demographic data from this population, especially Nahirì Rivera Barreto and Giselle Caraballo Cruz. We thank Sierra Sams and Arianne Mercer for help generating methylation libraries; Alice Baniel, India Schneider-Crease, and the Snyder-Mackler Lab for helpful feedback. We also sincerely thank the many Zooniverse volunteers, without whom the blood smear cell count analysis would not be possible. This work was supported by the University of Washington Department of Biology, a Royal Society Research Grant (RGS/R1/191182), and NIH (F31-AG072787, R00-AG051764, Office of Research Infrastructure Programs [ORIP] P40-OD012217, R01-AG060931, R01-MH096875, R01-MH089484, R01- MH118203, F32-AG062120, R01-AG075914). Cayo Santiago Field Station is supported by the ORIP of the NIH (2P40OD012217).

Author Contributions

M.M.W., M.J.M., C.B.R.U., J.E.H., M.I.M., J.P.H., L.J.N.B., M.L.P., A.J.L., and N.S.-M. designed research; M.M.W., K.L.C., E.A.G., M.J.M., R.P., S.P., C.C., J.E.H., performed research; M.M.W., A.J.L., and N.S.-M. analyzed data; and M.M.W., A.J.L. and N.S.-M. wrote the paper.

Figures

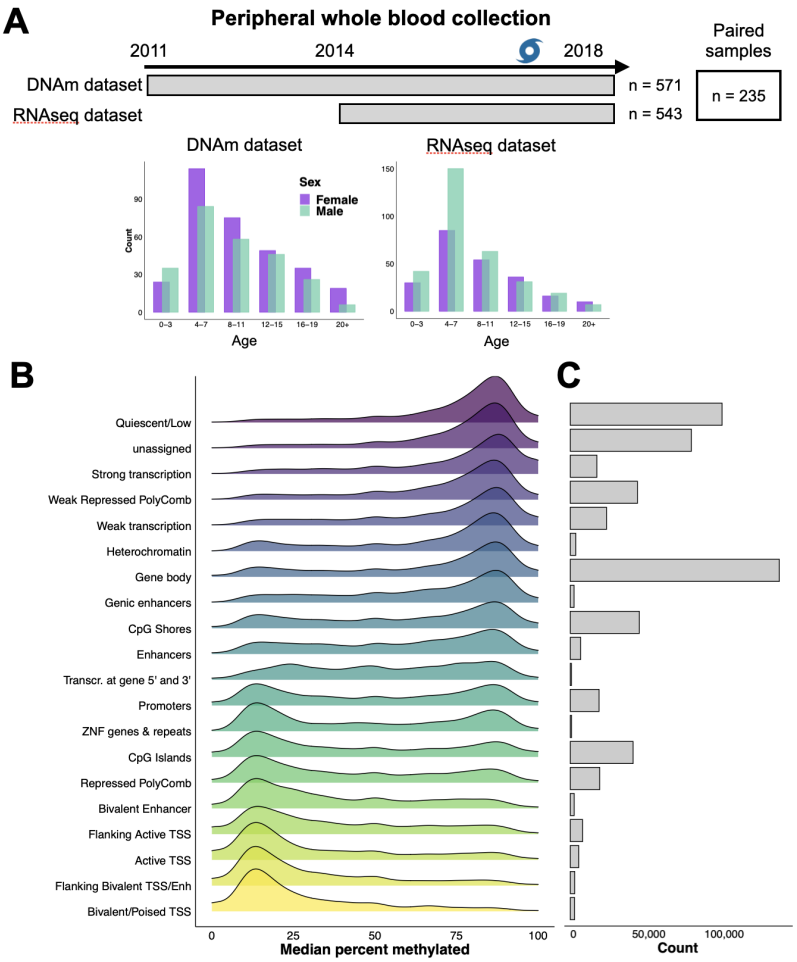

Fig. 1. Sampling design and RRBS coverage. (A) Schematic summary of sampling design. Peripheral whole blood was collected from rhesus macaques on Cayo Santiago from 2010-2018 and stabilized RNA was collected from 2014-2018. Sampling did not occur in 2017 due to Hurricane Maria. Both datasets include animals from infancy to old age, with an approximately even split of females and males. For 235 samples, we have paired DNA methylation and RNA sequencing data. (B) The median percent methylation of sites within each genomic region, after removing sites methylated >90% and <10% (i.e., invariably methylated), in at least 100 samples, and with 5-500x coverage. (C) The number of sites in each genomic region retained for downstream analysis after filtering.

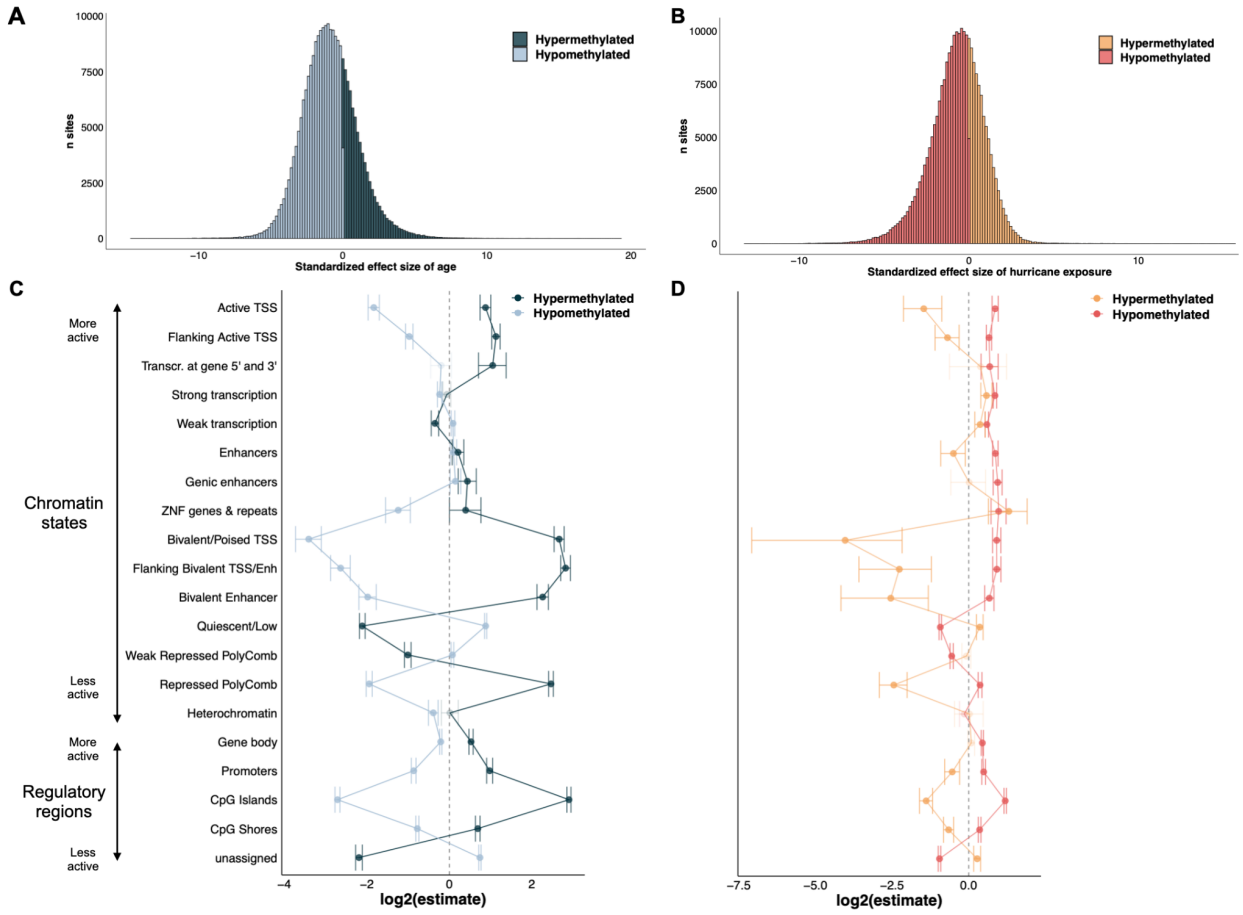

Fig. 2. Global hypomethylation in response to aging and environmental adversity. The distribution of standardized effect size of (A) age and (B) hurricane exposure. Enrichment of hyper- and hypomethylated (C) age-associated and (D) hurricane-associated sites in different genomic regions and chromatin states. Confidence intervals crossing the dotted line at zero are not significantly enriched and are denoted with a lighter color.

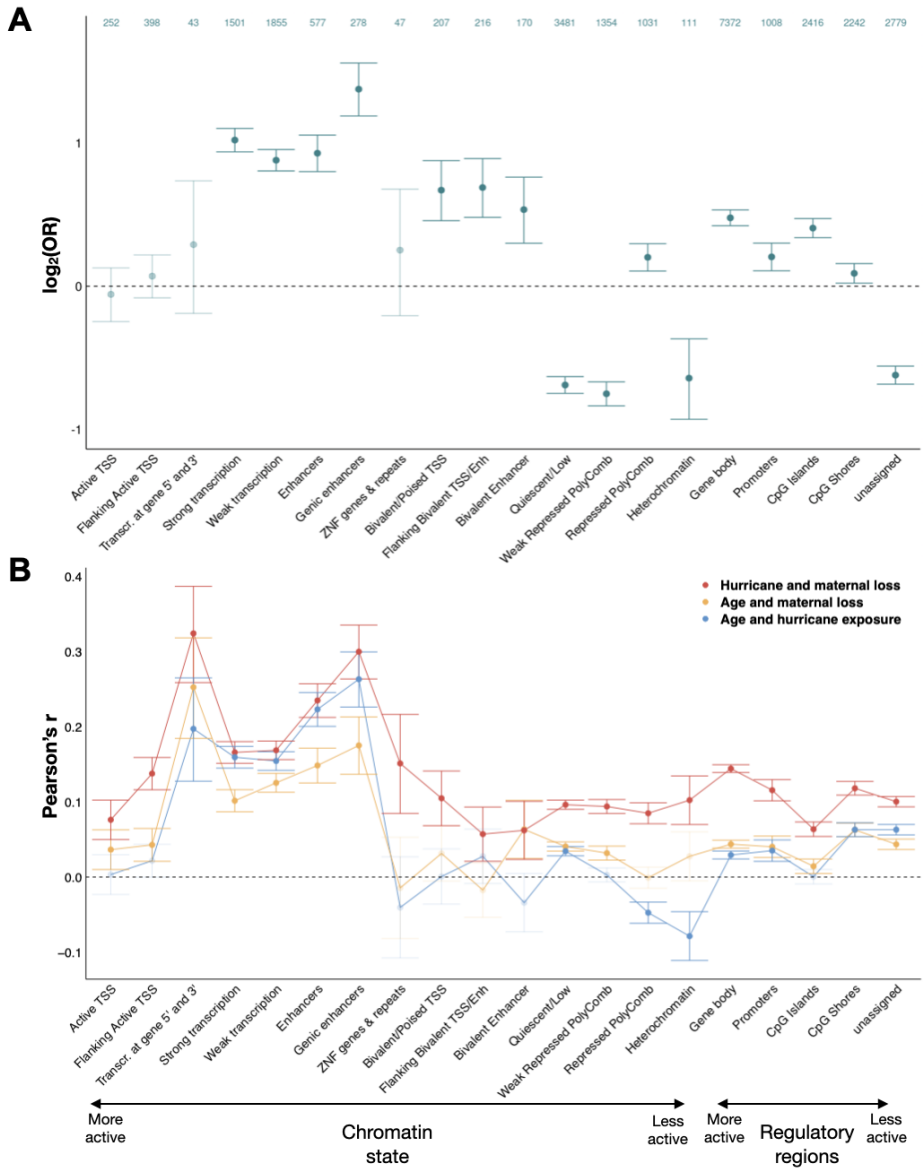

Fig. 3. Primary and secondary age effects are enriched and more correlated in areas of active gene regulation. (A) Enrichment of overlapping significant effects of age and hurricane exposure. Bars crossing 0 are not significantly enriched and are shown in lighter color. The number of CpG sites in each region is noted at the top of the plot. (B) Correlation between the effects of primary and secondary aging and between adversities is shown for all CpG sites within each genomic region and chromatin state. Points with confidence intervals crossing the dotted line at zero are not significantly correlated and are shown in lighter color (transparency).

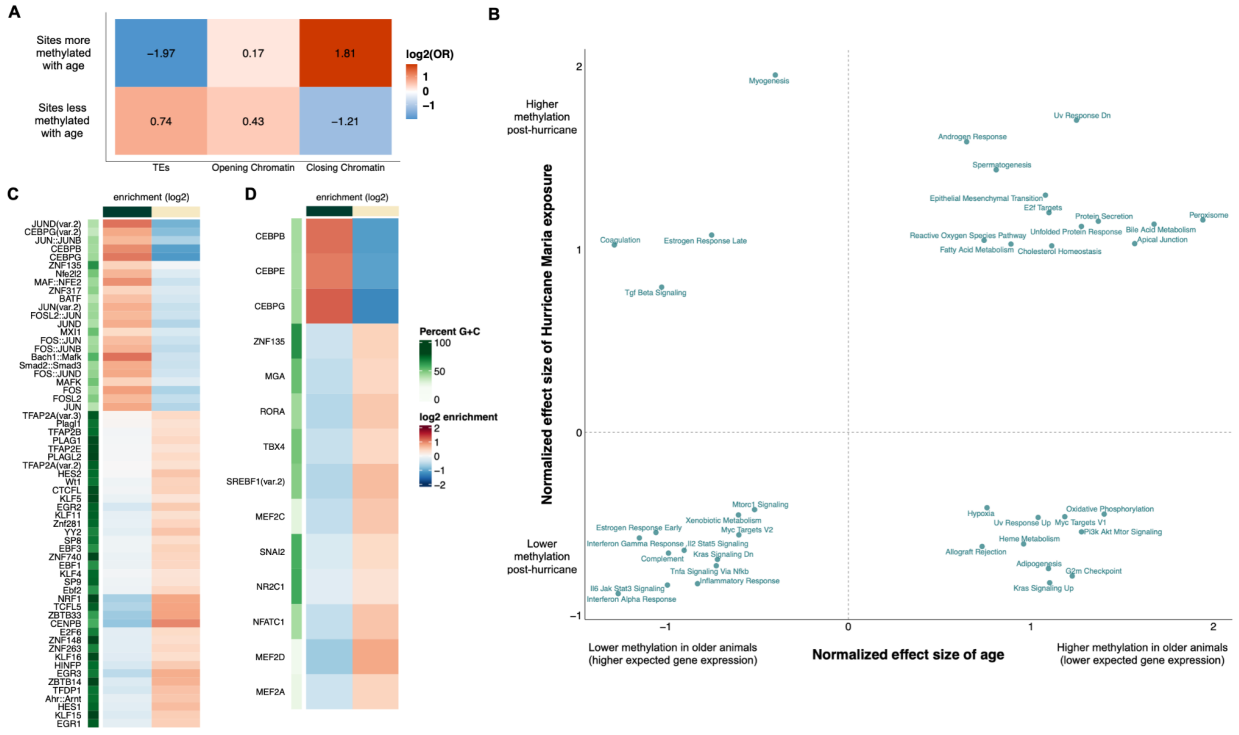

Fig. 4. Age and hurricane exposure have similar effects on inflammatory pathways. (A) Enrichment of age-associated CpG sites in TEs and differentially accessible chromatin (chromatin accessibility characterized by Márquez et al., 2020). Age-associated sites in transposable elements were more likely to be hypomethylated in older animals. Sites hypomethylated with age were enriched in chromatin regions that open with age, while sites hypermethylated with age were enriched in chromatin regions that close with age. (B) Age and (C) hurricane-associated DMR transcription factor binding site enrichment. The green bar on the x-axis shows enrichment statistics for hypomethylated DMRs while the white bar represents hypermethylated DMRs. (D) Gene set enrichment terms are correlated and enriched for the same direction of effect between the effects of aging and hurricane exposure.

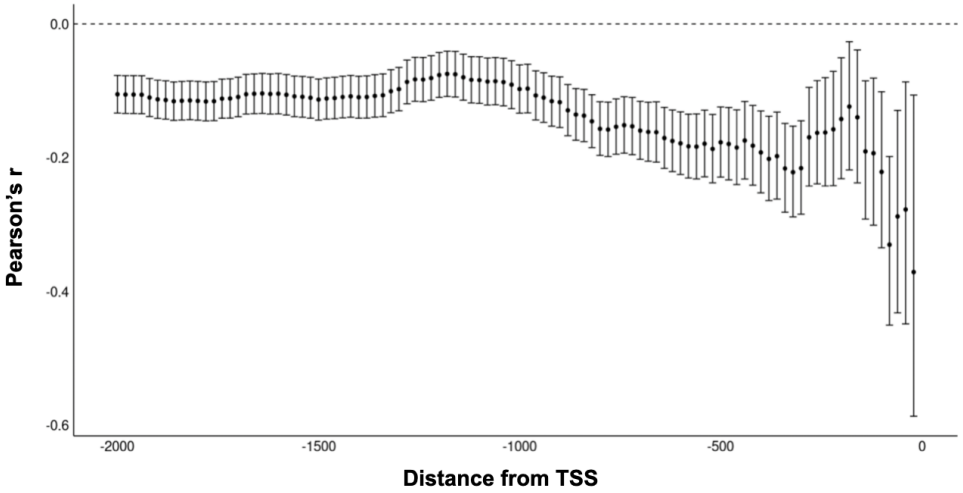

Fig. 5. Correlation of the effects of age between within CpG sites in promoter regions and downstream genes. Points show the median Pearson's r value (among all CpGs) for the correlation between the effects of age on CpG methylation and gene expression, with 95% confidence intervals shown. Bins represent 20 base pair units.

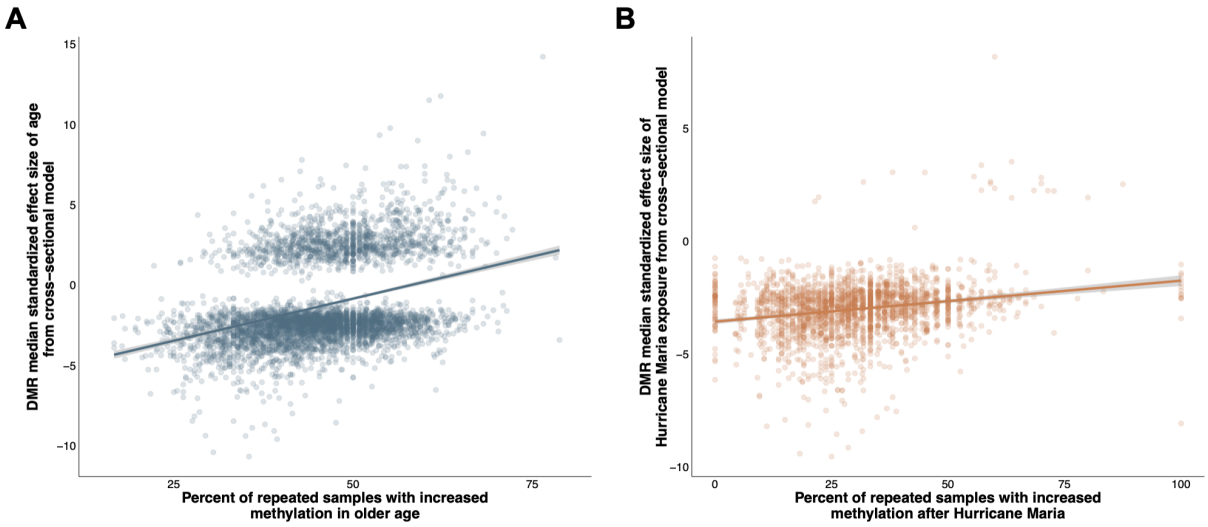

Fig. 6. Cross-sectional results are correlated with inter-individual changes in DNA methylation across aging and exposure to extreme natural disaster. (A) The percent of repeated samples (i.e., same individual) that had greater proportion methylation at older age, compared to the standardized effect sizes of age for CpG sites. (B) The percent of repeated samples with more methylation in post-hurricane samples compared to samples taken pre-hurricane, versus the median standardized effect size of Hurricane Maria exposure.

References

1. Alexa, A., & Rahnenfuhrer, J. (2020). *TopGO: Enrichment Analysis for Gene Ontology*.
2. Andrenacci, D., Cavaliere, V., & Lattanzi, G. (2020). The role of transposable elements activity in aging and their

possible involvement in laminopathic diseases. *Ageing Research Reviews*, *57*, 100995. https://doi.org/10.1016/j.arr.2019.100995
3. Bray, N. L., Pimentel, H., Melsted, P., & Pachter, L. (2016). Near-optimal probabilistic RNA-seq quantification. *Nature Biotechnology*, *34*(5), 525–527. https://doi.org/10.1038/nbt.3519
4. Cassandri, M., Smirnov, A., Novelli, F., Pitolli, C., Agostini, M., Malewicz, M., Melino, G., & Raschellà, G. (2017). Zinc-finger proteins in health and disease. *Cell Death Discovery*, *3*(1), Article 1. https://doi.org/10.1038/cddiscovery.2017.71
5. Chen, H. P., Zhao, Y. T., & Zhao, T. C. (2015). Histone Deacetylases and Mechanisms of Regulation of Gene Expression (Histone deacetylases in cancer). *Critical Reviews in Oncogenesis*, *20*(1–2), 35–47.
6. Chénais, B. (2022). Transposable Elements and Human Diseases: Mechanisms and Implication in the Response to Environmental Pollutants. *International Journal of Molecular Sciences*, *23*(5), Article 5. https://doi.org/10.3390/ijms23052551
7. Cheng, Z.-Y., He, T.-T., Gao, X.-M., Zhao, Y., & Wang, J. (2021). ZBTB Transcription Factors: Key Regulators of the Development, Differentiation and Effector Function of T Cells. *Frontiers in Immunology*, *12*, 713294. https://doi.org/10.3389/fimmu.2021.713294
8. Chiou, K. L., Montague, M. J., Goldman, E. A., Watowich, M. M., Sierra, N., Horvath, J. E., Ruiz-lambides, A. V., Melween, I., & Snyder-mackler, N. (2020). Rhesus macaques as a tractable physiological model of human ageing. *Phil. Trans. R. Soc. B*, *375*(20190612). http://dx.doi.org/10.1098/rstb.2019.0612
9. Cunningham, F., Allen, J. E., Allen, J., Alvarez-Jarreta, J., Amode, M. R., Armean, I. M., Austine-Orimoloye, O., Azov, A. G., Barnes, I., Bennett, R., Berry, A., Bhai, J., Bignell, A., Billis, K., Boddu, S., Brooks, L., Charkhchi, M., Cummins, C., Da Rin Fioretto, L., … Flicek, P. (2022). Ensembl 2022. *Nucleic Acids Research*, *50*(D1), D988–D995. https://doi.org/10.1093/nar/gkab1049
10. De Cecco, M., Ito, T., Petrashen, A. P., Elias, A. E., Skvir, N. J., Criscione, S. W., Caligiana, A., Brocculi, G., Adney, E. M., Boeke, J. D., Le, O., Beauséjour, C., Ambati, J., Ambati, K., Simon, M., Seluanov, A., Gorbunova, V., Slagboom, P. E., Helfand, S. L., … Sedivy, J. M. (2019). L1 drives IFN in senescent cells and promotes age-associated inflammation. *Nature*, *566*(7742), Article 7742. https://doi.org/10.1038/s41586-018-0784-9
11. Dmitrijeva, M., Ossowski, S., Serrano, L., & Schaefer, M. H. (2018). Tissue-specific DNA methylation loss during ageing and carcinogenesis is linked to chromosome structure, replication timing and cell division rates. *Nucleic Acids Research*, *46*(14), 7022–7039. https://doi.org/10.1093/nar/gky498
12. Durinck, S., Moreau, Y., Kasprzyk, A., Davis, S., De Moor, B., Brazma, A., & Huber, W. (2005). BioMart and Bioconductor: A powerful link between biological databases and microarray data analysis. *Bioinformatics*, *21*, 3439–3440.
13. Durinck, S., Spellman, P., E, B., & Huber, W. (2009). Mapping identifiers for the integration of genomic datasets with the R/Bioconductor package biomaRt. *Nature Protocols*, *4*, 1184–1191.
14. Ernst, J., & Kellis, M. (2012). ChromHMM: Automating chromatin-state discovery and characterization. *Nature Methods*, *9*(3), Article 3. https://doi.org/10.1038/nmeth.1906
15. Fornes, O., Castro-Mondragon, J. A., Khan, A., van der Lee, R., Zhang, X., Richmond, P. A., Modi, B. P., Correard, S., Gheorghe, M., Baranašić, D., Santana-Garcia, W., Tan, G., Chèneby, J., Ballester, B., Parcy, F., Sandelin, A., Lenhard, B., Wasserman, W. W., & Mathelier, A. (2020). JASPAR 2020: Update of the open-access database of transcription factor binding profiles. *Nucleic Acids Research*, *48*(D1), D87–D92. https://doi.org/10.1093/nar/gkz1001
16. Garces de los Fayos Alonso, I., Liang, H.-C., Turner, S. D., Lagger, S., Merkel, O., & Kenner, L. (2018). The Role of Activator Protein-1 (AP-1) Family Members in CD30-Positive Lymphomas. *Cancers*, *10*(4), 93. https://doi.org/10.3390/cancers10040093
17. Gladyshev, V. N., Kritchevsky, S. B., Clarke, S. G., Cuervo, A. M., Fiehn, O., de Magalhães, J. P., Mau, T., Maes, M., Moritz, R. L., Niedernhofer, L. J., Van Schaftingen, E., Tranah, G. J., Walsh, K., Yura, Y., Zhang, B., & Cummings, S. R. (2021). Molecular damage in aging. *Nature Aging*, *1*(12), Article 12. https://doi.org/10.1038/s43587-021-00150-3
18. Gorbunova, V., Seluanov, A., Mita, P., McKerrow, W., Fenyö, D., Boeke, J. D., Linker, S. B., Gage, F. H., Kreiling, J. A., Petrashen, A. P., Woodham, T. A., Taylor, J. R., Helfand, S. L., & Sedivy, J. M. (2021). The role of retrotransposable elements in ageing and age-associated diseases. *Nature*, *596*(7870), 43–53. https://doi.org/10.1038/s41586-021-03542-y
19. Hoffman, M. M., Ernst, J., Wilder, S. P., Kundaje, A., Harris, R. S., Libbrecht, M., Giardine, B., Ellenbogen, P. M., Bilmes, J. A., Birney, E., Hardison, R. C., Dunham, I., Kellis, M., & Noble, W. S. (2013). Integrative annotation of chromatin elements from ENCODE data. *Nucleic Acids Research*, *41*(2), 827–841. https://doi.org/10.1093/nar/gks1284

20. Holloszy, J. O. (2000). The biology of aging. *Mayo Clinic Proceedings*, *75 Suppl*, S3-8; discussion S8-9.
21. Horváth, V., Merenciano, M., & González, J. (2017). Revisiting the Relationship between Transposable Elements and the Eukaryotic Stress Response. *Trends in Genetics*, *33*(11), 832–841. https://doi.org/10.1016/j.tig.2017.08.007
22. *ID 715739—BioProject—NCBI*. (n.d.). Retrieved November 11, 2022, from https://www.ncbi.nlm.nih.gov/bioproject/?term=PRJNA715739
23. Jones, M. J., Goodman, S. J., & Kobor, M. S. (2015). DNA methylation and healthy human aging. *Aging Cell*, *14*(6), 924–932. https://doi.org/10.1111/acel.12349
24. Karolchik D, Hinrichs AS, Furey TS, Roskin KM, Sugnet CW, Haussler D, & Kent WJ. (2004). The UCSC Table Browser data retrieval tool. *Nucleic Acids Res*, *32*, 493–496.
25. Kent, W. J., Sugnet, C. W., Furey, T. S., Roskin, K. M., Pringle, T. H., Zahler, A. M., & Haussler, and D. (2002). The Human Genome Browser at UCSC. *Genome Research*, *12*(6), 996–1006. https://doi.org/10.1101/gr.229102
26. Krueger, F., & Andrews, S. (2011). Bismark: A flexible aligner and methylation caller for Bisulfite-Seq applications. *Bioinformatics*, *27*, 1571–1572. https://doi.org/10.1093/bioinformatics/btr167
27. Lea, A. J., Altmann, J., Alberts, S. C., & Tung, J. (2016). Resource base influences genome-wide DNA methylation levels in wild baboons (Papio cynocephalus). *Molecular Ecology*, *25*(8), 1681–1696. https://doi.org/10.1111/mec.13436
28. Lea, A. J., Tung, J., & Zhou, X. (2015). A flexible, efficient binomial mixed model for identifying differential DNA methylation in bisulfite sequencing data. *PLoS Genetics*, *11*(11), 1–31. https://doi.org/10.1371/journal.pgen.1005650
29. Li, M., Zou, D., Li, Z., Gao, R., Sang, J., Zhang, Y., Li, R., Xia, L., Zhang, T., Niu, G., Bao, Y., & Zhang, Z. (2019). EWAS Atlas: A curated knowledgebase of epigenome-wide association studies. *Nucleic Acids Research*, *47*(D1), D983–D988. https://doi.org/10.1093/nar/gky1027
30. López-Otín, C., Blasco, M. A., Partridge, L., Serrano, M., & Kroemer, G. (2013). The Hallmarks of Aging. *Cell*, *153*(6), 1194–1217. https://doi.org/10.1016/j.cell.2013.05.039
31. Manichaikul, A., Mychaleckyj, J. C., Rich, S. S., Daly, K., Sale, M., & Chen, W.-M. (2010). Robust relationship inference in genome-wide association studies. *Bioinformatics*, *26*(22), 2867–2873. https://doi.org/10.1093/bioinformatics/btq559
32. Márquez, E. J., Chung, C. han, Marches, R., Rossi, R. J., Nehar-Belaid, D., Eroglu, A., Mellert, D. J., Kuchel, G. A., Banchereau, J., & Ucar, D. (2020). Sexual-dimorphism in human immune system aging. *Nature Communications*, *11*(1). https://doi.org/10.1038/s41467-020-14396-9
33. Pages, H. (2022). *BSgenome: Software infrastructure for efficient representation of full genomes and their SNPs.* [R package version 1.66.1]. https://bioconductor.org/packages/BSgenome.
34. Pallares, L. F., Picard, S., & Ayroles, J. F. (2020). Tm3'Seq: A tagmentation-mediated 3' sequencing approach for improving scalability of RNAseq experiments. *G3: Genes, Genomes, Genetics*, *10*(1), 143–150. https://doi.org/10.1534/g3.119.400821
35. Pappalardo, A. M., Ferrito, V., Biscotti, M. A., Canapa, A., & Capriglione, T. (2021). Transposable Elements and Stress in Vertebrates: An Overview. *International Journal of Molecular Sciences*, *22*(4), 1970. https://doi.org/10.3390/ijms22041970
36. Pon, J. R., & Marra, M. A. (2015). MEF2 transcription factors: Developmental regulators and emerging cancer genes. *Oncotarget*, *7*(3), 2297–2312. https://doi.org/10.18632/oncotarget.6223
37. Quinlan, A. R., & Hall, I. M. (2010). BEDTools: A flexible suite of utilities for comparing genomic features. *Bioinformatics*, *26*(6), 841–842. https://doi.org/10.1093/bioinformatics/btq033
38. Ritchie, M. E., Phipson, B., Wu, D., Hu, Y., Law, C. W., Shi, W., & Smyth, G. K. (2015). Limma powers differential expression analyses for RNA-sequencing and microarray studies. *Nucleic Acids Research*, *43*(7), e47. https://doi.org/10.1093/nar/gkv007
39. Seale, K., Horvath, S., Teschendorff, A., Eynon, N., & Voisin, S. (2022). Making sense of the ageing methylome. *Nature Reviews Genetics*, *23*(10), 585–605. https://doi.org/10.1038/s41576-022-00477-6
40. Snyder-Mackler, N., Sanz, J., Kohn, J. N., Voyles, T., Pique-Regi, R., Wilson, M. E., Barreiro, L. B., & Tung, J. (2019). Social status alters chromatin accessibility and the gene regulatory response to glucocorticoid stimulation in rhesus macaques. *Proceedings of the National Academy of Sciences*, *116*(4), 1219–1228. https://doi.org/10.1073/pnas.1811758115
41. Sriraman, A., Debnath, T. K., Xhemalce, B., & Miller, K. M. (2020). Making it or breaking it: DNA methylation and genome integrity. *Essays in Biochemistry*, *64*(5), 687–703. https://doi.org/10.1042/EBC20200009
42. Sun, A. S., Zhu, J., & Zhou, X. (2018). *Package 'PQLseq'* (pp. 1–7).
43. Sun, S., Zhu, J., Mozaffari, S., Ober, C., Chen, M., & Zhou, X. (2019). Heritability estimation and differential analysis of count data with generalized linear mixed models in genomic sequencing studies. *Bioinformatics*, *35*(3), 487–496. https://doi.org/10.1093/bioinformatics/bty644

44. Thompson, R. F., Atzmon, G., Gheorghe, C., Liang, H. Q., Lowes, C., Greally, J. M., & Barzilai, N. (2010). Tissue-specific dysregulation of DNA methylation in aging. *Aging Cell*, *9*(4), 506–518. https://doi.org/10.1111/j.1474-9726.2010.00577.x
45. Tobi, E. W., Goeman, J. J., Monajemi, R., Gu, H., Putter, H., Zhang, Y., Slieker, R. C., Stok, A. P., Thijssen, P. E., Müller, F., Van Zwet, E. W., Bock, C., Meissner, A., Lumey, L. H., Eline Slagboom, P., & Heijmans, B. T. (2014). DNA methylation signatures link prenatal famine exposure to growth and metabolism. *Nature Communications*, *5*. https://doi.org/10.1038/ncomms6592
46. Trivedi, M., Shah, J., Hodgson, N., Byun, H.-M., & Deth, R. (2014). Morphine Induces Redox-Based Changes in Global DNA Methylation and Retrotransposon Transcription by Inhibition of Excitatory Amino Acid Transporter Type 3–Mediated Cysteine Uptake. *Molecular Pharmacology*, *85*(5), 747–757. https://doi.org/10.1124/mol.114.091728
47. Tung, J., Archie, E. A., Altmann, J., & Alberts, S. C. (2016). Cumulative early life adversity predicts longevity in wild baboons. *Nature Communications*, *7*, 1–7. https://doi.org/10.1038/ncomms11181
48. Unternaehrer, E., Luers, P., Mill, J., Dempster, E., Meyer, A. H., Staehli, S., Lieb, R., Hellhammer, D. H., & Meinlschmidt, G. (2012). Dynamic changes in DNA methylation of stress-associated genes (OXTR, BDNF) after acute psychosocial stress. *Translational Psychiatry*, *2*(8), Article 8. https://doi.org/10.1038/tp.2012.77
49. Watowich, M. M., Chiou, K. L., Montague, M. J., Cayo Biobank Research Unit, Simons, N. D., Horvath, J. E., Ruiz-Lambides, A. V., Martínez, M. I., Higham, J. P., Brent, L. J. N., Platt, M. L., Snyder-Mackler, N., Brent, L. J. N., Higham, J. P., Martínez, M. I., Montague, M. J., Platt, M. L., & Snyder-Mackler, N. (2022). Natural disaster and immunological aging in a nonhuman primate. *Proceedings of the National Academy of Sciences*, *119*(8), e2121663119. https://doi.org/10.1073/pnas.2121663119
50. Wood, J. G., Jones, B. C., Jiang, N., Chang, C., Hosier, S., Wickremesinghe, P., Garcia, M., Hartnett, D. A., Burhenn, L., Neretti, N., & Helfand, S. L. (2016). Chromatin-modifying genetic interventions suppress age-associated transposable element activation and extend life span in Drosophila. *Proceedings of the National Academy of Sciences*, *113*(40), 11277–11282. https://doi.org/10.1073/pnas.1604621113
51. Xiong, Z., Yang, F., Li, M., Ma, Y., Zhao, W., Wang, G., Li, Z., Zheng, X., Zou, D., Zong, W., Kang, H., Jia, Y., Li, R., Zhang, Z., & Bao, Y. (2022). EWAS Open Platform: Integrated data, knowledge and toolkit for epigenome-wide association study. *Nucleic Acids Research*, *50*(D1), D1004–D1009. https://doi.org/10.1093/nar/gkab972
52. Zannas, A. S., Arloth, J., Carrillo-Roa, T., Iurato, S., Röh, S., Ressler, K. J., Nemeroff, C. B., Smith, A. K., Bradley, B., Heim, C., Menke, A., Lange, J. F., Brückl, T., Ising, M., Wray, N. R., Erhardt, A., Binder, E. B., & Mehta, D. (2015). Lifetime stress accelerates epigenetic aging in an urban, African American cohort: Relevance of glucocorticoid signaling. *Genome Biology*, *16*(1), 266. https://doi.org/10.1186/s13059-015-0828-5
53. Zipple, M. N., Altmann, J., Campos, F. A., Cords, M., Fedigan, L. M., Lawler, R. R., Lonsdorf, E. V., Perry, S., Pusey, A. E., Stoinski, T. S., Strier, K. B., & Alberts, S. C. (2021). Maternal death and offspring fitness in multiple wild primates.

Data Availability and Code

Data availability for each chapter is documented within the chapter text.

Code used to complete analyses for each chapter are available in the following locations:

Chapter 1: https://github.com/mwatowich/Dog-cognition-across-aging

Chapter 2: https://github.com/mwatowich/Natural-disaster-accelerates-immune-aging

Chapter 3: https://github.com/mwatowich/aging_hurricane_DNAm